



UvA-DARE (Digital Academic Repository)

Search for B -L R-parity-violating top squarks in $\sqrt{s} = 13$ TeV pp collisions with the ATLAS experiment

Aaboud, M.; The ATLAS Collaboration

DOI

[10.1103/PhysRevD.97.032003](https://doi.org/10.1103/PhysRevD.97.032003)

Publication date

2018

Document Version

Final published version

Published in

Physical Review D. Particles and Fields

License

CC BY

[Link to publication](#)

Citation for published version (APA):

Aaboud, M., & The ATLAS Collaboration (2018). Search for *B -L R-parity-violating top squarks in $\sqrt{s} = 13$ TeV pp collisions with the ATLAS experiment.* *Physical Review D. Particles and Fields*, 97(3), [032003]. <https://doi.org/10.1103/PhysRevD.97.032003>

General rights

It is not permitted to download or to forward/distribute the text or part of it without the consent of the author(s) and/or copyright holder(s), other than for strictly personal, individual use, unless the work is under an open content license (like Creative Commons).

Disclaimer/Complaints regulations

If you believe that digital publication of certain material infringes any of your rights or (privacy) interests, please let the Library know, stating your reasons. In case of a legitimate complaint, the Library will make the material inaccessible and/or remove it from the website. Please Ask the Library: <https://uba.uva.nl/en/contact>, or a letter to: Library of the University of Amsterdam, Secretariat, Singel 425, 1012 WP Amsterdam, The Netherlands. You will be contacted as soon as possible.

UvA-DARE is a service provided by the library of the University of Amsterdam (<https://dare.uva.nl>)

Search for $B-L$ R -parity-violating top squarks in $\sqrt{s} = 13$ TeV pp collisions with the ATLAS experiment

M. Aaboud *et al.**
(ATLAS Collaboration)

 (Received 16 October 2017; published 6 February 2018)

A search is presented for the direct pair production of the stop, the supersymmetric partner of the top quark, that decays through an R -parity-violating coupling to a final state with two leptons and two jets, at least one of which is identified as a b -jet. The data set corresponds to an integrated luminosity of 36.1 fb^{-1} of proton-proton collisions at a center-of-mass energy of $\sqrt{s} = 13$ TeV, collected in 2015 and 2016 by the ATLAS detector at the LHC. No significant excess is observed over the Standard Model background, and exclusion limits are set on stop pair production at a 95% confidence level. Lower limits on the stop mass are set between 600 GeV and 1.5 TeV for branching ratios above 10% for decays to an electron or muon and a b -quark.

DOI: [10.1103/PhysRevD.97.032003](https://doi.org/10.1103/PhysRevD.97.032003)

I. INTRODUCTION

The extension of the Standard Model (SM) of particle physics with supersymmetry (SUSY) [1–6] leads to processes that violate both baryon number (B) and lepton number (L), such as rapid proton decay. A common theoretical approach to reconcile the strong constraints from the nonobservation of these processes is to introduce a multiplicative quantum number called R -parity [7], defined as $R = (-1)^{3(B-L)+2s}$ where s is the spin of the particle. If R -parity is conserved, then SUSY particles are produced in pairs, and the lightest supersymmetric particle (LSP) is stable. The LSP cannot carry electric charge or color charge without coming into conflict with astrophysical data [8,9].

A number of theoretical models beyond the Standard Model (BSM) predict R -parity violation (RPV) [10–13]. The benchmark model for this search considers an additional local symmetry $U(1)_{B-L}$ to the $SU(3)_C \times SU(2)_L \times U(1)_Y$ Standard Model with right-handed neutrino supermultiplets. The minimal supersymmetric extension then only needs a vacuum expectation value for a right-handed scalar neutrino in order to spontaneously break the $B-L$ symmetry [14–18]. This minimal $B-L$ model violates lepton number but not baryon number. The couplings for RPV are highly suppressed as they are related to the neutrino masses, and the model is consistent with the experimental bounds on proton decay and lepton number

violation. At the LHC, the most noticeable effect is that the LSP is no longer stable and can now decay via RPV processes, and it also may now carry color and electric charge. This leads to unique signatures that are forbidden in conventional models with R -parity conservation. A novel possibility is a top squark or stop (\tilde{t}) as the LSP with a rapid RPV decay. The supersymmetric partners of the left- and right-handed top quarks, \tilde{t}_L and \tilde{t}_R , mix to form two mass eigenstates consisting of the lighter \tilde{t}_1 and heavier \tilde{t}_2 . Given the large top quark mass, the lighter \tilde{t}_1 is expected to be significantly lighter than the other squarks due to renormalization group effects [19,20]. The lighter \tilde{t}_1 , denoted \tilde{t} for simplicity, is the target of this analysis.

This paper presents a search performed by ATLAS for direct stop pair production, with the RPV decay of each \tilde{t} to a b -quark and a charged lepton ($\tilde{t} \rightarrow b\ell$), as shown in Fig. 1. In contrast to R -parity-conserving searches for \tilde{t} , there is no significant missing transverse momentum in the

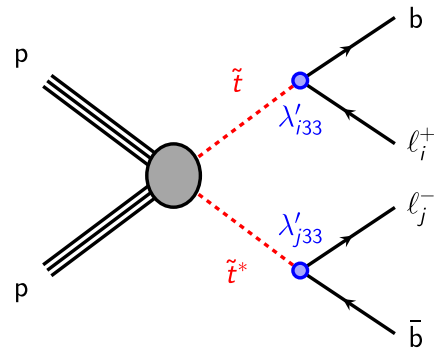


FIG. 1. Feynman diagram for stop pair production, with \tilde{t} and anti- \tilde{t}^* decay to a charged lepton of any flavor and a b -quark through an R -parity-violating coupling λ' .

*Full author list given at the end of the article.

Published by the American Physical Society under the terms of the [Creative Commons Attribution 4.0 International license](https://creativecommons.org/licenses/by/4.0/). Further distribution of this work must maintain attribution to the author(s) and the published article's title, journal citation, and DOI. Funded by SCOAP³.

decay. The \tilde{t} decay branching ratios to each lepton flavor are related to the neutrino mass hierarchy [21,22], and a large phase space in the branching ratio plane is currently available. With an inverted mass hierarchy, the branching ratio to the $b\ell$ final state may be as large as 100%, and with a normal mass hierarchy the branching ratio to the $b\mu$ final state may be as high as 90%. The experimental signature is therefore two oppositely charged leptons of any flavor and two b -jets. In this analysis, only events with electron or muon signatures are selected, and final states are split by flavor into ee , $e\mu$, and $\mu\mu$ selections. At least one of the two jets is required to be identified as initiated by a b -quark, improving the selection efficiency of signal events over a requirement of two b -jets. Events are chosen in which the two reconstructed $b\ell$ pairs have roughly equal mass.

Previous searches with similar final states have targeted the pair production of first-, second-, and third-generation leptoquarks at ATLAS [23,24] and at CMS [25,26]. However, they consider final states within the same generation ($eejj$, $\mu\mu jj$, $\tau\tau bb$, where j indicates a light-flavor jet) and do not focus on final states with both b -jets and electrons or muons ($eebb$, $\mu\mu bb$), nor consider final states with both electrons and muons ($e\mu bb$). The results of the Run 1 leptoquark searches were reinterpreted for the \tilde{t} mass and its decay branching ratios in the $B-L$ model [21,22], setting lower mass limits between 424 and 900 GeV at a 95% confidence level.

The ATLAS detector and the data set collected during Run 2 of the LHC are described in Sec. II, with the corresponding Monte Carlo simulation samples presented in Sec. III. The identification and reconstruction of jets and leptons is presented in Sec. IV, and the discriminating variables used to construct the signal regions are described in Sec. V. The method of background estimation is described in Sec. VI, and the systematic uncertainties are detailed in Sec. VII. The results are presented in Sec. VIII, and the conclusions are given in Sec. IX.

II. ATLAS DETECTOR AND DATA SET

The ATLAS detector [27] consists of an inner detector tracking system, electromagnetic and hadronic sampling calorimeters, and a muon spectrometer. Charged-particle tracks are reconstructed in the inner detector (ID), which spans the pseudorapidity¹ range $|\eta| < 2.5$, and consists of three subdetectors: a silicon pixel tracker, a silicon

¹ATLAS uses a right-handed coordinate system with its origin at the nominal interaction point (IP) in the center of the detector and the z axis along the beam pipe. The x axis points from the IP to the center of the LHC ring, and the y axis points upward. Cylindrical coordinates (r, ϕ) are used in the transverse plane, ϕ being the azimuthal angle around the z axis. The pseudorapidity is defined in terms of the polar angle θ as $\eta = -\ln \tan(\theta/2)$. Rapidity is defined as $y = 0.5 \ln [(E + p_z)/(E - p_z)]$ where E denotes the energy and p_z is the component of the momentum along the beam direction.

microstrip tracker, and a straw-tube transition radiation tracker. The ID is surrounded by a thin superconducting solenoid providing an axial magnetic field of 2 T, allowing the measurement of charged-particle momenta. In preparation for Run 2, a new innermost layer of the silicon pixel tracker, the insertable B-layer (IBL) [28], was introduced at a radial distance of 3.3 cm from the beam line to improve track reconstruction and the identification of jets initiated by b -quarks.

The ATLAS calorimeter system consists of high-granularity electromagnetic and hadronic sampling calorimeters covering the region $|\eta| < 4.9$. The electromagnetic calorimeter uses liquid argon (LAr) as the active material with lead absorbers in the region $|\eta| < 3.2$. The central hadronic calorimeter incorporates plastic scintillator tiles and steel absorbers in the region $|\eta| < 1.7$. The hadronic endcap calorimeter ($1.5 < |\eta| < 3.2$) and the forward calorimeters ($3.1 < |\eta| < 4.9$) use LAr with copper or tungsten absorbers.

The muon spectrometer (MS) surrounds the calorimeters and measures muon tracks within $|\eta| < 2.7$ using three layers of precision tracking chambers and dedicated trigger chambers. A system of three superconducting air-core toroidal magnets provides a magnetic field for measuring muon momenta.

The ATLAS trigger system begins with a hardware-based level-1 (L1) trigger followed by a software-based high-level trigger (HLT) [29]. The L1 trigger is designed to accept events at an average rate of 100 kHz, and the HLT is designed to accept events to write out to disk at an average rate of 1 kHz. Electrons are triggered in the pseudorapidity range $|\eta| < 2.5$, where the electromagnetic calorimeter is finely segmented and track reconstruction is available. Compact electromagnetic energy deposits triggered at L1 are used as the seeds for HLT algorithms that are designed to identify electrons based on calorimeter and fast track reconstruction. The muon trigger at L1 is based on a coincidence of trigger chamber layers. The parameters of muon candidate tracks are then derived in the HLT by fast reconstruction algorithms in both the ID and MS.

The data sample used for this search was collected from proton-proton collisions at a center-of-mass energy of $\sqrt{s} = 13$ TeV in 2015 and 2016. An integrated luminosity of 36.1 fb^{-1} was collected while all tracking detectors, calorimeters, muon chambers, and magnets were fully operational. The uncertainty in the combined 2015 and 2016 integrated luminosity is 3.2%. It is derived from a preliminary calibration of the luminosity scale using x - y beam-separation scans performed in August 2015 and May 2016, following a methodology similar to that detailed in Ref. [30]. The LHC collided protons with bunch-crossing intervals of 25 ns, and the average number of interactions per bunch crossing was estimated to be $\langle \mu \rangle = 23.7$.

For this analysis, events are selected using single-electron and single-muon triggers requiring leptons above

a transverse momentum (p_T) threshold and satisfying various lepton identification and isolation criteria. The trigger-level criteria for the p_T , identification, and isolation of the leptons are less stringent than those applied in the event selection to ensure that trigger efficiencies are constant in the analysis phase space.

III. MONTE CARLO SIMULATION

Monte Carlo (MC) simulation is used to predict the backgrounds from SM processes, estimate the detector response and efficiency to reconstruct the signal process, and estimate systematic uncertainties. The largest sources of SM background with different-flavor leptons are top quark pair production ($t\bar{t}$) and single-top-quark production (single-top), while the largest source with same-flavor leptons is Z + jets production. The yields of these three backgrounds are estimated through data-driven methods described in Sec. VI. The smaller backgrounds are W + jets, diboson, and $t\bar{t} + W/Z$ production and are estimated directly from MC simulation. The contribution from events with jets misreconstructed as leptons or with nonprompt leptons is evaluated with the MC simulation and is negligible. Details of the MC simulations are given below and are summarized in Table I.

The $t\bar{t}$ and single-top processes were simulated [37] at next-to-leading-order (NLO) accuracy in perturbative QCD using the POWHEG-BOX v2 event generator [38] for $t\bar{t}$, Wt , and s -channel single-top production, and using the POWHEG-BOX v1 generator for the electroweak t -channel single-top production. For these processes the spin correlations in top quark production and decay were preserved, and the top quark mass was set to 172.5 GeV. The matrix element was interfaced with the CT10 parton distribution function (PDF) set [39], and the parton shower (PS), fragmentation, and underlying event were simulated with PYTHIA 6.428 [40] using the CTEQ6L1 PDF set [41] and the P2012 underlying-event tuned parameters (UE tune) [42], with additional radiation simulated to the leading-logarithm approximation through p_T -ordered parton showers [43].

The Z + jets and W + jets samples were generated at NLO [44] with the SHERPA 2.2.1 event generator [45].

Matrix elements were calculated for up to two partons at NLO and four partons at LO using Comix [46] and OpenLoops [47], and merged with the SHERPA PS [48] using the ME + PS@NLO prescription [49]. The NNPDF3.0 PDF set [50] was used in conjunction with a dedicated PS tuning developed by the SHERPA authors. Diboson samples with two, three, or four leptons were similarly generated with SHERPA 2.2.1. The diboson matrix elements contain all diagrams with four electroweak vertices, and were calculated for up to one (ZZ) or zero (WW, WZ) partons at NLO and up to three partons at LO. Electroweak- and loop-induced diboson events were simulated with SHERPA 2.1.1, using the same prescriptions as above but with the CT10 PDF set used in conjunction with the dedicated SHERPA PS tuning. The production of $t\bar{t}$ with a W or Z boson ($t\bar{t} + V$) was simulated at NLO using MADGRAPH5_aMC@NLO (MG5_AMC@NLO) 2.2.3 [51] and interfaced to PYTHIA 8.212 [52] with the CKKW-L prescription [53]. These samples are generated with the A14 UE tune [54] and NNPDF2.3 PDF set [55].

The RPV stop signal events were generated at leading order using the MG5_AMC@NLO 2.2.3 event generator with the NNPDF2.3 PDF set and interfaced to PYTHIA 8.186 [52] using the A14 UE tune. The matrix element was matched to the PS using the CKKW-L prescription, with the matching scale set to one quarter of the generated stop mass. All other supersymmetric particles are assumed to be decoupled. The signal cross sections are calculated to NLO accuracy in the strong coupling constant, adding the resummation of soft gluon emission at next-to-leading-logarithm accuracy (NLO + NLL) [56–59]. The nominal cross section and the uncertainty for each mass value are taken from a combination of cross-section predictions using different PDF sets and factorization and renormalization scales, as described in Ref. [36]. Stop samples were generated at masses between 600 and 1000 GeV in steps of 100 GeV and between 1000 and 1600 GeV in steps of 50 GeV. The cross section ranges from 175 ± 23 fb for a \tilde{t} mass of 600 GeV to 0.141 ± 0.038 fb for a mass of 1600 GeV. The generated stops decay promptly through $\tilde{t} \rightarrow b\ell$ with a 1/3 branching ratio (\mathcal{B}) for each lepton flavor. When optimizing the signal event selection, the generated events are reweighted to have

TABLE I. MC simulation details by physics process.

Process	Event generator	PS and hadronization	UE tune	PDF	Cross section
$t\bar{t}$	POWHEG-BOX v2	PYTHIA 6.428	P2012	CT10	NNLO + NNLL [31]
single-top (Wt and s -channel)	POWHEG-BOX v2	PYTHIA 6.428	P2012	CT10	NNLO + NNLL [32,33]
(t -channel)	POWHEG-BOX v1	PYTHIA 6.428	P2012	CT10	NNLO + NNLL [34]
Z/W + jets	SHERPA 2.2.1	SHERPA 2.2.1	Default	NNPDF3.0	NNLO [35]
Diboson	SHERPA 2.2.1	SHERPA 2.2.1	Default	NNPDF3.0	NLO
Diboson (EW/loop)	SHERPA 2.1.1	SHERPA 2.1.1	Default	CT10	NLO
$t\bar{t} + W/Z$	MG5_AMC@NLO 2.2.3	PYTHIA 8.212	A14	NNPDF2.3	NLO
\tilde{t}^*	MG5_AMC@NLO 2.2.3	PYTHIA 8.1868.186	A14	NNPDF2.3	NLO + NLL [36]

$\mathcal{B}(\tilde{t} \rightarrow be) = \mathcal{B}(\tilde{t} \rightarrow b\mu) = 0.5$ and $\mathcal{B}(\tilde{t} \rightarrow b\tau) = 0$, and various weightings are used to derive limits for different branching ratio assumptions.

All background samples are normalized using the available NLO or next-to-next-to-leading order (NNLO) cross sections, as indicated in Table I. The modeling of c -hadron and b -hadron decays in samples generated with POWHEG-BOX or MG5_AMC@NLO was performed with EVTGEN 1.2.0 [60]. Generated events were propagated through a full simulation of the ATLAS detector [61] based on Geant4 [62], which describes the interactions of the particles with the detector. A parametrized simulation of the ATLAS calorimeter called AtIfast-II [61] was used for faster detector simulation of signal samples, and was found to agree well with the full simulation. Multiple overlapping pp interactions (pileup) were included by overlaying simulated minimum-bias events onto the simulated hard-scatter event. Minimum-bias events were generated using PYTHIA 8.186 with the A2 UE tune [63] and MSTW2008LO PDF set [64]. The simulated events are weighted such that the distribution of the average number of pp interactions per bunch crossing agrees with data.

IV. EVENT RECONSTRUCTION

Events and individual leptons and jets are required to satisfy several quality criteria to be considered by the analysis. Events recorded during stable beam and detector conditions are required to satisfy data-quality criteria [65]. Each event is required to have a primary reconstructed vertex with two or more associated tracks with $p_T > 400$ MeV, where the primary vertex is chosen as the vertex with the highest Σp_T^2 of associated tracks. Two stages of quality and kinematic requirements are applied to leptons and jets. The looser baseline requirements are first applied, and baseline leptons and jets are used to resolve any misidentification or overlap between electrons, muons, and jets. The subsequent tighter signal requirements are then applied to identify high-quality leptons and jets in the kinematic phase space of interest.

Electron candidates are reconstructed from energy deposits in the electromagnetic calorimeter matched to a charged-particle track in the ID. Baseline electron candidates must have $p_T > 10$ GeV, $|\eta| < 2.47$, and satisfy a loose electron likelihood identification [66]. Signal electrons must pass the baseline electron selection, have $p_T > 40$ GeV, and satisfy a tight electron likelihood identification. In addition, they must be isolated from nearby activity, satisfying a loose p_T -dependent track-based criterion [67]. Finally, their trajectory must be consistent with the primary vertex, such that their impact parameter in the transverse plane (d_0^{PV}) satisfies $|d_0^{\text{PV}}|/\sigma_{d_0^{\text{PV}}} < 5$, where $\sigma_{d_0^{\text{PV}}}$ is the uncertainty in d_0^{PV} . Each signal electron must have a longitudinal impact parameter with respect to the primary vertex (z_0^{PV}) that satisfies $|z_0^{\text{PV}} \sin \theta| < 0.5$ mm.

Muon candidates are reconstructed by combining tracks in the ID with tracks in the MS. Baseline muon candidates must have $p_T > 10$ GeV, $|\eta| < 2.7$, and satisfy the medium muon identification criteria [68]. Signal muons must pass the baseline muon selection, have $p_T > 40$ GeV, $|\eta| < 2.5$, $|z_0^{\text{PV}} \sin \theta| < 0.5$ mm, and $|d_0^{\text{PV}}|/\sigma_{d_0^{\text{PV}}} < 3$. As with electrons, muons must satisfy the p_T -dependent loose track-based isolation criteria. Events containing a poorly measured signal muon, as determined by having incompatible momentum measurements in the ID and the MS, are rejected. Absolute requirements of $|z_0^{\text{PV}}| < 1$ mm and $|d_0^{\text{PV}}| < 0.2$ mm on the impact parameters of signal muons are applied to reject cosmic muons.

Jets are reconstructed using the anti- k_r algorithm [69,70] with a radius parameter $R = 0.4$ from clusters of energy deposits in the calorimeters [71]. Jets are corrected for pileup contamination on an event-by-event basis using the jet area subtraction method [72,73]. Jets are further calibrated to account for the predicted detector response in MC simulation, and a residual calibration of jets in data is derived through *in situ* measurements [74]. Baseline jet candidates are required to have $p_T > 20$ GeV and $|\eta| < 2.8$. Jets with $p_T < 60$ GeV and $|\eta| < 2.4$ are required to satisfy pileup-rejection criteria based on charged-particle tracks and implemented through the jet vertex tagger algorithm [72]. Signal jets must pass the baseline jet selection and have $p_T > 60$ GeV. Events are rejected if they contain a jet that fails the loose quality criteria [75], reducing contamination from calorimeter noise bursts and noncollision backgrounds. Jets within $|\eta| < 2.5$ that are initiated by b -quarks are identified using the multivariate MV2c10 b -tagging algorithm [76,77], which exploits the impact parameters of charged-particle tracks, the parameters of reconstructed secondary vertices, and the topology of b - and c -hadron decays inside a jet. The working point is chosen to provide a b -tagging efficiency of 77% per b -jet in simulated $t\bar{t}$ events with a rejection factor of approximately 130 for jets initiated by gluons or light-flavor quarks and 6 for jets initiated by c -quarks [77]. Correction factors are applied to events to compensate for differences between data and MC simulation in the b -tagging efficiency for b -jets, c -jets, and light-flavor jets.

To avoid reconstructing a single detector signature as multiple leptons or jets, an overlap removal procedure is performed on baseline leptons and jets. The requirements are applied sequentially, and failing particles are removed from consideration in the subsequent steps. If an electron and muon share a track in the ID, the electron is removed. Any jet that is not b -tagged and is within a distance² $\Delta R(\ell, \text{jet}) \leq 0.2$ of a lepton is removed. If the jet is

²The distance between two four-momenta is defined as $\Delta R = \sqrt{(\Delta y)^2 + (\Delta \phi)^2}$, where Δy is their distance in rapidity and $\Delta \phi$ is their azimuthal distance. The distance with respect to a jet is calculated from its central axis.

b -tagged, the lepton is removed instead in order to suppress leptons from semileptonic decays of c - and b -hadrons. Finally, any lepton that is $\Delta R(\ell, \text{jet}) \leq 0.4$ from a jet is removed.

The trigger, reconstruction, identification, and isolation efficiencies of electrons [67] and muons [68] in MC simulation are corrected using events in data with leptonic Z and J/ψ decays. Similarly, corrections to the b -tagging

efficiency and mis-tag rate in MC simulation are derived from various control regions in data [77].

V. EVENT SELECTION

To identify the pair production of stops, events are required to have at least two leptons and two jets. If more than two leptons or two jets are found, the two highest- p_T

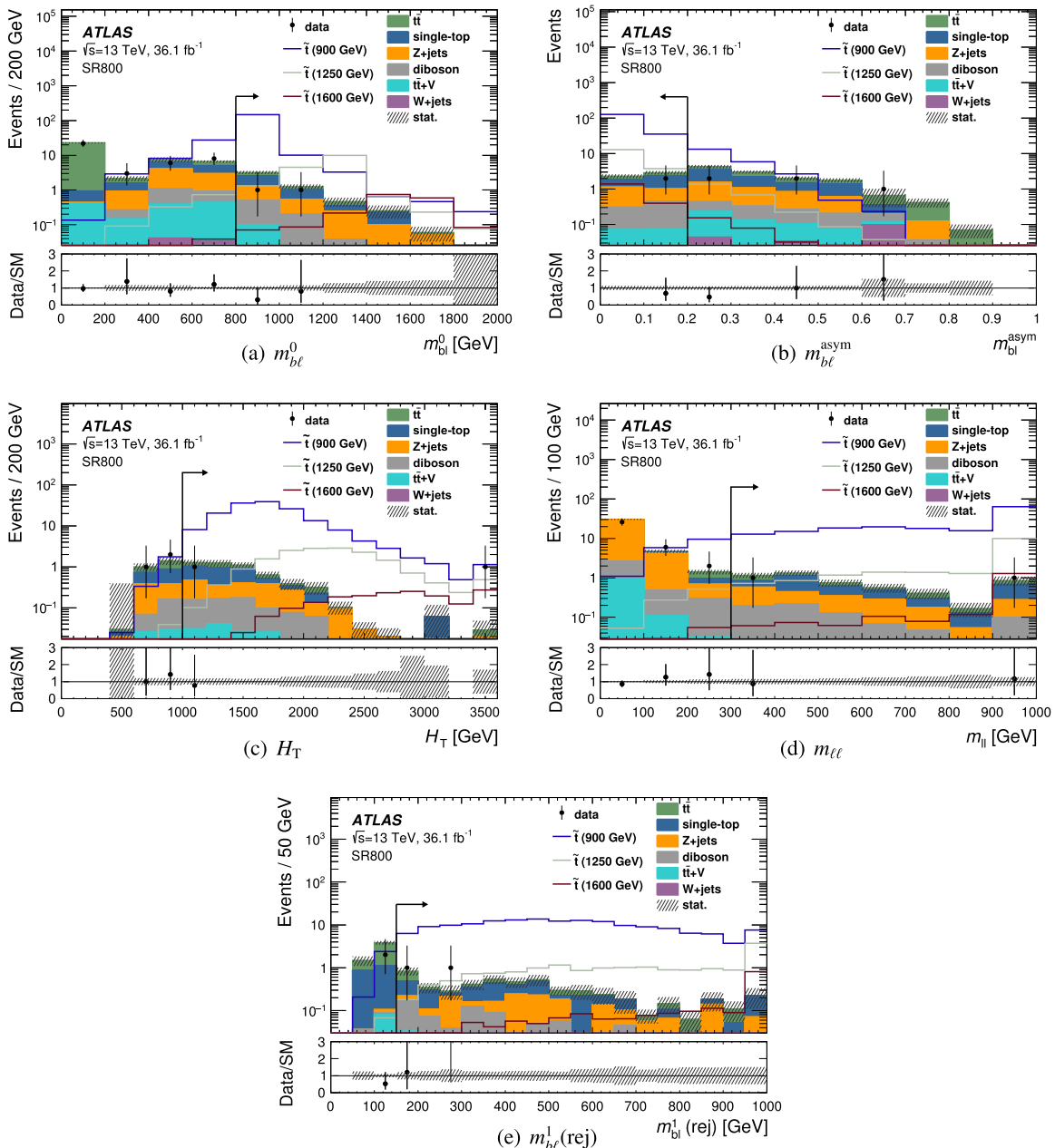


FIG. 2. Distributions of (a) $m_{b\ell}^0$, (b) $m_{b\ell}^{\text{asym}}$, (c) H_T , (d) $m_{\ell\ell}$, and (e) $m_{b\ell}^1(\text{rej})$ in the SR800 signal region for the data and postfit MC prediction. The SR800 event selections are applied for each distribution except the selection on the variable shown, which is indicated by an arrow. Normalization factors are derived from the background-only estimation discussed in Sec. VI and are applied to the dominant $t\bar{t}$, single-top, and $Z + \text{jets}$ processes. Benchmark signal models generated with \tilde{t} masses of 900, 1250, and 1600 GeV are included for comparison. The bottom panel shows the ratio between the data and the postfit MC prediction. The hatched uncertainty band includes the statistical uncertainties in the background prediction. The last bin includes the overflow events.

leptons and jets are selected. At least one of the two leading jets must be b -tagged. The selected leptons are required to have opposite charge, and one of them must be consistent with the associated single-lepton trigger. This trigger requirement is highly efficient for signal events, with an efficiency of 93% for the $\mu\mu$ channel, 95% for the $e\mu$ channel, and 98% for the ee channel.

The lepton-jet pair from each \tilde{t} decay generally reconstructs the invariant mass $m_{b\ell}$ of the original \tilde{t} . In an event with two leptons and two jets, two pairings are possible; one that reconstructs the correct \tilde{t} masses, and one which inverts the pairing and incorrectly reconstructs the masses. As the two masses should be roughly equal, the pairing that minimizes the mass asymmetry between $m_{b\ell}^0$ and $m_{b\ell}^1$ is chosen, defined as

$$m_{b\ell}^{\text{asym}} = \frac{m_{b\ell}^0 - m_{b\ell}^1}{m_{b\ell}^0 + m_{b\ell}^1}.$$

Here $m_{b\ell}^0$ is chosen to be the larger of the two masses. Events are further selected to have small mass asymmetry $m_{b\ell}^{\text{asym}} < 0.2$. This reduces the contamination from background processes, whose random pairings lead to a more uniform $m_{b\ell}^{\text{asym}}$ distribution.

Two nested signal regions (SRs) are constructed to optimize the identification of signal over background events. The signal regions are optimized using MC signal and background predictions, assuming \tilde{t} decays of $\mathcal{B}(\tilde{t} \rightarrow b\ell) = \mathcal{B}(\tilde{t} \rightarrow b\mu) = 50\%$. A primary kinematic selection of the signal regions is on $m_{b\ell}^0$, with SR800 requiring $m_{b\ell}^0 > 800$ GeV and SR1100 requiring $m_{b\ell}^0 > 1100$ GeV. By defining two signal regions the sensitivity to high-mass signals above 1100 GeV is improved, while maintaining sensitivity to lower-mass signals. Several other kinematic selections, common to both SRs, are defined to reduce the contribution from the largest backgrounds. As the \tilde{t} decay products are generally very energetic, a selection on their p_T sum,

$$H_T = \sum_{i=1}^2 p_T^{\ell_i} + \sum_{j=1}^2 p_T^{\text{jet}_j}$$

is applied, such that $H_T > 1000$ GeV. To reduce contamination from $Z + \text{jets}$ events, a requirement is placed on the invariant mass of two same-flavor leptons, with $m_{\ell\ell} > 300$ GeV. A large fraction of the background from processes involving a top quark is suppressed through the requirement on $m_{b\ell}^0$ and $m_{b\ell}^{\text{asym}}$, with correctly reconstructed top quark masses falling well below the signal region requirements. However, top quark decays in which the lepton and b -jet decay products are mispaired can enter the SRs if the incorrectly reconstructed masses happen to be large. In such cases it is the rejected pairing that properly reconstructs the top quark decay, with one of the two $b\ell$

pair masses below the kinematic limit for a top quark decay. To suppress such backgrounds, events are rejected if the subleading $b\ell$ mass of the rejected pairing, $m_{b\ell}^1(\text{rej})$, is compatible with that of a reconstructed top quark, with $m_{b\ell}^1(\text{rej}) < 150$ GeV.

The distribution of predicted signal and background events is shown for the SR800 region in Fig. 2 for $m_{b\ell}^0$, H_T , $m_{b\ell}^{\text{asym}}$, $m_{\ell\ell}$, and $m_{b\ell}^1(\text{rej})$, demonstrating the potential for background rejection. For the model with a \tilde{t} mass of 1000 GeV (1500 GeV), the SR800 selections are 21% (24%) efficient for events with two $\tilde{t} \rightarrow b\ell$ decays, 16% (16%) for events with two $\tilde{t} \rightarrow b\mu$ decays, and 0.1% (0.3%) for events with two $\tilde{t} \rightarrow b\tau$ decays.

VI. BACKGROUND ESTIMATION

For each of the relevant backgrounds in the signal regions, one of two methods is used to estimate the contribution. The minor backgrounds from diboson, $t\bar{t} + V$, and $W + \text{jets}$ processes are estimated directly from MC simulation and the normalization is corrected to the highest-order theoretical cross section available. For the dominant $t\bar{t}$, single-top, and $Z + \text{jets}$ backgrounds, the expected yield in the SRs is estimated by scaling each MC prediction by a normalization factor (NF) derived from three dedicated control regions (CRs), one for each background process. Each control region is defined to be kinematically close to the SRs while inverting or relaxing specific selections to enhance the contribution from the targeted background process while reducing the contamination from other backgrounds and the benchmark signals.

To derive a background-only estimate, the normalizations of the $t\bar{t}$, single-top, and $Z + \text{jets}$ backgrounds are determined through a likelihood fit [78] performed simultaneously to the observed number of events in each CR. The expected yield in each region is given by the inclusive sum over all background processes in the ee , $e\mu$, and $\mu\mu$ channels. The NF for each of the $t\bar{t}$, single-top, and $Z + \text{jets}$ backgrounds are free parameters of the fit. The systematic uncertainties are treated as nuisance parameters in the fit and are not significantly constrained.

Several validation regions (VRs) are defined to test the extrapolation from the CRs to SRs over the relevant kinematic variables. The VRs are disjoint from both the CRs and SRs, and are constructed to fall between one or more CRs and the SRs in one of the extrapolated variables. The VRs are not included in the fit, but provide a statistically independent cross-check of the background prediction in regions with a negligible signal contamination. Three VRs are constructed to test the extrapolation in the $m_{b\ell}^0$, $m_{b\ell}^1(\text{rej})$, and H_T observables. A fourth VR is constructed to validate the extrapolation of the $Z + \text{jets}$ CR in $m_{\ell\ell}$. Details of the selection criteria in each CR and VR are presented below, and a summary of the selections is provided in Table II.

TABLE II. Summary of the selections of the signal, control, and validation regions. All regions require at least two oppositely charged leptons and at least two jets. Each region requires at least one of the two leading jets to be b -tagged with the exception of CRst, which requires both leading jets to be b -tagged, and VRZ, which requires zero b -tagged jets in the event. A mass asymmetry selection of $m_{b\ell}^{\text{asym}} < 0.2$ is applied to all regions. The contranverse mass selection m_{CT} [Eq. (1)] is only applied to events in CRtt with exactly two b -tagged jets, as indicated by the *, ensuring the region is orthogonal to CRst.

Region	N_b	$m_{b\ell}^0$ [GeV]	H_T [GeV]	$m_{b\ell}^1(\text{rej})$ [GeV]	$m_{\ell\ell}$ [GeV]	m_{CT} [GeV]
SR800	≥ 1	> 800	> 1000	> 150	> 300	...
SR1100	≥ 1	> 1100	> 1000	> 150	> 300	...
CRst	$= 2$	[200,500]	< 800	< 150	> 120	> 200
CRtt	≥ 1	[200,500]	[600,800]	< 150	> 300	$< 200^*$
CRZ	≥ 1	> 700	> 1000	...	[76.2,106.2]	...
$\text{VR}m_{b\ell}^0$	≥ 1	> 500	[600,800]	< 150	> 300	...
$\text{VR}m_{b\ell}^1(\text{rej})$	≥ 1	[200,500]	[600,800]	> 150	> 300	...
$\text{VR}H_T$	≥ 1	[200,500]	> 800	< 150	> 300	...
VRZ	$= 0$	[500,800]	> 1000	> 150	> 300	...

A. Single-top control region

The single-top background enters the SR through the Wt process, when the b -jet and lepton produced in the semi-leptonic top quark decay are incorrectly paired with the lepton from the W decay and an additional jet, respectively. The CRst control region is designed to target the Wt production in a less-energetic kinematic region or where the rejected $b\ell$ pairing correctly combines the decay products of the top quark. To separate CRst from the SRs, the H_T and $m_{b\ell}^0$ requirements are reversed such that $H_T < 800$ GeV and $200 < m_{b\ell}^0 < 500$ GeV. To target events in which the top quark is reconstructed in the rejected $b\ell$ pairing, the selection on $m_{b\ell}^1(\text{rej})$ is reversed, requiring $m_{b\ell}^1(\text{rej}) < 150$ GeV. As there is no dilepton resonance in this background process the $m_{\ell\ell}$ selection is lowered to increase the CRst yield and improve the statistical precision of the constraint.

After these selections the control region is dominated by $t\bar{t}$ production, which has a significantly higher cross section than the Wt process. The contranverse mass (m_{CT}) [79] is introduced to discriminate between Wt and $t\bar{t}$ events and increase the Wt purity in the CRst. The m_{CT} observable attempts to reconstruct the invariant mass of pair-produced particles which decay into visible and invisible decay products. For two identical decays of top quarks into two visible b -quarks b_1 and b_2 , and two W bosons, each of whose decay products may include an invisible particle, m_{CT} is defined as

$$m_{\text{CT}}^2(b_1, b_2) = [E_T(b_1) + E_T(b_2)]^2 - [\mathbf{p}_T(b_1) - \mathbf{p}_T(b_2)]^2, \quad (1)$$

where $E_T = \sqrt{p_T^2 + m^2}$ is calculated from the kinematics of the reconstructed b -jet. For an event with two top quarks, the m_{CT} observable therefore has a kinematic endpoint at

$$m_{\text{CT}}^{\text{max}} = \frac{m_t^2 - m_W^2}{m_t},$$

where m_t and m_W are the masses of the top quark and W boson, respectively. Requiring this variable to exceed a minimum value is effective in suppressing the $t\bar{t}$ contribution, for which m_{CT} has a kinematic endpoint of about 135 GeV, and a strict requirement of $m_{\text{CT}} > 200$ GeV is applied in CRst. The m_{CT} variable is only effective in rejecting $t\bar{t}$ events in which the b -quark decay products of both top quarks are properly identified, and both leading jets (and only the leading jets) are required to be b -tagged in CRst, such that $N_b = 2$. The m_{CT} distribution of the backgrounds in CRst is shown in Fig. 3(a) when no m_{CT} requirement is applied, and a significant single-top contribution above 55% is seen for $m_{\text{CT}} > 200$ GeV.

B. $t\bar{t}$ control region

The CRtt control region is constructed to target $t\bar{t}$ events with kinematics similar to the SRs. As with CRst, the H_T and $m_{b\ell}^0$ requirements are inverted such that $600 < H_T < 800$ GeV and $200 < m_{b\ell}^0 < 500$ GeV. The selection on $m_{b\ell}^1(\text{rej})$ is also inverted, requiring $m_{b\ell}^1(\text{rej}) < 150$ GeV, such that one of the two top quarks is reconstructed in the rejected $b\ell$ pairings. The distribution of $m_{b\ell}^1(\text{rej})$ in CRtt is shown in Fig. 3(b), showing the mispairing of $t\bar{t}$ events is well modeled in MC simulation. Due to the larger cross section of the $t\bar{t}$ process, contamination from Wt events is minimal. However, to maintain orthogonality with CRst, a requirement of $m_{\text{CT}} < 200$ GeV is applied to events in which both leading jets (and only the leading jets) are b -tagged, with $N_b = 2$.

C. Z + jets control region

The CRZ control region targets Z + jets events by applying a selection on the invariant mass of the dilepton

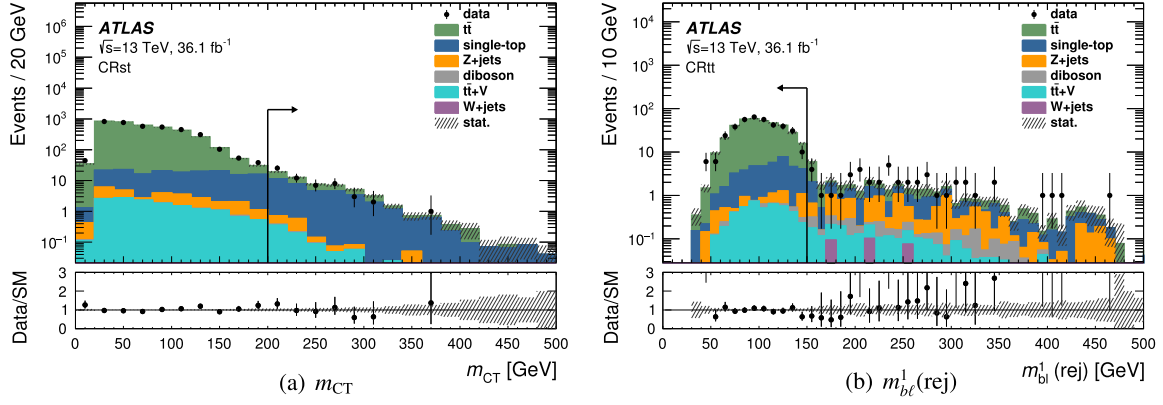


FIG. 3. Distributions of (a) m_{CT} in CRst and (b) $m_{b\ell}^1(\text{rej})$ in CRtt for the data and postfit MC prediction. The relevant CR event selections are applied for each distribution except the selection on the variable shown, which is indicated by an arrow. Normalization factors are derived from the background-only fit configuration and are applied to the dominant $t\bar{t}$, single-top, and $Z + \text{jets}$ processes. The bottom panel shows the ratio between the data and the post-fit MC prediction. The hatched uncertainty band includes the statistical uncertainties in the background prediction. The last bin includes the overflow events.

pair $m_{\ell\ell}$, requiring it to be within 15 GeV of the Z mass. Both leptons are required to be of the same flavor. The $m_{\ell\ell}$ selection is effective in removing signal contamination, and the SR H_T selection is left unchanged, while the $m_{b\ell}^0$ selection is slightly relaxed to $m_{b\ell}^0 > 700$ GeV to enhance the event yield.

D. Validation regions

Four disjoint validation regions are used to test the extrapolation of the background fit from the CRs to the SRs. A full list of the region selections is given in Table II. The $VRm_{b\ell}^0$, $VRm_{b\ell}^1(\text{rej})$, and VRH_T test the extrapolation from CRst and CRtt to the SRs in the $m_{b\ell}^0$, $m_{b\ell}^1(\text{rej})$, and H_T observables by requiring $m_{b\ell}^0 > 500$ GeV, $m_{b\ell}^1(\text{rej}) > 150$ GeV, and $H_T > 800$ GeV, respectively. In this way

$VRm_{b\ell}^0$, $VRm_{b\ell}^1(\text{rej})$, and VRH_T all lie between the SRs and both CRtt and CRst, with signal contamination below 1% for all signal mass values. No requirement is placed on m_{CT} in any VR, allowing both the $t\bar{t}$ and Wt contributions to be validated.

A fourth validation region, VRZ, is used to test the extrapolation from CRZ to the SRs in the $m_{\ell\ell}$ observable, requiring $m_{\ell\ell} > 300$ GeV. As the $m_{\ell\ell}$ variable provides the only separation between CRZ and the SRs, the requirement on $m_{b\ell}^0$ is relaxed to $500 < m_{b\ell}^0 < 800$ GeV, and any event with a b -tagged jet is rejected, such that $N_b = 0$. The $Z + \text{jets}$ MC prediction is found to model the data well in both $m_{b\ell}$ and N_b , with a signal contamination in VRZ below 5% for mass values above 1000 GeV.

The observed data yield and the postfit background prediction for each CR and VR are shown in Fig. 4. Good agreement is seen in all validation regions, with differences between the data and SM prediction below 1σ . The modeling of the extrapolated variable for each VR is shown in Fig. 5, demonstrating good agreement in the shape of the variables of interest.

VII. SYSTEMATIC UNCERTAINTIES

Systematic uncertainties in the signal and background predictions arise from theoretical uncertainties in the expected yield and MC modeling, and from experimental sources. The dominant uncertainties are summarized in Table III.

Experimental uncertainties reflect the precision of the energy and momentum calibration of jets and leptons, as well as the assumptions about the identification and reconstruction efficiencies in MC simulation. The dominant experimental uncertainties are related to jets, including those in the jet energy scale and resolution [80,81] and the calibration of the b -tagging efficiency for b -jets, c -jets, and

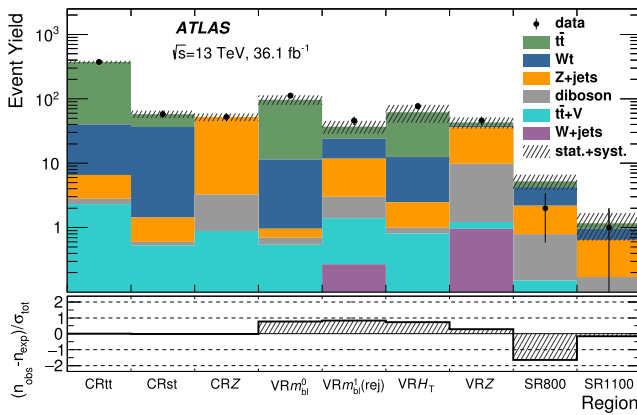


FIG. 4. Comparison of the observed data and expected numbers of events in the CRs, VRs, and SRs. The background prediction is derived with the background-only fit configuration, and the hatched band includes the total uncertainty in the background prediction. The bottom panel shows the significance of the difference between data and the background prediction.

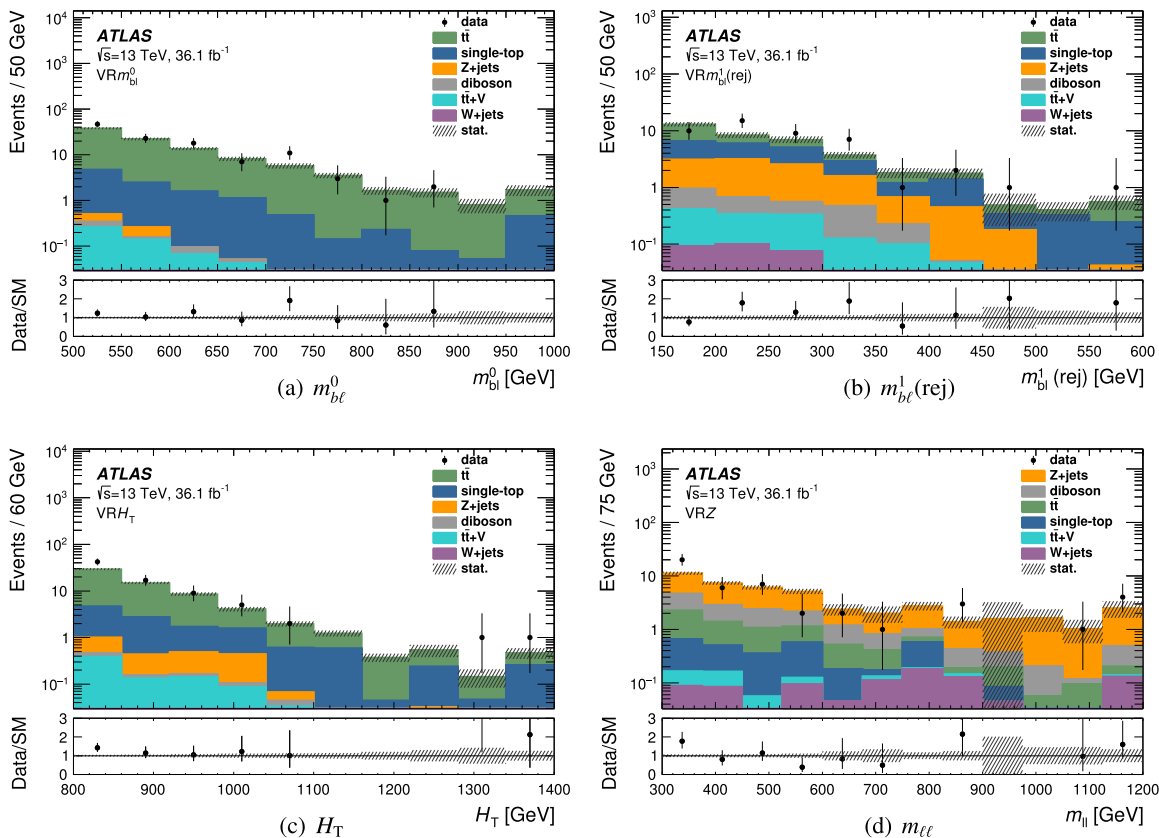


FIG. 5. Distributions of (a) $m_{b\ell}^0$ in $VRm_{b\ell}^0$, (b) $m_{b\ell}^1(\text{rej})$ in $VRm_{b\ell}^1(\text{rej})$ for the data and postfit MC prediction, (c) H_T in VRH_T , and (d) $m_{\ell\ell}$ in VRZ . Normalization factors are derived from the background-only fit configuration and are applied to the dominant $t\bar{t}$, single-top, and $Z + \text{jets}$ processes. The bottom panel shows the ratio between the data and the postfit MC prediction. The hatched uncertainty band includes the statistical uncertainties in the background prediction. The last bin includes the overflow events.

TABLE III. Summary of the dominant experimental and theoretical uncertainties in SR800 and SR1100 before the likelihood fits, quoted relative to the total prefit MC background predictions. The individual uncertainties can be correlated, and do not necessarily add in quadrature to the total postfit background uncertainty.

Source \ Region	SR800	SR1100
Experimental uncertainty		
b -tagging	3%	5%
Jet energy resolution	2%	10%
Jet energy scale	1%	3%
Electrons	1%	4%
Muons	1%	3%
Theoretical modeling uncertainty		
MC statistical uncertainty	8%	17%
$t\bar{t}$	8%	45%
Single-top	21%	22%
$Z + \text{jets}$	2%	4%
Diboson	4%	3%
$t\bar{t} + W/Z$	1%	1%
$W + \text{jets}$	1%	1%

light-flavor jets [77]. The largest experimental uncertainties in the fitted background prediction in SR800 (SR1100) are from the b -tagging efficiency of light-flavor jets and the jet energy resolution. The experimental uncertainties associated with leptons each have a small impact on the final measurement, and include uncertainties in the energy scale and resolution of electrons [67] and muons [68], and the calibration of the lepton trigger, identification, reconstruction, and isolation efficiencies. The 3.2% uncertainty in the measured integrated luminosity also has a marginal effect on the final result.

Theoretical and MC modeling uncertainties of the $t\bar{t}$ and Wt backgrounds account for the choice of event generator, underlying-event tune, and their parameters. The uncertainties are derived separately for each background process and are treated as uncorrelated nuisance parameters. As the $t\bar{t}$ (Wt) background normalization is constrained in the likelihood fits, the uncertainties are derived on the transfer of the NF from the CRtt (CRst) to both SR800 and SR1100 by comparing CR-to-SR yield ratios in alternative models. The uncertainty in the background estimate due to the choice of MC event generator is estimated for $t\bar{t}$ and Wt by

comparing the CR-to-SR yield ratios derived using MG5_AMC@NLO 2.2.3 with the one derived using POWHEG-BOX v2, both showered with Herwig++ v2.7.1 [82] using the UEEE5 UE tune [83]. The generator uncertainties are found to be conservative due to the limited statistical precision of the MG5_AMC@NLO samples. The hadronization and fragmentation modeling uncertainty is similarly estimated in both $t\bar{t}$ and Wt by comparing the nominal POWHEG + PYTHIA sample with the same POWHEG + HERWIG sample. The uncertainty due to the choice of parameters in the POWHEG + PYTHIA generator and P2012 underlying-event tune are derived by varying the parameters related to the amount of initial- and final-state radiation, the factorization and renormalization scales, and (for $t\bar{t}$ only) the p_T of the first additional emission beyond the Born level [37]. An uncertainty in the single-top yield due to the destructive interference between the $t\bar{t}$ and Wt processes is estimated by using inclusively generated $WWbb$ events in a comparison with the combined yield of $t\bar{t}$ and Wt samples, all generated at LO with MG5_AMC@NLO 2.5.5.

The theoretical uncertainties of the Z + jets, diboson, and $t\bar{t} + V$ samples are estimated by varying event generator parameters related to the factorization, renormalization, resummation, and CKKW matching scales. The envelope of these variations is taken as the theoretical uncertainty in the predicted yield in each SR. As the diboson and $t\bar{t} + V$ samples are not normalized in the CRs, the uncertainty in the theoretical cross section is also

included. The uncertainty in the NLO cross section is taken to be 6% for the diboson process [84] and 13% for the $t\bar{t} + V$ process [51]. A 50% uncertainty is applied to the small W + jets yield in both SRs.

The stop signal model uncertainties are dominated by the cross-section uncertainty, derived from the envelope of cross-section predictions from several distinct PDF sets and varying the factorization and renormalization scales, as described in Ref. [36]. The uncertainty in the cross section varies from 13% for the 600 GeV mass value to 27% for the 1600 GeV mass value. The electron efficiency uncertainties are between 3% and 4% for the various stop masses when assuming $\mathcal{B}(\tilde{t} \rightarrow be) = \mathcal{B}(\tilde{t} \rightarrow b\mu) = 50\%$, and are between 5% and 8% when assuming $\mathcal{B}(\tilde{t} \rightarrow be) = 100\%$. Similarly, the muon efficiency uncertainties are between 2% and 4% when assuming $\mathcal{B}(\tilde{t} \rightarrow be) = \mathcal{B}(\tilde{t} \rightarrow b\mu) = 50\%$, and rise to 6% when assuming $\mathcal{B}(\tilde{t} \rightarrow b\mu) = 100\%$. The electron, muon, and jet energy scale and resolution uncertainties are generally below 1% for the stop signal models, reaching 1% for masses near the $m_{b\ell}$ threshold of 800 GeV for SR800 and 1100 GeV for SR1100. The b -tagging efficiency uncertainties are between 1% and 3%, reaching the largest value for the 600 GeV signal model.

VIII. RESULTS

The observed yields and fitted background predictions in SR800 and SR1100 are shown in Table IV. One event is

TABLE IV. The observed and total postfit expected background yields in SR800 and SR1100. Both the MC background expectation before the fit and the background-only postfit yields are shown, with each broken down into single-top, Z + jets, $t\bar{t}$, diboson, $t\bar{t} + V$ and W + jets background processes. Model-independent upper limits are set at a 95% C.L. on the visible number of expected (S_{exp}^{95}) and observed (S_{obs}^{95}) events and on the visible cross section (σ_{vis}) of a generic BSM process. Results are shown in each flavor channel and inclusively. The background estimates and their uncertainties are derived from a background-only fit configuration.

	SR800				SR1100			
	inclusive	ee	$e\mu$	$\mu\mu$	inclusive	ee	$e\mu$	$\mu\mu$
Observed yield	2	0	0	2	1	0	0	1
Total postfit bkg yield	5.2 ± 1.4	1.8 ± 0.5	2.1 ± 0.8	1.35 ± 0.32	$1.2^{+0.6}_{-0.5}$	$0.51^{+0.22}_{-0.20}$	$0.44^{+0.39}_{-0.33}$	0.22 ± 0.13
Postfit single-top yield	2.0 ± 1.3	0.6 ± 0.4	1.1 ± 0.7	0.32 ± 0.20	0.32 ± 0.29	0.11 ± 0.10	0.21 ± 0.19	...
Postfit Z + jets yield	1.40 ± 0.33	0.80 ± 0.24	0.01 ± 0.01	0.59 ± 0.14	0.47 ± 0.15	0.28 ± 0.10	...	0.19 ± 0.11
Postfit $t\bar{t}$ yield	1.0 ± 0.5	0.27 ± 0.14	0.54 ± 0.25	0.21 ± 0.10	$0.21^{+0.55}_{-0.21}$	$0.06^{+0.16}_{-0.06}$	$0.13^{+0.34}_{-0.13}$	$0.01^{+0.03}_{-0.01}$
Postfit diboson yield	0.64 ± 0.23	0.14 ± 0.05	0.31 ± 0.12	0.19 ± 0.08	0.13 ± 0.05	0.06 ± 0.03	0.07 ± 0.03	0.01 ± 0.01
Postfit $t\bar{t} + V$ yield	0.12 ± 0.03	0.01 ± 0.01	0.07 ± 0.02	0.04 ± 0.02	0.03 ± 0.01	...	0.01 ± 0.01	0.01 ± 0.01
Postfit W + jets yield	0.03 ± 0.03	...	0.04 ± 0.04	...	$0.01^{+0.02}_{-0.01}$...	$0.01^{+0.02}_{-0.01}$...
Total MC bkg yield	4.9 ± 1.2	1.7 ± 0.4	2.0 ± 0.7	1.23 ± 0.28	$1.1^{+0.6}_{-0.5}$	$0.46^{+0.21}_{-0.19}$	$0.43^{+0.40}_{-0.33}$	0.18 ± 0.10
MC single-top yield	1.9 ± 1.0	0.57 ± 0.34	1.0 ± 0.6	0.29 ± 0.17	0.29 ± 0.25	0.10 ± 0.08	0.19 ± 0.17	...
MC Z + jets yield	1.15 ± 0.21	0.65 ± 0.17	0.01 ± 0.01	0.48 ± 0.09	0.38 ± 0.10	0.23 ± 0.07	...	0.15 ± 0.09
MC $t\bar{t}$ yield	1.1 ± 0.5	0.29 ± 0.14	0.57 ± 0.26	0.22 ± 0.10	$0.22^{+0.57}_{-0.22}$	$0.07^{+0.18}_{-0.07}$	$0.14^{+0.36}_{-0.14}$	$0.01^{+0.03}_{-0.01}$
MC diboson yield	0.64 ± 0.23	0.14 ± 0.05	0.31 ± 0.12	0.19 ± 0.08	0.13 ± 0.05	0.06 ± 0.03	0.07 ± 0.03	0.01 ± 0.01
MC $t\bar{t} + V$ yield	0.12 ± 0.03	0.01 ± 0.01	0.07 ± 0.02	0.04 ± 0.02	0.03 ± 0.01	...	0.01 ± 0.01	0.01 ± 0.01
MC W + jets yield	0.03 ± 0.03	...	0.04 ± 0.04	...	$0.01^{+0.02}_{-0.01}$...	$0.01^{+0.02}_{-0.01}$...
S_{exp}^{95}	$6.4^{+3.0}_{-1.9}$	$4.1^{+1.8}_{-1.1}$	$4.0^{+2.2}_{-0.9}$	$3.9^{+1.6}_{-0.7}$	$3.9^{+2.4}_{-0.5}$	$3.0^{+1.3}_{-0.0}$	$3.0^{+1.3}_{-0.0}$	$3.1^{+0.6}_{-0.1}$
S_{obs}^{95}	4.0	3.0	3.0	4.8	3.9	3.0	3.1	4.1
σ_{vis} [fb]	0.11	0.08	0.08	0.13	0.11	0.08	0.08	0.11

observed in SR1100 and two are observed in SR800, in agreement with the SM prediction. The SR1100 event is included in SR800 by definition, and both events are found in the $\mu\mu$ channel. The SR1100 event has a high H_T due to a high- p_T muon with a large p_T uncertainty. The observed and predicted $m_{b\ell}^0$, H_T , $m_{b\ell}^{\text{asym}}$, $m_{\ell\ell}$, and $m_{b\ell}^1(\text{rej})$ distributions in SR800 are shown in Fig. 2.

For each SR, model-independent upper limits are derived on the visible cross section of potential BSM processes at a 95% confidence level (C.L.). A likelihood fit is performed to the number of observed events in all three CRs and the target SR, and a generic BSM process is assumed to contribute to the SR only. No theoretical or systematic uncertainties are considered for the signal model except the luminosity uncertainty. The observed (S_{obs}^{95}) and expected (S_{exp}^{95}) limits on the number of BSM events are derived at 95% C.L. in each flavor channel and inclusively, and are shown in the lower rows of Table IV. Also shown are the observed limits on the visible cross section σ_{vis} , defined as

S_{obs}^{95} normalized to the integrated luminosity, and representing the product of the production cross section, acceptance, and selection efficiency of a generic BSM signal. Limits on σ_{vis} are set between 0.08 and 0.13 fb, with the weaker limit set in the $\mu\mu$ channel due to the two observed events.

Exclusion limits are derived at 95% C.L. for the \tilde{t} signal samples. Limits are obtained through a profile log-likelihood ratio test using the CL_s prescription [85], following the simultaneous fit to the CRs and a target SR [78]. The signal contributions in both the SR and CRs are accounted for in the fit, although they are negligible in the latter. Exclusion fits are performed separately for various branching ratio assumptions, sampling values of $\mathcal{B}(\tilde{t} \rightarrow be)$, $\mathcal{B}(\tilde{t} \rightarrow b\mu)$, and $\mathcal{B}(\tilde{t} \rightarrow b\tau)$ whose sum is unity in steps of 5%, and reweighting events in the signal samples according to the generated decays. For both SR800 and SR1100, limits are derived in the ee , $e\mu$, $\mu\mu$, and inclusive channels. Observed limits are reported for the SR and channel combination with the lowest expected

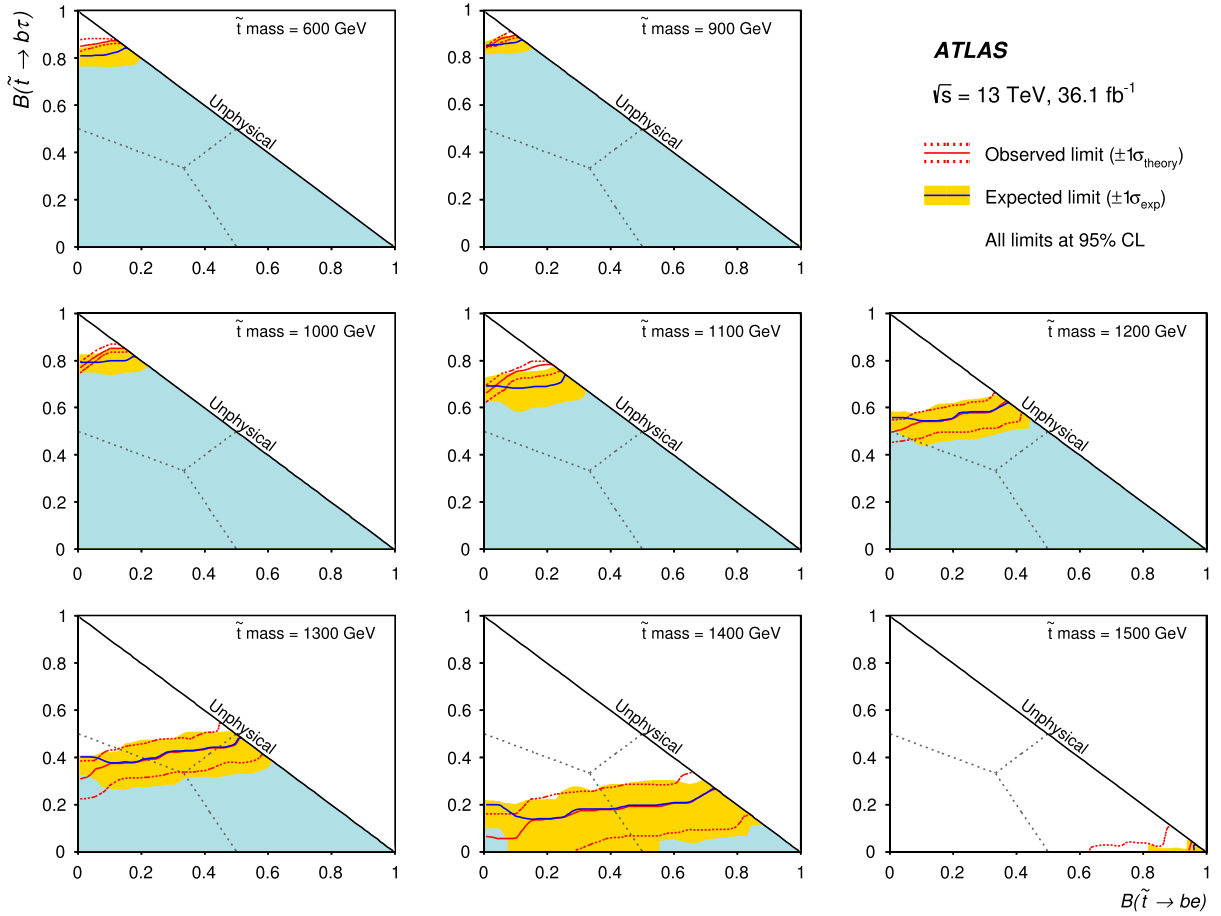


FIG. 6. Expected (dashed blue line) and observed (solid red line) limit curves as a function of \tilde{t} branching ratios for various mass values between 600 and 1500 GeV. The sum of $\mathcal{B}(\tilde{t} \rightarrow be)$, $\mathcal{B}(\tilde{t} \rightarrow b\mu)$, and $\mathcal{B}(\tilde{t} \rightarrow b\tau)$ is assumed to be unity everywhere, and points of equality are marked by a dotted gray line. The yellow band reflects the $\pm 1\sigma$ uncertainty of the expected limit due to theoretical, experimental, and MC statistical uncertainties. The shaded blue area represents the branching ratios that are expected to be excluded beyond 1σ . The dotted red lines correspond to the $\pm 1\sigma$ cross section uncertainty of the observed limit derived by varying the signal cross section by the theoretical uncertainties.

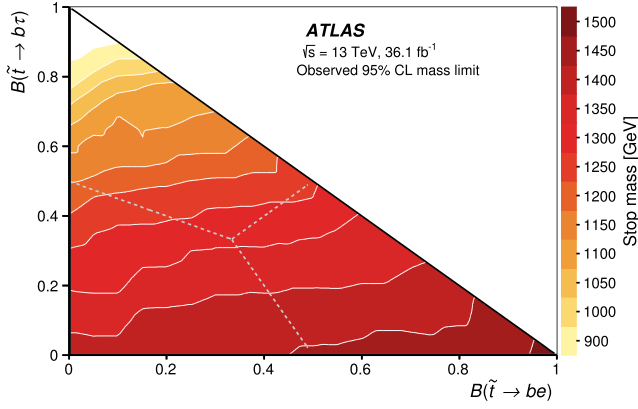


FIG. 7. The observed lower limits on the \tilde{t} mass at 95% C.L. as a function of \tilde{t} branching ratios. The sum of $\mathcal{B}(\tilde{t} \rightarrow be)$, $\mathcal{B}(\tilde{t} \rightarrow b\mu)$, and $\mathcal{B}(\tilde{t} \rightarrow b\tau)$ is assumed to be unity everywhere, and points of equality are marked by a dotted gray line. The limits are obtained using the nominal \tilde{t} cross-section predictions. As the branching ratio $\mathcal{B}(\tilde{t} \rightarrow b\tau)$ increases, the expected number of events with electrons or muons in the final state decreases, reducing the mass reach of the exclusion.

CL_s value, and therefore best expected sensitivity, at a given mass value and branching ratio. The inclusive channel typically has the stronger expected sensitivity when $\mathcal{B}(\tilde{t} \rightarrow be)$ and $\mathcal{B}(\tilde{t} \rightarrow b\mu)$ are both above 15%, while the ee ($\mu\mu$) channel is more sensitive when $\mathcal{B}(\tilde{t} \rightarrow b\mu)$ ($\mathcal{B}(\tilde{t} \rightarrow be)$) is below 15%. The inclusive channel is always more sensitive than the $e\mu$ channel because a substantial fraction of signal events has two leptons of the same flavor, regardless of individual branching ratios.

The expected and observed exclusion contours for the branching ratios are shown in Fig. 6 for each simulated \tilde{t} mass. The limits are strongest at low values of $\mathcal{B}(\tilde{t} \rightarrow b\tau)$, where the expected number of events with electrons or muons in the final state is largest. Expected limits are slightly stronger for increasing $\mathcal{B}(\tilde{t} \rightarrow be)$, reflecting a higher trigger efficiency for electrons than for muons. Stops with $\mathcal{B}(\tilde{t} \rightarrow b\tau)$ up to 80% or more are excluded for masses between 600 and 1000 GeV, while those with larger $\mathcal{B}(\tilde{t} \rightarrow be)$ or $\mathcal{B}(\tilde{t} \rightarrow b\mu)$ may be excluded up to 1500 GeV. Observed limits are stronger than expected for \tilde{t} masses of 1100 GeV or below, reflecting the lower-than-expected event yield in SR800 in the ee channel and inclusively. Exclusion contours reflecting the highest \tilde{t} mass excluded at a 95% C.L. for a given point in the branching ratio plane are shown in Fig. 7.

IX. CONCLUSIONS

This paper presents the first ATLAS results on the search for the pair production of stops, each decaying via an R -parity-violating coupling to a b -quark and a lepton. The final state requires two jets, at least one of which is

b -tagged, and two light, oppositely charged leptons (electron or muon). The search uses 36.1 fb^{-1} of $\sqrt{s} = 13 \text{ TeV}$ proton-proton collision data collected with the ATLAS detector at the LHC in 2015 and 2016. No significant excess of events over the Standard Model prediction is observed, and limits are set on the \tilde{t} mass at a 95% confidence level. These results significantly extend the lower-mass exclusion limits on the $B-L$ stop model from reinterpretations of Run 1 leptoquark searches. Model-independent upper limits are set on the cross section of potential BSM processes in the ee , $e\mu$, and $\mu\mu$ channels and inclusively. A scan of various \tilde{t} branching ratios is performed to set branching-ratio-dependent limits on decays to be , $b\mu$, and $b\tau$ for various \tilde{t} mass models. Limits are set on \tilde{t} masses between 600 GeV for large $b\tau$ decay branching ratios and 1500 GeV for a be branching ratio of 100%.

ACKNOWLEDGMENTS

We thank CERN for the very successful operation of the LHC, as well as the support staff from our institutions without whom ATLAS could not be operated efficiently. We acknowledge the support of ANPCyT, Argentina; YerPhI, Armenia; ARC, Australia; BMWFW and FWF, Austria; ANAS, Azerbaijan; SSTC, Belarus; CNPq and FAPESP, Brazil; NSERC, NRC and CFI, Canada; CERN; CONICYT, Chile; CAS, MOST and NSFC, China; COLCIENCIAS, Colombia; MSMT CR, MPO CR and VSC CR, Czech Republic; DNRF and DNSRC, Denmark; IN2P3-CNRS, CEA-DRF/IRFU, France; SRNSF, Georgia; BMBF, HGF, and MPG, Germany; GSRT, Greece; RGC, Hong Kong SAR, China; ISF, I-CORE and Benozziyo Center, Israel; INFN, Italy; MEXT and JSPS, Japan; CNRST, Morocco; NWO, Netherlands; RCN, Norway; MNiSW and NCN, Poland; FCT, Portugal; MNE/IFA, Romania; MES of Russia and NRC KI, Russian Federation; JINR; MESTD, Serbia; MSSR, Slovakia; ARRS and MIZŠ, Slovenia; DST/NRF, South Africa; MINECO, Spain; SRC and Wallenberg Foundation, Sweden; SERI, SNSF and Cantons of Bern and Geneva, Switzerland; MOST, Taiwan; TAEK, Turkey; STFC, United Kingdom; DOE and NSF, USA. In addition, individual groups and members have received support from BCKDF, the Canada Council, CANARIE, CRC, Compute Canada, FQRNT, and the Ontario Innovation Trust, Canada; EPLANET, ERC, ERDF, FP7, Horizon 2020 and Marie Skłodowska-Curie Actions, European Union; Investissements d'Avenir Labex and Idex, ANR, Région Auvergne and Fondation Partager le Savoir, France; DFG and AvH Foundation, Germany; Herakleitos, Thales and Aristeia programmes co-financed by EU-ESF and the Greek NSRF; BSF, GIF and Minerva, Israel; BRF, Norway; CERCA Programme Generalitat de Catalunya, Generalitat Valenciana, Spain; the Royal Society and Leverhulme

Trust, United Kingdom. The crucial computing support from all WLCG partners is acknowledged gratefully, in particular from CERN, the ATLAS Tier-1 facilities at TRIUMF (Canada), NDGF (Denmark, Norway, Sweden), CC-IN2P3 (France), KIT/GridKA (Germany),

INFN-CNAF (Italy), NL-T1 (Netherlands), PIC (Spain), ASGC (Taiwan), RAL (UK) and BNL (USA), the Tier-2 facilities worldwide and large non-WLCG resource providers. Major contributors of computing resources are listed in Ref. [86].

-
- [1] Yu. A. Golfand and E. P. Likhtman, Extension of the algebra of Poincare group generators and violation of P invariance, *Pis'ma Zh. Eksp. Teor. Fiz.* **13**, 452 (1971) [*JETP Lett.* **13**, 323 (1971)].
- [2] D. V. Volkov and V. P. Akulov, Is the neutrino a Goldstone particle?, *Phys. Lett.* **46B**, 109 (1973).
- [3] J. Wess and B. Zumino, Supergauge transformations in four-dimensions, *Nucl. Phys.* **B70**, 39 (1974).
- [4] J. Wess and B. Zumino, Supergauge invariant extension of quantum electrodynamics, *Nucl. Phys.* **B78**, 1 (1974).
- [5] S. Ferrara and B. Zumino, Supergauge invariant Yang-Mills theories, *Nucl. Phys.* **B79**, 413 (1974).
- [6] A. Salam and J. A. Strathdee, Supersymmetry and non-Abelian gauges, *Phys. Lett. B* **51**, 353 (1974).
- [7] G. R. Farrar and P. Fayet, Phenomenology of the production, decay, and detection of new hadronic states associated with supersymmetry, *Phys. Lett. B* **76**, 575 (1978).
- [8] J. R. Ellis, J. S. Hagelin, D. V. Nanopoulos, K. A. Olive, and M. Srednicki, Supersymmetric relics from the big bang, *Nucl. Phys.* **B238**, 453 (1984).
- [9] M. Pospelov, Particle Physics Catalysis of Thermal Big Bang Nucleosynthesis, *Phys. Rev. Lett.* **98**, 231301 (2007).
- [10] H. K. Dreiner, An introduction to explicit R-parity violation, *Adv. Ser. Dir. High Energy Phys.* **21**, 565 (2010).
- [11] R. Barbier *et al.*, R-parity violating supersymmetry, *Phys. Rep.* **420**, 1 (2005).
- [12] P. Fileviez Perez and S. Spinner, Supersymmetry at the LHC and the theory of R-parity, *Phys. Lett. B* **728**, 489 (2014).
- [13] D. Restrepo, W. Porod, and J. W. F. Valle, Broken R-parity, stop decays, and neutrino physics, *Phys. Rev. D* **64**, 055011 (2001).
- [14] P. Fileviez Perez and S. Spinner, Spontaneous R-parity breaking and left-right symmetry, *Phys. Lett. B* **673**, 251 (2009).
- [15] V. Barger, P. Fileviez Perez, and S. Spinner, Minimal Gauged $U(1)_{B-L}$ Model with Spontaneous R-Parity Violation, *Phys. Rev. Lett.* **102**, 181802 (2009).
- [16] L. L. Everett, P. Fileviez Perez, and S. Spinner, The right side of TeV scale spontaneous R-parity violation, *Phys. Rev. D* **80**, 055007 (2009).
- [17] V. Braun, Y.-H. He, B. A. Ovrut, and T. Pantev, A heterotic standard model, *Phys. Lett. B* **618**, 252 (2005).
- [18] R. Deen, B. A. Ovrut, and A. Purves, The minimal SUSY $B - L$ model: Simultaneous Wilson lines and string thresholds, *J. High Energy Phys.* **07** (2016) 043.
- [19] R. Barbieri and G. Giudice, Upper bounds on supersymmetric particle masses, *Nucl. Phys.* **B306**, 63 (1988).
- [20] B. de Carlos and J. A. Casas, One loop analysis of the electroweak breaking in supersymmetric models and the fine tuning problem, *Phys. Lett. B* **309**, 320 (1993).
- [21] Z. Marshall, B. A. Ovrut, A. Purves, and S. Spinner, LSP squark decays at the LHC and the neutrino mass hierarchy, *Phys. Rev. D* **90**, 015034 (2014).
- [22] Z. Marshall, B. A. Ovrut, A. Purves, and S. Spinner, Spontaneous R-parity breaking, stop LSP decays and the neutrino mass hierarchy, *Phys. Lett. B* **732**, 325 (2014).
- [23] ATLAS Collaboration, Search for scalar leptoquarks in pp collisions at $\sqrt{s} = 13$ TeV with the ATLAS experiment, *New J. Phys.* **18**, 093016 (2016).
- [24] ATLAS Collaboration, Searches for scalar leptoquarks in pp collisions at $\sqrt{s} = 8$ TeV with the ATLAS detector, *Eur. Phys. J. C* **76**, 5 (2016).
- [25] CMS Collaboration, Search for third-generation scalar leptoquarks and heavy right-handed neutrinos in final states with two tau leptons and two jets in proton-proton collisions at $\sqrt{s} = 13$ TeV, *J. High Energy Phys.* **07** (2017) 121.
- [26] CMS Collaboration, Search for pair production of first and second generation leptoquarks in proton-proton collisions at $\sqrt{s} = 8$ TeV, *Phys. Rev. D* **93**, 032004 (2016).
- [27] ATLAS Collaboration, The ATLAS experiment at the CERN Large Hadron Collider, *J. Instrum.* **3**, S08003 (2008).
- [28] ATLAS Collaboration, Report No. ATLAS-TDR-19, 2010, <https://cds.cern.ch/record/1291633>; Report No. ATLAS-TDR-19-ADD-1, 2012, <https://cds.cern.ch/record/1451888>.
- [29] ATLAS Collaboration, Performance of the ATLAS trigger system in 2015, *Eur. Phys. J. C* **77**, 317 (2017).
- [30] ATLAS Collaboration, Luminosity determination in pp collisions at $\sqrt{s} = 8$ TeV using the ATLAS detector at the LHC, *Eur. Phys. J. C* **76**, 653 (2016).
- [31] M. Czakon and A. Mitov, Top++: A program for the calculation of the top-pair cross-section at hadron colliders, *Comput. Phys. Commun.* **185**, 2930 (2014).
- [32] N. Kidonakis, Two-loop soft anomalous dimensions for single top quark associated production with a W^- or H^- , *Phys. Rev. D* **82**, 054018 (2010).
- [33] N. Kidonakis, NNLL resummation for s-channel single top quark production, *Phys. Rev. D* **81**, 054028 (2010).
- [34] N. Kidonakis, Next-to-next-to-leading-order collinear and soft gluon corrections for t-channel single top quark production, *Phys. Rev. D* **83**, 091503 (2011).
- [35] S. Catani, L. Cieri, G. Ferrera, D. de Florian, and M. Grazzini, Vector Boson Production at Hadron Colliders: A Fully Exclusive QCD Calculation at NNLO, *Phys. Rev. Lett.* **103**, 082001 (2009).

- [36] C. Borschensky, M. Krämer, A. Kulesza, M. Mangano, S. Padhi, T. Plehn, and X. Portell, Squark and gluino production cross sections in pp collisions at $\sqrt{s} = 13, 14, 33$ and 100 TeV, *Eur. Phys. J. C* **74**, 3174 (2014).
- [37] ATLAS Collaboration, Report No. ATL-PHYS-PUB-2016-004, 2016, <https://cds.cern.ch/record/2120417>.
- [38] S. Alioli, P. Nason, C. Oleari, and E. Re, A general framework for implementing NLO calculations in shower Monte Carlo programs: The POWHEG BOX, *J. High Energy Phys.* **06** (2010) 043.
- [39] H.-L. Lai, M. Guzzi, J. Huston, Z. Li, P. M. Nadolsky, J. Pumplin, and C.-P. Yuan, New parton distributions for collider physics, *Phys. Rev. D* **82**, 074024 (2010).
- [40] T. Sjöstrand, S. Mrenna, and P. Z. Skands, PYTHIA 6.4 physics and manual, *J. High Energy Phys.* **05** (2006) 026.
- [41] J. Pumplin, D. R. Stump, J. Huston, H.-L. Lai, P. Nadolsky, and W.-K. Tung, New generation of parton distributions with uncertainties from global QCD analysis, *J. High Energy Phys.* **07** (2002) 012.
- [42] P. Z. Skands, Tuning Monte Carlo generators: The Perugia tunes, *Phys. Rev. D* **82**, 074018 (2010).
- [43] R. Corke and T. Sjöstrand, Improved parton showers at large transverse momenta, *Eur. Phys. J. C* **69**, 1 (2010).
- [44] ATLAS Collaboration, Report No. ATL-PHYS-PUB-2016-003, 2016, <https://cds.cern.ch/record/2120133>.
- [45] T. Gleisberg, S. Höche, F. Krauss, M. Schönherr, S. Schumann, F. Siegert, and J. Winter, Event generation with SHERPA 1.1, *J. High Energy Phys.* **02** (2009) 007.
- [46] T. Gleisberg and S. Hoeche, Comix, A new matrix element generator, *J. High Energy Phys.* **12** (2008) 039.
- [47] F. Cascioli, P. Maierhofer, and S. Pozzorini, Scattering Amplitudes with Open Loops, *Phys. Rev. Lett.* **108**, 111601 (2012).
- [48] S. Schumann and F. Krauss, A parton shower algorithm based on Catani-Seymour dipole factorisation, *J. High Energy Phys.* **03** (2008) 038.
- [49] S. Hoeche, F. Krauss, M. Schonherr, and F. Siegert, QCD matrix elements + parton showers: The NLO case, *J. High Energy Phys.* **04** (2013) 027.
- [50] R. D. Ball *et al.*, Parton distributions for the LHC run II, *J. High Energy Phys.* **04** (2015) 040.
- [51] J. Alwall, R. Frederix, S. Frixione, V. Hirschi, F. Maltoni, O. Mattelaer, H.-S. Shao, T. Stelzer, P. Torrielli, and M. Zaro, The automated computation of tree-level and next-to-leading order differential cross sections, and their matching to parton shower simulations, *J. High Energy Phys.* **07** (2014) 079.
- [52] T. Sjöstrand, S. Mrenna, and P. Z. Skands, A brief introduction to PYTHIA 8.1, *Comput. Phys. Commun.* **178**, 852 (2008).
- [53] L. Lönlblad and S. Prestel, Matching tree-level matrix elements with interleaved showers, *J. High Energy Phys.* **03** (2012) 019.
- [54] ATLAS Collaboration, Report No. ATL-PHYS-PUB-2014-021, 2014, <https://cds.cern.ch/record/1966419>.
- [55] R. D. Ball *et al.*, Parton distributions with LHC data, *Nucl. Phys.* **B867**, 244 (2013).
- [56] M. Krämer *et al.*, Supersymmetry production cross sections in pp collisions at $\sqrt{s} = 7$ TeV, [arXiv:1206.2892](https://arxiv.org/abs/1206.2892).
- [57] W. Beenakker, M. Krämer, T. Plehn, M. Spira, and P. Zerwas, Stop production at hadron colliders, *Nucl. Phys.* **B515**, 3 (1998).
- [58] W. Beenakker, S. Brensing, M. Krämer, A. Kulesza, E. Laenen, and I. Niessen, Supersymmetric top and bottom squark production at hadron colliders, *J. High Energy Phys.* **08** (2010) 098.
- [59] W. Beenakker, S. Brensing, M. Krämer, A. Kulesza, E. Laenen, L. Motyka, and I. Niessen, Squark and gluino hadroproduction, *Int. J. Mod. Phys. A* **26**, 2637 (2011).
- [60] D. J. Lange, The EvtGen particle decay simulation package, *Nucl. Instrum. Methods Phys. Res., Sect. A* **462**, 152 (2001).
- [61] ATLAS Collaboration, The ATLAS simulation infrastructure, *Eur. Phys. J. C* **70**, 823 (2010).
- [62] S. Agostinelli *et al.*, GEANT4: A simulation toolkit, *Nucl. Instrum. Methods Phys. Res., Sect. A* **506**, 250 (2003).
- [63] ATLAS Collaboration, Report No. ATL-PHYS-PUB-2012-003, 2012, <https://cds.cern.ch/record/1474107>.
- [64] A. D. Martin, W. J. Stirling, R. S. Thorne, and G. Watt, Parton distributions for the LHC, *Eur. Phys. J. C* **63**, 189 (2009).
- [65] P. Laycock *et al.*, Report No. ATL-DAPR-PROC-2017-001, CERN, 2017, <https://cds.cern.ch/record/2253427>.
- [66] ATLAS Collaboration, Report No. ATL-PHYS-PUB-2016-015, 2016, <https://cds.cern.ch/record/2203514>.
- [67] ATLAS Collaboration, Report No. ATLAS-CONF-2016-024, 2016, <https://cds.cern.ch/record/2157687>.
- [68] ATLAS Collaboration, Muon reconstruction performance of the ATLAS detector in proton-proton collision data at $\sqrt{s} = 13$ TeV, *Eur. Phys. J. C* **76**, 292 (2016).
- [69] M. Cacciari, G. P. Salam, and G. Soyez, The anti- k_t jet clustering algorithm, *J. High Energy Phys.* **04** (2008) 063.
- [70] M. Cacciari, G. P. Salam, and G. Soyez, FastJet user manual, *Eur. Phys. J. C* **72**, 1896 (2012).
- [71] ATLAS Collaboration, Topological cell clustering in the ATLAS calorimeters and its performance in LHC Run 1, *Eur. Phys. J. C* **77**, 490 (2017).
- [72] ATLAS Collaboration, Performance of pile-up mitigation techniques for jets in pp collisions at $\sqrt{s} = 8$ TeV using the ATLAS detector, *Eur. Phys. J. C* **76**, 581 (2016).
- [73] M. Cacciari and G. P. Salam, Pileup subtraction using jet areas, *Phys. Lett. B* **659**, 119 (2008).
- [74] ATLAS Collaboration, Jet energy scale measurements and their systematic uncertainties in proton-proton collisions at $\sqrt{s} = 13$ TeV with the ATLAS detector, *Phys. Rev. D* **96**, 072002 (2017).
- [75] ATLAS Collaboration, Report No. ATLAS-CONF-2015-029, 2015, <https://cds.cern.ch/record/2037702>.
- [76] ATLAS Collaboration, Performance of b-jet identification in the ATLAS experiment, *J. Instrum.* **11**, P04008 (2016).
- [77] ATLAS Collaboration, Report No. ATL-PHYS-PUB-2016-012, 2016, <https://cds.cern.ch/record/2160731>.
- [78] M. Baak, G. J. Besjes, D. Côté, A. Koutsman, J. Lorenz, and D. Short, HistFitter software framework for statistical data analysis, *Eur. Phys. J. C* **75**, 153 (2015).
- [79] D. R. Tovey, On measuring the masses of pair-produced semi-invisibly decaying particles at hadron colliders, *J. High Energy Phys.* **04** (2008) 034.
- [80] ATLAS Collaboration, Jet energy resolution in proton-proton collisions at $\sqrt{s} = 7$ TeV recorded in 2010

- with the ATLAS detector, *Eur. Phys. J. C* **73**, 2306 (2013).
- [81] ATLAS Collaboration, Report No. ATL-PHYS-PUB-2015-015, 2015, <https://cds.cern.ch/record/2037613>.
- [82] G. Marchesini, B. R. Webber, G. Abbiendi, I. G. Knowles, M. H. Seymour, and L. Stanco, HERWIG: A Monte Carlo event generator for simulating hadron emission reactions with interfering gluons. Version 5.1, April 1991, *Comput. Phys. Commun.* **67**, 465 (1992).
- [83] S. Gieseke, C. Rohr, and A. Siodmok, Colour reconnections in herwig++, *Eur. Phys. J. C* **72**, 2225 (2012).
- [84] ATLAS Collaboration, Report No. ATL-PHYS-PUB-2016-002, 2016, <https://cds.cern.ch/record/2119986>.
- [85] A. L. Read, Presentation of search results: The CL(s) technique, *J. Phys. G* **28**, 2693 (2002).
- [86] ATLAS Collaboration, Report No. ATL-GEN-PUB-2016-002, <https://cds.cern.ch/record/2202407>.

M. Aaboud,^{137d} G. Aad,⁸⁸ B. Abbott,¹¹⁵ O. Abidinov,^{12,†} B. Abeloos,¹¹⁹ S. H. Abidi,¹⁶¹ O. S. AbouZeid,¹³⁹ N. L. Abraham,¹⁵¹ H. Abramowicz,¹⁵⁵ H. Abreu,¹⁵⁴ R. Abreu,¹¹⁸ Y. Abulaiti,^{148a,148b} B. S. Acharya,^{167a,167b,a} S. Adachi,¹⁵⁷ L. Adamczyk,^{41a} J. Adelman,¹¹⁰ M. Adersberger,¹⁰² T. Auyeub,¹³³ A. A. Affolder,¹³⁹ Y. Afik,¹⁵⁴ T. Agatonovic-Jovin,¹⁴ C. Agheorghiesei,^{28c} J. A. Aguilar-Saavedra,^{128a,128f} S. P. Ahlen,²⁴ F. Ahmadov,^{68,b} G. Aielli,^{135a,135b} S. Akatsuka,⁷¹ H. Akerstedt,^{148a,148b} T. P. A. Åkesson,⁸⁴ E. Akilli,⁵² A. V. Akimov,⁹⁸ G. L. Alberghi,^{22a,22b} J. Albert,¹⁷² P. Albicocco,⁵⁰ M. J. Alconada Verzini,⁷⁴ S. C. Alderweireldt,¹⁰⁸ M. Aleksa,³² I. N. Aleksandrov,⁶⁸ C. Alexa,^{28b} G. Alexander,¹⁵⁵ T. Alexopoulos,¹⁰ M. Alhroob,¹¹⁵ B. Ali,¹³⁰ M. Aliev,^{76a,76b} G. Alimonti,^{94a} J. Alison,³³ S. P. Alkire,³⁸ B. M. M. Allbrooke,¹⁵¹ B. W. Allen,¹¹⁸ P. P. Allport,¹⁹ A. Aloisio,^{106a,106b} A. Alonso,³⁹ F. Alonso,⁷⁴ C. Alpigiani,¹⁴⁰ A. A. Alshehri,⁵⁶ M. I. Alstary,⁸⁸ B. Alvarez Gonzalez,³² D. Álvarez Piqueras,¹⁷⁰ M. G. Alviggi,^{106a,106b} B. T. Amadio,¹⁶ Y. Amaral Coutinho,^{26a} C. Amelung,²⁵ D. Amidei,⁹² S. P. Amor Dos Santos,^{128a,128c} S. Amoroso,³² G. Amundsen,²⁵ C. Anastopoulos,¹⁴¹ L. S. Ancu,⁵² N. Andari,¹⁹ T. Andeen,¹¹ C. F. Anders,^{60b} J. K. Anders,⁷⁷ K. J. Anderson,³³ A. Andreazza,^{94a,94b} V. Andrei,^{60a} S. Angelidakis,³⁷ I. Angelozzi,¹⁰⁹ A. Angerami,³⁸ A. V. Anisenkov,^{111,c} N. Anjos,¹³ A. Annovi,^{126a,126b} C. Antel,^{60a} M. Antonelli,⁵⁰ A. Antonov,^{100,†} D. J. Antrim,¹⁶⁶ F. Anulli,^{134a} M. Aoki,⁶⁹ L. Aperio Bella,³² G. Arabidze,⁹³ Y. Arai,⁶⁹ J. P. Araque,^{128a} V. Araujo Ferraz,^{26a} A. T. H. Arce,⁴⁸ R. E. Ardell,⁸⁰ F. A. Arduh,⁷⁴ J-F. Arguin,⁹⁷ S. Argyropoulos,⁶⁶ M. Arik,^{20a} A. J. Armbruster,³² L. J. Armitage,⁷⁹ O. Arnaez,¹⁶¹ H. Arnold,⁵¹ M. Arratia,³⁰ O. Arslan,²³ A. Artamonov,^{99,†} G. Artoni,¹²² S. Artz,⁸⁶ S. Asai,¹⁵⁷ N. Asbah,⁴⁵ A. Ashkenazi,¹⁵⁵ L. Asquith,¹⁵¹ K. Assamagan,²⁷ R. Astalos,^{146a} M. Atkinson,¹⁶⁹ N. B. Atlay,¹⁴³ K. Augsten,¹³⁰ G. Avolio,³² B. Axen,¹⁶ M. K. Ayoub,^{35a} G. Azuelos,^{97,d} A. E. Baas,^{60a} M. J. Baca,¹⁹ H. Bachacou,¹³⁸ K. Bachas,^{76a,76b} M. Backes,¹²² P. Bagnaia,^{134a,134b} M. Bahmani,⁴² H. Bahrasemani,¹⁴⁴ J. T. Baines,¹³³ M. Bajic,³⁹ O. K. Baker,¹⁷⁹ P. J. Bakker,¹⁰⁹ E. M. Baldin,^{111,c} P. Balek,¹⁷⁵ F. Balli,¹³⁸ W. K. Balunas,¹²⁴ E. Banas,⁴² A. Bandyopadhyay,²³ Sw. Banerjee,^{176,e} A. A. E. Bannoura,¹⁷⁸ L. Barak,¹⁵⁵ E. L. Barberio,⁹¹ D. Barberis,^{53a,53b} M. Barbero,⁸⁸ T. Barillari,¹⁰³ M-S Barisits,³² J. T. Barkeloo,¹¹⁸ T. Barklow,¹⁴⁵ N. Barlow,³⁰ S. L. Barnes,^{36c} B. M. Barnett,¹³³ R. M. Barnett,¹⁶ Z. Barnovska-Blenessy,^{36a} A. Baroncelli,^{136a} G. Barone,²⁵ A. J. Barr,¹²² L. Barranco Navarro,¹⁷⁰ F. Barreiro,⁸⁵ J. Barreiro Guimarães da Costa,^{35a} R. Bartoldus,¹⁴⁵ A. E. Barton,⁷⁵ P. Bartos,^{146a} A. Basalaeu,¹²⁵ A. Bassalat,^{119,f} R. L. Bates,⁵⁶ S. J. Batista,¹⁶¹ J. R. Batley,³⁰ M. Battaglia,¹³⁹ M. Bauce,^{134a,134b} F. Bauer,¹³⁸ H. S. Bawa,^{145,g} J. B. Beacham,¹¹³ M. D. Beattie,⁷⁵ T. Beau,⁸³ P. H. Beauchemin,¹⁶⁵ P. Bechtel,²³ H. P. Beck,^{18,h} H. C. Beck,⁵⁷ K. Becker,¹⁶ M. Becker,⁸⁶ C. Becot,¹¹² A. J. Beddall,^{20e} A. Beddall,^{20b} V. A. Bednyakov,⁶⁸ M. Bedognetti,¹⁰⁹ C. P. Bee,¹⁵⁰ T. A. Beermann,³² M. Begalli,^{26a} M. Begel,²⁷ J. K. Behr,⁴⁵ A. S. Bell,⁸¹ G. Bella,¹⁵⁵ L. Bellagamba,^{22a} A. Bellerive,³¹ M. Bellomo,¹⁵⁴ K. Belotskiy,¹⁰⁰ O. Beltramello,³² N. L. Belyaev,¹⁰⁰ O. Benary,^{155,†} D. Bencheikroun,^{137a} M. Bender,¹⁰² N. Benekos,¹⁰ Y. Benhammou,¹⁵⁵ E. Benhar Nocchioli,¹⁷⁹ J. Benitez,⁶⁶ D. P. Benjamin,⁴⁸ M. Benoit,⁵² J. R. Bensinger,²⁵ S. Bentvelsen,¹⁰⁹ L. Beresford,¹²² M. Beretta,⁵⁰ D. Berge,¹⁰⁹ E. Bergeas Kuutmann,¹⁶⁸ N. Berger,⁵ J. Beringer,¹⁶ S. Berlendis,⁵⁸ N. R. Bernard,⁸⁹ G. Bernardi,⁸³ C. Bernius,¹⁴⁵ F. U. Bernlochner,²³ T. Berry,⁸⁰ P. Berta,⁸⁶ C. Bertella,^{35a} G. Bertoli,^{148a,148b} I. A. Bertram,⁷⁵ C. Bertsche,⁴⁵ D. Bertsche,¹¹⁵ G. J. Besjes,³⁹ O. Bessidskaia Bylund,^{148a,148b} M. Bessner,⁴⁵ N. Besson,¹³⁸ A. Bethani,⁸⁷ S. Bethke,¹⁰³ A. Betti,²³ A. J. Bevan,⁷⁹ J. Beyer,¹⁰³ R. M. Bianchi,¹²⁷ O. Biebel,¹⁰² D. Biedermann,¹⁷ R. Bielski,⁸⁷ K. Bierwagen,⁸⁶ N. V. Biesuz,^{126a,126b} M. Biglietti,^{136a} T. R. V. Billoud,⁹⁷ H. Bilokon,⁵⁰ M. Bindi,⁵⁷ A. Bingul,^{20b} C. Bini,^{134a,134b} S. Biondi,^{22a,22b} T. Bisanz,⁵⁷ C. Bittrich,⁴⁷ D. M. Bjergaard,⁴⁸ J. E. Black,¹⁴⁵ K. M. Black,²⁴ R. E. Blair,⁶ T. Blazek,^{146a} I. Bloch,⁴⁵ C. Blocker,²⁵ A. Blue,⁵⁶ W. Blum,^{86,†} U. Blumenschein,⁷⁹ S. Blunier,^{34a} G. J. Bobbink,¹⁰⁹ V. S. Bobrovnikov,^{111,c} S. S. Bocchetta,⁸⁴ A. Bocci,⁴⁸ C. Bock,¹⁰² M. Boehler,⁵¹ D. Boerner,¹⁷⁸ D. Bogavac,¹⁰² A. G. Bogdanchikov,¹¹¹ C. Bohm,^{148a} V. Boisvert,⁸⁰ P. Bokan,^{168,i} T. Bold,^{41a} A. S. Boldyrev,¹⁰¹

A. E. Bolz,^{60b} M. Bomben,⁸³ M. Bona,⁷⁹ M. Boonekamp,¹³⁸ A. Borisov,¹³² G. Borisov,⁷⁵ J. Bortfeldt,³² D. Bortoletto,¹²² V. Bortolotto,^{62a} D. Boscherini,^{22a} M. Bosman,¹³ J. D. Bossio Sola,²⁹ J. Boudreau,¹²⁷ J. Bouffard,² E. V. Bouhova-Thacker,⁷⁵ D. Boumediene,³⁷ C. Bourdarios,¹¹⁹ S. K. Boutle,⁵⁶ A. Boveia,¹¹³ J. Boyd,³² I. R. Boyko,⁶⁸ A. J. Bozson,⁸⁰ J. Bracinik,¹⁹ A. Brandt,⁸ G. Brandt,⁵⁷ O. Brandt,^{60a} F. Braren,⁴⁵ U. Bratzler,¹⁵⁸ B. Brau,⁸⁹ J. E. Brau,¹¹⁸ W. D. Breaden Madden,⁵⁶ K. Brendlinger,⁴⁵ A. J. Brennan,⁹¹ L. Brenner,¹⁰⁹ R. Brenner,¹⁶⁸ S. Bressler,¹⁷⁵ D. L. Briglin,¹⁹ T. M. Bristow,⁴⁹ D. Britton,⁵⁶ D. Britzger,⁴⁵ F. M. Brochu,³⁰ I. Brock,²³ R. Brock,⁹³ G. Brooijmans,³⁸ T. Brooks,⁸⁰ W. K. Brooks,^{34b} J. Brosamer,¹⁶ E. Brost,¹¹⁰ J. H. Broughton,¹⁹ P. A. Bruckman de Renstrom,⁴² D. Bruncko,^{146b} A. Bruni,^{22a} G. Bruni,^{22a} L. S. Bruni,¹⁰⁹ S. Bruno,^{135a,135b} BH Brunt,³⁰ M. Bruschi,^{22a} N. Bruscinio,¹²⁷ P. Bryant,³³ L. Bryngemark,⁴⁵ T. Buanes,¹⁵ Q. Buat,¹⁴⁴ P. Buchholz,¹⁴³ A. G. Buckley,⁵⁶ I. A. Budagov,⁶⁸ F. Buehrer,⁵¹ M. K. Bugge,¹²¹ O. Bulekov,¹⁰⁰ D. Bullock,⁸ T. J. Burch,¹¹⁰ S. Burdin,⁷⁷ C. D. Burgard,⁵¹ A. M. Burger,⁵ B. Burghgrave,¹¹⁰ K. Burka,⁴² S. Burke,¹³³ I. Burmeister,⁴⁶ J. T. P. Burr,¹²² E. Busato,³⁷ D. Büscher,⁵¹ V. Büscher,⁸⁶ P. Bussey,⁵⁶ J. M. Butler,²⁴ C. M. Buttar,⁵⁶ J. M. Butterworth,⁸¹ P. Butti,³² W. Buttinger,²⁷ A. Buzatu,¹⁵³ A. R. Buzykaev,^{111,c} S. Cabrera Urbán,¹⁷⁰ D. Caforio,¹³⁰ H. Cai,¹⁶⁹ V. M. Cairo,^{40a,40b} O. Cakir,^{4a} N. Calace,⁵² P. Calafiura,¹⁶ A. Calandri,⁸⁸ G. Calderini,⁸³ P. Calfayan,⁶⁴ G. Callea,^{40a,40b} L. P. Caloba,^{26a} S. Calvente Lopez,⁸⁵ D. Calvet,³⁷ S. Calvet,³⁷ T. P. Calvet,⁸⁸ R. Camacho Toro,³³ S. Camarda,³² P. Camarri,^{135a,135b} D. Cameron,¹²¹ R. Caminal Armadans,¹⁶⁹ C. Camincher,⁵⁸ S. Campana,³² M. Campanelli,⁸¹ A. Camplani,^{94a,94b} A. Campoverde,¹⁴³ V. Canale,^{106a,106b} M. Cano Bret,^{36c} J. Cantero,¹¹⁶ T. Cao,¹⁵⁵ M. D. M. Capeans Garrido,³² I. Caprini,^{28b} M. Caprini,^{28b} M. Capua,^{40a,40b} R. M. Carbone,³⁸ R. Cardarelli,^{135a} F. Cardillo,⁵¹ I. Carli,¹³¹ T. Carli,³² G. Carlino,^{106a} B. T. Carlson,¹²⁷ L. Carminati,^{94a,94b} R. M. D. Carney,^{148a,148b} S. Caron,¹⁰⁸ E. Carquin,^{34b} S. Carrá,^{94a,94b} G. D. Carrillo-Montoya,³² D. Casadei,¹⁹ M. P. Casado,^{13j} M. Casolino,¹³ D. W. Casper,¹⁶⁶ R. Castelijns,¹⁰⁹ V. Castillo Gimenez,¹⁷⁰ N. F. Castro,^{128a,k} A. Catinaccio,³² J. R. Catmore,¹²¹ A. Cattai,³² J. Caudron,²³ V. Cavaliere,¹⁶⁹ E. Cavallaro,¹³ D. Cavalli,^{94a} M. Cavalli-Sforza,¹³ V. Cavasinni,^{126a,126b} E. Celebi,^{20d} F. Ceradini,^{136a,136b} L. Cerda Alberich,¹⁷⁰ A. S. Cerqueira,^{26b} A. Cerri,¹⁵¹ L. Cerrito,^{135a,135b} F. Cerutti,¹⁶ A. Cervelli,^{22a,22b} S. A. Cetin,^{20d} A. Chafaq,^{137a} D. Chakraborty,¹¹⁰ S. K. Chan,⁵⁹ W. S. Chan,¹⁰⁹ Y. L. Chan,^{62a} P. Chang,¹⁶⁹ J. D. Chapman,³⁰ D. G. Charlton,¹⁹ C. C. Chau,³¹ C. A. Chavez Barajas,¹⁵¹ S. Che,¹¹³ S. Cheatham,^{167a,167c} A. Chegwidan,⁹³ S. Chekanov,⁶ S. V. Chekulaev,^{163a} G. A. Chelkov,^{68,l} M. A. Chelstowska,³² C. Chen,^{36a} C. Chen,⁶⁷ H. Chen,²⁷ J. Chen,^{36a} S. Chen,^{35b} S. Chen,¹⁵⁷ X. Chen,^{35c,m} Y. Chen,⁷⁰ H. C. Cheng,⁹² H. J. Cheng,^{35a} A. Cheplakov,⁶⁸ E. Cheremushkina,¹³² R. Cherkaoui El Moursli,^{137e} E. Cheu,⁷ K. Cheung,⁶³ L. Chevalier,¹³⁸ V. Chiarella,⁵⁰ G. Chiarelli,^{126a,126b} G. Chiodini,^{76a} A. S. Chisholm,³² A. Chitan,^{28b} Y. H. Chiu,¹⁷² M. V. Chizhov,⁶⁸ K. Choi,⁶⁴ A. R. Chomont,³⁷ S. Chouridou,¹⁵⁶ Y. S. Chow,^{62a} V. Christodoulou,⁸¹ M. C. Chu,^{62a} J. Chudoba,¹²⁹ A. J. Chuinard,⁹⁰ J. J. Chwastowski,⁴² L. Chytka,¹¹⁷ A. K. Ciftci,^{4a} D. Cinca,⁴⁶ V. Cindro,⁷⁸ I. A. Cioara,²³ A. Ciocio,¹⁶ F. Ciotto,^{106a,106b} Z. H. Citron,¹⁷⁵ M. Citterio,^{94a} M. Ciubancan,^{28b} A. Clark,⁵² B. L. Clark,⁵⁹ M. R. Clark,³⁸ P. J. Clark,⁴⁹ R. N. Clarke,¹⁶ C. Clement,^{148a,148b} Y. Coadou,⁸⁸ M. Cobal,^{167a,167c} A. Coccaro,⁵² J. Cochran,⁶⁷ L. Colasurdo,¹⁰⁸ B. Cole,³⁸ A. P. Colijn,¹⁰⁹ J. Collot,⁵⁸ T. Colombo,¹⁶⁶ P. Conde Muño,^{128a,128b} E. Coniavitis,⁵¹ S. H. Connell,^{147b} I. A. Connelly,⁸⁷ S. Constantinescu,^{28b} G. Conti,³² F. Conventi,^{106a,n} M. Cooke,¹⁶ A. M. Cooper-Sarkar,¹²² F. Cormier,¹⁷¹ K. J. R. Cormier,¹⁶¹ M. Corradi,^{134a,134b} F. Corriveau,^{90,o} A. Cortes-Gonzalez,³² G. Costa,^{94a} M. J. Costa,¹⁷⁰ D. Costanzo,¹⁴¹ G. Cottin,³⁰ G. Cowan,⁸⁰ B. E. Cox,⁸⁷ K. Cranmer,¹¹² S. J. Crawley,⁵⁶ R. A. Creager,¹²⁴ G. Cree,³¹ S. Crépe-Renaudin,⁵⁸ F. Crescioli,⁸³ W. A. Cribbs,^{148a,148b} M. Cristinziani,²³ V. Croft,¹¹² G. Crosetti,^{40a,40b} A. Cueto,⁸⁵ T. Cuhadar Donszelmann,¹⁴¹ A. R. Cukierman,¹⁴⁵ J. Cummings,¹⁷⁹ M. Curatolo,⁵⁰ J. Cúth,⁸⁶ S. Czekiarda,⁴² P. Czodrowski,³² G. D'amen,^{22a,22b} S. D'Auria,⁵⁶ L. D'eraimo,⁸³ M. D'Onofrio,⁷⁷ M. J. Da Cunha Sargedas De Sousa,^{128a,128b} C. Da Via,⁸⁷ W. Dabrowski,^{41a} T. Dado,^{146a} T. Dai,⁹² O. Dale,¹⁵ F. Dallaire,⁹⁷ C. Dallapiccola,⁸⁹ M. Dam,³⁹ J. R. Dandoy,¹²⁴ M. F. Daneri,²⁹ N. P. Dang,¹⁷⁶ A. C. Daniells,¹⁹ N. S. Dann,⁸⁷ M. Danninger,¹⁷¹ M. Dano Hoffmann,¹³⁸ V. Dao,¹⁵⁰ G. Darbo,^{53a} S. Darmora,⁸ J. Dassoulas,³ A. Dattagupta,¹¹⁸ T. Daubney,⁴⁵ W. Davey,²³ C. David,⁴⁵ T. Davidek,¹³¹ D. R. Davis,⁴⁸ P. Davison,⁸¹ E. Dawe,⁹¹ I. Dawson,¹⁴¹ K. De,⁸ R. de Asmundis,^{106a} A. De Benedetti,¹¹⁵ S. De Castro,^{22a,22b} S. De Cecco,⁸³ N. De Groot,¹⁰⁸ P. de Jong,¹⁰⁹ H. De la Torre,⁹³ F. De Lorenzi,⁶⁷ A. De Maria,⁵⁷ D. De Pedis,^{134a} A. De Salvo,^{134a} U. De Sanctis,^{135a,135b} A. De Santo,¹⁵¹ K. De Vasconcelos Corga,⁸⁸ J. B. De Vivie De Regie,¹¹⁹ R. Debbe,²⁷ C. Debenedetti,¹³⁹ D. V. Dedovich,⁶⁸ N. Dehghanian,³ I. Deigaard,¹⁰⁹ M. Del Gaudio,^{40a,40b} J. Del Peso,⁸⁵ D. Delgove,¹¹⁹ F. Deliot,¹³⁸ C. M. Delitzsch,⁷ A. Dell'Acqua,³² L. Dell'Asta,²⁴ M. Dell'Orso,^{126a,126b} M. Della Pietra,^{106a,106b} D. della Volpe,⁵² M. Delmastro,⁵ C. Delporte,¹¹⁹ P. A. Delsart,⁵⁸ D. A. DeMarco,¹⁶¹ S. Demers,¹⁷⁹ M. Demichev,⁶⁸ A. Demilly,⁸³ S. P. Denisov,¹³² D. Denysiuk,¹³⁸ D. Derendarz,⁴² J. E. Derkaoui,^{137d} F. Derue,⁸³ P. Dervan,⁷⁷ K. Desch,²³ C. Deterre,⁴⁵ K. Dette,¹⁶¹ M. R. Devesa,²⁹

P. O. Deviveiros,³² A. Dewhurst,¹³³ S. Dhaliwal,²⁵ F. A. Di Bello,⁵² A. Di Ciaccio,^{135a,135b} L. Di Ciaccio,⁵ W. K. Di Clemente,¹²⁴ C. Di Donato,^{106a,106b} A. Di Girolamo,³² B. Di Girolamo,³² B. Di Micco,^{136a,136b} R. Di Nardo,³² K. F. Di Petrillo,⁵⁹ A. Di Simone,⁵¹ R. Di Sipio,¹⁶¹ D. Di Valentino,³¹ C. Diaconu,⁸⁸ M. Diamond,¹⁶¹ F. A. Dias,³⁹ M. A. Diaz,^{34a} E. B. Diehl,⁹² J. Dietrich,¹⁷ S. Díez Cornell,⁴⁵ A. Dimitrievska,¹⁴ J. Dingfelder,²³ P. Dita,^{28b} S. Dita,^{28b} F. Dittus,³² F. Djama,⁸⁸ T. Djobava,^{54b} J. I. Djuvsland,^{60a} M. A. B. do Vale,^{26c} D. Dobos,³² M. Dobre,^{28b} D. Dodsworth,²⁵ C. Doglioni,⁸⁴ J. Dolejsi,¹³¹ Z. Dolezal,¹³¹ M. Donadelli,^{26d} S. Donati,^{126a,126b} P. Dondero,^{123a,123b} J. Donini,³⁷ J. Dopke,¹³³ A. Doria,^{106a} M. T. Dova,⁷⁴ A. T. Doyle,⁵⁶ E. Drechsler,⁵⁷ M. Dris,¹⁰ Y. Du,^{36b} J. Duarte-Camperderros,¹⁵⁵ A. Dubreuil,⁵² E. Duchovni,¹⁷⁵ G. Duckeck,¹⁰² A. Ducourthial,⁸³ O. A. Ducu,^{97,p} D. Duda,¹⁰⁹ A. Dudarev,³² A. Chr. Dudder,⁸⁶ E. M. Duffield,¹⁶ L. Dufлот,¹¹⁹ M. Dührssen,³² C. Dulsen,¹⁷⁸ M. Dumancic,¹⁷⁵ A. E. Dumitriu,^{28b} A. K. Duncan,⁵⁶ M. Dunford,^{60a} A. Duperrin,⁸⁸ H. Duran Yildiz,^{4a} M. Düren,⁵⁵ A. Durglishvili,^{54b} D. Duschinger,⁴⁷ B. Dutta,⁴⁵ D. Duvnjak,¹ M. Dyndal,⁴⁵ B. S. Dziedzic,⁴² C. Eckardt,⁴⁵ K. M. Ecker,¹⁰³ R. C. Edgar,⁹² T. Eifert,³² G. Eigen,¹⁵ K. Einsweiler,¹⁶ T. Ekelof,¹⁶⁸ M. El Kacimi,^{137c} R. El Kosseifi,⁸⁸ V. Ellajosyula,⁸⁸ M. Ellert,¹⁶⁸ S. Elles,⁵ F. Ellinghaus,¹⁷⁸ A. A. Elliot,¹⁷² N. Ellis,³² J. Elmsheuser,²⁷ M. Elsing,³² D. Emeliyanov,¹³³ Y. Enari,¹⁵⁷ O. C. Endner,⁸⁶ J. S. Ennis,¹⁷³ M. B. Epland,⁴⁸ J. Erdmann,⁴⁶ A. Ereditato,¹⁸ M. Ernst,²⁷ S. Errede,¹⁶⁹ M. Escalier,¹¹⁹ C. Escobar,¹⁷⁰ B. Esposito,⁵⁰ O. Estrada Pastor,¹⁷⁰ A. I. Etienvre,¹³⁸ E. Etzion,¹⁵⁵ H. Evans,⁶⁴ A. Ezhilov,¹²⁵ M. Ezzi,^{137e} F. Fabbri,^{22a,22b} L. Fabbri,^{22a,22b} V. Fabiani,¹⁰⁸ G. Facini,⁸¹ R. M. Fakhrutdinov,¹³² S. Falciano,^{134a} R. J. Falla,⁸¹ J. Faltova,³² Y. Fang,^{35a} M. Fanti,^{94a,94b} A. Farbin,⁸ A. Farilla,^{136a} C. Farina,¹²⁷ E. M. Farina,^{123a,123b} T. Farooque,⁹³ S. Farrell,¹⁶ S. M. Farrington,¹⁷³ P. Farthouat,³² F. Fassi,^{137e} P. Fassnacht,³² D. Fassouliotis,⁹ M. Fauci Giannelli,⁴⁹ A. Favareto,^{53a,53b} W. J. Fawcett,¹²² L. Fayard,¹¹⁹ O. L. Fedin,^{125,q} W. Fedorko,¹⁷¹ S. Feigl,¹²¹ L. Feligioni,⁸⁸ C. Feng,^{36b} E. J. Feng,³² M. J. Fenton,⁵⁶ A. B. Fenyuk,¹³² L. Feremenga,⁸ P. Fernandez Martinez,¹⁷⁰ S. Fernandez Perez,¹³ J. Ferrando,⁴⁵ A. Ferrari,¹⁶⁸ P. Ferrari,¹⁰⁹ R. Ferrari,^{123a} D. E. Ferreira de Lima,^{60b} A. Ferrer,¹⁷⁰ D. Ferrere,⁵² C. Ferretti,⁹² F. Fiedler,⁸⁶ A. Filipčič,⁷⁸ M. Filipuzzi,⁴⁵ F. Filthaut,¹⁰⁸ M. Fincke-Keeler,¹⁷² K. D. Finelli,¹⁵² M. C. N. Fiolhais,^{128a,128c,r} L. Fiorini,¹⁷⁰ A. Fischer,² C. Fischer,¹³ J. Fischer,¹⁷⁸ W. C. Fisher,⁹³ N. Flaschel,⁴⁵ I. Fleck,¹⁴³ P. Fleischmann,⁹² R. R. M. Fletcher,¹²⁴ T. Flick,¹⁷⁸ B. M. Flierl,¹⁰² L. R. Flores Castillo,^{62a} M. J. Flowerdew,¹⁰³ G. T. Forcolin,⁸⁷ A. Formica,¹³⁸ F. A. Förster,¹³ A. Forti,⁸⁷ A. G. Foster,¹⁹ D. Fournier,¹¹⁹ H. Fox,⁷⁵ S. Fracchia,¹⁴¹ P. Francavilla,⁸³ M. Franchini,^{22a,22b} S. Franchino,^{60a} D. Francis,³² L. Franconi,¹²¹ M. Franklin,⁵⁹ M. Frate,¹⁶⁶ M. Fraternali,^{123a,123b} D. Freeborn,⁸¹ S. M. Fressard-Batraneanu,³² B. Freund,⁹⁷ D. Froidevaux,³² J. A. Frost,¹²² C. Fukunaga,¹⁵⁸ T. Fusayasu,¹⁰⁴ J. Fuster,¹⁷⁰ O. Gabizon,¹⁵⁴ A. Gabrielli,^{22a,22b} A. Gabrielli,¹⁶ G. P. Gach,^{41a} S. Gadatsch,³² S. Gadomski,⁸⁰ G. Gagliardi,^{53a,53b} L. G. Gagnon,⁹⁷ C. Galea,¹⁰⁸ B. Galhardo,^{128a,128c} E. J. Gallas,¹²² B. J. Gallop,¹³³ P. Gallus,¹³⁰ G. Galster,³⁹ K. K. Gan,¹¹³ S. Ganguly,³⁷ Y. Gao,⁷⁷ Y. S. Gao,^{145,g} F. M. Garay Walls,^{34a} C. García,¹⁷⁰ J. E. García Navarro,¹⁷⁰ J. A. García Pascual,^{35a} M. Garcia-Sciveres,¹⁶ R. W. Gardner,³³ N. Garelli,¹⁴⁵ V. Garonne,¹²¹ A. Gascon Bravo,⁴⁵ K. Gasnikova,⁴⁵ C. Gatti,⁵⁰ A. Gaudiello,^{53a,53b} G. Gaudio,^{123a} I. L. Gavrilenko,⁹⁸ C. Gay,¹⁷¹ G. Gaycken,²³ E. N. Gazis,¹⁰ C. N. P. Gee,¹³³ J. Geisen,⁵⁷ M. Geisen,⁸⁶ M. P. Geisler,^{60a} K. Gellerstedt,^{148a,148b} C. Gemme,^{53a} M. H. Genest,⁵⁸ C. Geng,⁹² S. Gentile,^{134a,134b} C. Gentsos,¹⁵⁶ S. George,⁸⁰ D. Gerbaudo,¹³ G. Geßner,⁴⁶ S. Ghasemi,¹⁴³ M. Ghneimat,²³ B. Giacobbe,^{22a} S. Giagu,^{134a,134b} N. Giangiacomi,^{22a,22b} P. Giannetti,^{126a,126b} S. M. Gibson,⁸⁰ M. Gignac,¹⁷¹ M. Gilchriese,¹⁶ D. Gillberg,³¹ G. Gilles,¹⁷⁸ D. M. Gingrich,^{3,d} M. P. Giordani,^{167a,167c} F. M. Giorgi,^{22a} P. F. Giraud,¹³⁸ P. Giromini,⁵⁹ G. Giugliarelli,^{167a,167c} D. Giugni,^{94a} F. Giuli,¹²² C. Giuliani,¹⁰³ M. Giulini,^{60b} B. K. Gjelsten,¹²¹ S. Gkaitatzis,¹⁵⁶ I. Gkialas,^{9,s} E. L. Gkoukousis,¹³ P. Gkoutoumis,¹⁰ L. K. Gladilin,¹⁰¹ C. Glasman,⁸⁵ J. Glatzer,¹³ P. C. F. Glaysher,⁴⁵ A. Glazov,⁴⁵ M. Goblirsch-Kolb,²⁵ J. Godlewski,⁴² S. Goldfarb,⁹¹ T. Golling,⁵² D. Golubkov,¹³² A. Gomes,^{128a,128b,128d} R. Gonçalo,^{128a} R. Goncalves Gama,^{26a} J. Goncalves Pinto Firmino Da Costa,¹³⁸ G. Gonella,⁵¹ L. Gonella,¹⁹ A. Gongadze,⁶⁸ S. González de la Hoz,¹⁷⁰ S. Gonzalez-Sevilla,⁵² L. Goossens,³² P. A. Gorbounov,⁹⁹ H. A. Gordon,²⁷ I. Gorelov,¹⁰⁷ B. Gorini,³² E. Gorini,^{76a,76b} A. Gorišek,⁷⁸ A. T. Goshaw,⁴⁸ C. Gössling,⁴⁶ M. I. Gostkin,⁶⁸ C. A. Gottardo,²³ C. R. Goudet,¹¹⁹ D. Goujdami,^{137c} A. G. Goussiou,¹⁴⁰ N. Govender,^{147b,t} E. Gozani,¹⁵⁴ I. Grabowska-Bold,^{41a} P. O. J. Gradin,¹⁶⁸ J. Gramling,¹⁶⁶ E. Gramstad,¹²¹ S. Grancagnolo,¹⁷ V. Gratchev,¹²⁵ P. M. Gravila,^{28f} C. Gray,⁵⁶ H. M. Gray,¹⁶ Z. D. Greenwood,^{82,u} C. Grefe,²³ K. Gregersen,⁸¹ I. M. Gregor,⁴⁵ P. Grenier,¹⁴⁵ K. Grevtsov,⁵ J. Griffiths,⁸ A. A. Grillo,¹³⁹ K. Grimm,⁷⁵ S. Grinstein,^{13,v} Ph. Gris,³⁷ J.-F. Grivaz,¹¹⁹ S. Groh,⁸⁶ E. Gross,¹⁷⁵ J. Grosse-Knetter,⁵⁷ G. C. Grossi,⁸² Z. J. Grout,⁸¹ A. Grummer,¹⁰⁷ L. Guan,⁹² W. Guan,¹⁷⁶ J. Guenther,³² F. Guescini,^{163a} D. Guest,¹⁶⁶ O. Gueta,¹⁵⁵ B. Gui,¹¹³ E. Guido,^{53a,53b} T. Guillemin,⁵ S. Guindon,³² U. Gul,⁵⁶ C. Gumpert,³² J. Guo,^{36c} W. Guo,⁹² Y. Guo,^{36a,w} R. Gupta,⁴³ S. Gupta,¹²² S. Gurbuz,^{20a} G. Gustavino,¹¹⁵ B. J. Gutelman,¹⁵⁴ P. Gutierrez,¹¹⁵ N. G. Gutierrez Ortiz,⁸¹ C. Gutsche,⁸¹ C. Guyot,¹³⁸ M. P. Guzik,^{41a} C. Gwenlan,¹²² C. B. Gwilliam,⁷⁷ A. Haas,¹¹²

C. Haber,¹⁶ H. K. Hadavand,⁸ N. Haddad,^{137e} A. Hadeef,⁸⁸ S. Hageböck,²³ M. Hagihara,¹⁶⁴ H. Hakobyan,^{180,†} M. Haleem,⁴⁵ J. Haley,¹¹⁶ G. Halladjian,⁹³ G. D. Hallewell,⁸⁸ K. Hamacher,¹⁷⁸ P. Hamal,¹¹⁷ K. Hamano,¹⁷² A. Hamilton,^{147a} G. N. Hamity,¹⁴¹ P. G. Hamnett,⁴⁵ L. Han,^{36a} S. Han,^{35a} K. Hanagaki,^{69,x} K. Hanawa,¹⁵⁷ M. Hance,¹³⁹ B. Haney,¹²⁴ P. Hanke,^{60a} J. B. Hansen,³⁹ J. D. Hansen,³⁹ M. C. Hansen,²³ P. H. Hansen,³⁹ K. Hara,¹⁶⁴ A. S. Hard,¹⁷⁶ T. Harenberg,¹⁷⁸ F. Hariri,¹¹⁹ S. Harkusha,⁹⁵ P. F. Harrison,¹⁷³ N. M. Hartmann,¹⁰² Y. Hasegawa,¹⁴² A. Hasib,⁴⁹ S. Hassani,¹³⁸ S. Haug,¹⁸ R. Hauser,⁹³ L. Hauswald,⁴⁷ L. B. Havener,³⁸ M. Havranek,¹³⁰ C. M. Hawkes,¹⁹ R. J. Hawkings,³² D. Hayakawa,¹⁵⁹ D. Hayden,⁹³ C. P. Hays,¹²² J. M. Hays,⁷⁹ H. S. Hayward,⁷⁷ S. J. Haywood,¹³³ S. J. Head,¹⁹ T. Heck,⁸⁶ V. Hedberg,⁸⁴ L. Heelan,⁸ S. Heer,²³ K. K. Heidegger,⁵¹ S. Heim,⁴⁵ T. Heim,¹⁶ B. Heinemann,^{45,y} J. J. Heinrich,¹⁰² L. Heinrich,¹¹² C. Heinz,⁵⁵ J. Hejbal,¹²⁹ L. Helary,³² A. Held,¹⁷¹ S. Hellman,^{148a,148b} C. Hensens,³² R. C. W. Henderson,⁷⁵ Y. Heng,¹⁷⁶ S. Henkelmann,¹⁷¹ A. M. Henriques Correia,³² S. Henrot-Versille,¹¹⁹ G. H. Herbert,¹⁷ H. Herde,²⁵ V. Herget,¹⁷⁷ Y. Hernández Jiménez,^{147c} H. Herr,⁸⁶ G. Herten,⁵¹ R. Hertenberger,¹⁰² L. Hervas,³² T. C. Herwig,¹²⁴ G. G. Hesketh,⁸¹ N. P. Hesse,^{163a} J. W. Hetherly,⁴³ S. Higashino,⁶⁹ E. Higón-Rodríguez,¹⁷⁰ K. Hildebrand,³³ E. Hill,¹⁷² J. C. Hill,³⁰ K. H. Hiller,⁴⁵ S. J. Hillier,¹⁹ M. Hils,⁴⁷ I. Hinchliffe,¹⁶ M. Hirose,⁵¹ D. Hirschbuehl,¹⁷⁸ B. Hiti,⁷⁸ O. Hladik,¹²⁹ X. Hoad,⁴⁹ J. Hobbs,¹⁵⁰ N. Hod,^{163a} M. C. Hodgkinson,¹⁴¹ P. Hodgson,¹⁴¹ A. Hoecker,³² M. R. Hoferkamp,¹⁰⁷ F. Hoenig,¹⁰² D. Hohn,²³ T. R. Holmes,³³ M. Homann,⁴⁶ S. Honda,¹⁶⁴ T. Honda,⁶⁹ T. M. Hong,¹²⁷ B. H. Hooberman,¹⁶⁹ W. H. Hopkins,¹¹⁸ Y. Horii,¹⁰⁵ A. J. Horton,¹⁴⁴ J.-Y. Hostachy,⁵⁸ A. Hostiuc,¹⁴⁰ S. Hou,¹⁵³ A. Houmada,^{137a} J. Howarth,⁸⁷ J. Hoya,⁷⁴ M. Hrabovsky,¹¹⁷ J. Hrdinka,³² I. Hristova,¹⁷ J. Hrivnac,¹¹⁹ T. Hryn'ova,⁵ A. Hrynevich,⁹⁶ P. J. Hsu,⁶³ S.-C. Hsu,¹⁴⁰ Q. Hu,^{36a} S. Hu,^{36c} Y. Huang,^{35a} Z. Hubacek,¹³⁰ F. Hubaut,⁸⁸ F. Huegging,²³ T. B. Huffman,¹²² E. W. Hughes,³⁸ G. Hughes,⁷⁵ M. Huhtinen,³² R. F. H. Hunter,³¹ P. Huo,¹⁵⁰ N. Huseynov,^{68,b} J. Huston,⁹³ J. Huth,⁵⁹ R. Hyneman,⁹² G. Iacobucci,⁵² G. Iakovidis,²⁷ I. Ibragimov,¹⁴³ L. Iconomidou-Fayard,¹¹⁹ Z. Idrissi,^{137e} P. Inengo,³² O. Igonkina,^{109,z} T. Iizawa,¹⁷⁴ Y. Ikegami,⁶⁹ M. Ikeno,⁶⁹ Y. Ilchenko,^{11,aa} D. Iliadis,¹⁵⁶ N. Ilic,¹⁴⁵ F. Iltzsche,⁴⁷ G. Introzzi,^{123a,123b} P. Ioannou,^{9,†} M. Iodice,^{136a} K. Iordanidou,³⁸ V. Ippolito,⁵⁹ M. F. Isacson,¹⁶⁸ N. Ishijima,¹²⁰ M. Ishino,¹⁵⁷ M. Ishitsuka,¹⁵⁹ C. Issever,¹²² S. Istin,^{20a} F. Ito,¹⁶⁴ J. M. Iturbe Ponce,^{62a} R. Iuppa,^{162a,162b} H. Iwasaki,⁶⁹ J. M. Izen,⁴⁴ V. Izzo,^{106a} S. Jabbar,³ B. Jackson,¹²⁴ P. Jackson,¹ R. M. Jacobs,²³ V. Jain,² K. B. Jakobi,⁸⁶ K. Jakobs,⁵¹ S. Jakobsen,⁶⁵ T. Jakoubek,¹²⁹ D. O. Jamin,¹¹⁶ D. K. Jana,⁸² R. Jansky,⁵² J. Janssen,²³ M. Janus,⁵⁷ P. A. Janus,^{41a} G. Jarlskog,⁸⁴ N. Javadov,^{68,b} T. Javůrek,⁵¹ M. Javurkova,⁵¹ F. Jeanneau,¹³⁸ L. Jeanty,¹⁶ J. Jeljela,^{54a,ab} A. Jelinskas,¹⁷³ P. Jenni,^{51,ac} C. Jeske,¹⁷³ S. Jézéquel,⁵ H. Ji,¹⁷⁶ J. Jia,¹⁵⁰ H. Jiang,⁶⁷ Y. Jiang,^{36a} Z. Jiang,¹⁴⁵ S. Jiggins,⁸¹ J. Jimenez Pena,¹⁷⁰ S. Jin,^{35a} A. Jinaru,^{28b} O. Jinnouchi,¹⁵⁹ H. Jivan,^{147c} P. Johansson,¹⁴¹ K. A. Johns,⁷ C. A. Johnson,⁶⁴ W. J. Johnson,¹⁴⁰ K. Jon-And,^{148a,148b} R. W. L. Jones,⁷⁵ S. D. Jones,¹⁵¹ S. Jones,⁷ T. J. Jones,⁷⁷ J. Jongmanns,^{60a} P. M. Jorge,^{128a,128b} J. Jovicevic,^{163a} X. Ju,¹⁷⁶ A. Juste Rozas,^{13,v} M. K. Köhler,¹⁷⁵ A. Kaczmarska,⁴² M. Kado,¹¹⁹ H. Kagan,¹¹³ M. Kagan,¹⁴⁵ S. J. Kahn,⁸⁸ T. Kaji,¹⁷⁴ E. Kajomovitz,¹⁵⁴ C. W. Kalderon,⁸⁴ A. Kaluza,⁸⁶ S. Kama,⁴³ A. Kamenshchikov,¹³² N. Kanaya,¹⁵⁷ L. Kanjir,⁷⁸ V. A. Kantserov,¹⁰⁰ J. Kanzaki,⁶⁹ B. Kaplan,¹¹² L. S. Kaplan,¹⁷⁶ D. Kar,^{147c} K. Karakostas,¹⁰ N. Karastathis,¹⁰ M. J. Kareem,^{163b} E. Karentzos,¹⁰ S. N. Karpov,⁶⁸ Z. M. Karpova,⁶⁸ K. Karthik,¹¹² V. Kartvelishvili,⁷⁵ A. N. Karyukhin,¹³² K. Kasahara,¹⁶⁴ L. Kashif,¹⁷⁶ R. D. Kass,¹¹³ A. Kastanas,¹⁴⁹ Y. Kataoka,¹⁵⁷ C. Kato,¹⁵⁷ A. Katre,⁵² J. Katzy,⁴⁵ K. Kawade,⁷⁰ K. Kawagoe,⁷³ T. Kawamoto,¹⁵⁷ G. Kawamura,⁵⁷ E. F. Kay,⁷⁷ V. F. Kazanin,^{111,c} R. Keeler,¹⁷² R. Kehoe,⁴³ J. S. Keller,³¹ E. Kellermann,⁸⁴ J. J. Kempster,⁸⁰ J. Kendrick,¹⁹ H. Keoshkerian,¹⁶¹ O. Kepka,¹²⁹ B. P. Kerševan,⁷⁸ S. Kersten,¹⁷⁸ R. A. Keyes,⁹⁰ M. Khader,¹⁶⁹ F. Khalil-zada,¹² A. Khanov,¹¹⁶ A. G. Kharlamov,^{111,c} T. Kharlamova,^{111,c} A. Khodinov,¹⁶⁰ T. J. Khoo,⁵² V. Khovanskiy,^{99,†} E. Khramov,⁶⁸ J. Khubua,^{54b,ad} S. Kido,⁷⁰ C. R. Kilby,⁸⁰ H. Y. Kim,⁸ S. H. Kim,¹⁶⁴ Y. K. Kim,³³ N. Kimura,¹⁵⁶ O. M. Kind,¹⁷ B. T. King,⁷⁷ D. Kirchmeier,⁴⁷ J. Kirk,¹³³ A. E. Kiryunin,¹⁰³ T. Kishimoto,¹⁵⁷ D. Kisielewska,^{41a} V. Kitali,⁴⁵ O. Kivernyk,⁵ E. Kladiva,^{146b} T. Klapdor-Kleingrothaus,⁵¹ M. H. Klein,⁹² M. Klein,⁷⁷ U. Klein,⁷⁷ K. Kleinknecht,⁸⁶ P. Klimek,¹¹⁰ A. Klimentov,²⁷ R. Klingenberg,⁴⁶ T. Klingl,²³ T. Klioutchnikova,³² E.-E. Kluge,^{60a} P. Kluit,¹⁰⁹ S. Kluth,¹⁰³ E. Kneringer,⁶⁵ E. B. F. G. Knoops,⁸⁸ A. Knue,¹⁰³ A. Kobayashi,¹⁵⁷ D. Kobayashi,⁷³ T. Kobayashi,¹⁵⁷ M. Kobel,⁴⁷ M. Kocian,¹⁴⁵ P. Kodys,¹³¹ T. Koffas,³¹ E. Koffeman,¹⁰⁹ N. M. Köhler,¹⁰³ T. Koi,¹⁴⁵ M. Kolb,^{60b} I. Koletsou,⁵ A. A. Komar,^{98,†} T. Kondo,⁶⁹ N. Kondrashova,^{36c} K. Köneke,⁵¹ A. C. König,¹⁰⁸ T. Kono,^{69,ae} R. Konoplich,^{112,af} N. Konstantinidis,⁸¹ R. Kopeliansky,⁶⁴ S. Koperny,^{41a} A. K. Kopp,⁵¹ K. Korcyl,⁴² K. Kordas,¹⁵⁶ A. Korn,⁸¹ A. A. Korol,^{111,c} I. Korolkov,¹³ E. V. Korolkova,¹⁴¹ O. Kortner,¹⁰³ S. Kortner,¹⁰³ T. Kosek,¹³¹ V. V. Kostyukhin,²³ A. Kotwal,⁴⁸ A. Koulouris,¹⁰ A. Kourkoumeli-Charalampidi,^{123a,123b} C. Kourkoumelis,⁹ E. Kourlitis,¹⁴¹ V. Kouskoura,²⁷ A. B. Kowalewska,⁴² R. Kowalewski,¹⁷² T. Z. Kowalski,^{41a} C. Kozakai,¹⁵⁷ W. Kozanecki,¹³⁸ A. S. Kozhin,¹³² V. A. Kramarenko,¹⁰¹ G. Kramberger,⁷⁸ D. Krasnopevtsev,¹⁰⁰ M. W. Krasny,⁸³ A. Krasznahorkay,³² D. Krauss,¹⁰³ J. A. Kremer,^{41a}

J. Kretzschmar,⁷⁷ K. Kreuzfeldt,⁵⁵ P. Krieger,¹⁶¹ K. Krizka,¹⁶ K. Kroeninger,⁴⁶ H. Kroha,¹⁰³ J. Kroll,¹²⁹ J. Kroll,¹²⁴ J. Kroseberg,²³ J. Krstic,¹⁴ U. Kruchonak,⁶⁸ H. Krüger,²³ N. Krumnack,⁶⁷ M. C. Kruse,⁴⁸ T. Kubota,⁹¹ H. Kucuk,⁸¹ S. Kuday,^{4b} J. T. Kuechler,¹⁷⁸ S. Kuehn,³² A. Kugel,^{60a} F. Kuger,¹⁷⁷ T. Kuhl,⁴⁵ V. Kukhtin,⁶⁸ R. Kukla,⁸⁸ Y. Kulchitsky,⁹⁵ S. Kuleshov,^{34b} Y. P. Kulinich,¹⁶⁹ M. Kuna,^{134a,134b} T. Kunigo,⁷¹ A. Kupco,¹²⁹ T. Kupfer,⁴⁶ O. Kuprash,¹⁵⁵ H. Kurashige,⁷⁰ L. L. Kurchaninov,^{163a} Y. A. Kurochkin,⁹⁵ M. G. Kurth,^{35a} E. S. Kuwertz,¹⁷² M. Kuze,¹⁵⁹ J. Kvita,¹¹⁷ T. Kwan,¹⁷² D. Kyriazopoulos,¹⁴¹ A. La Rosa,¹⁰³ J. L. La Rosa Navarro,^{26d} L. La Rotonda,^{40a,40b} F. La Ruffa,^{40a,40b} C. Lacasta,¹⁷⁰ F. Lacava,^{134a,134b} J. Lacey,⁴⁵ D. P. J. Lack,⁸⁷ H. Lacker,¹⁷ D. Lacour,⁸³ E. Ladygin,⁶⁸ R. Lafaye,⁵ B. Laforge,⁸³ T. Lagouri,¹⁷⁹ S. Lai,⁵⁷ S. Lammers,⁶⁴ W. Lampl,⁷ E. Lançon,²⁷ U. Landgraf,⁵¹ M. P. J. Landon,⁷⁹ M. C. Lanfermann,⁵² V. S. Lang,⁴⁵ J. C. Lange,¹³ R. J. Langenberg,³² A. J. Lankford,¹⁶⁶ F. Lanni,²⁷ K. Lantzsich,²³ A. Lanza,^{123a} A. Lapertosa,^{53a,53b} S. Laplace,⁸³ J. F. Laporte,¹³⁸ T. Lari,^{94a} F. Lasagni Manghi,^{22a,22b} M. Lassnig,³² T. S. Lau,^{62a} P. Laurelli,⁵⁰ W. Lavrijsen,¹⁶ A. T. Law,¹³⁹ P. Laycock,⁷⁷ T. Lazovich,⁵⁹ M. Lazzaroni,^{94a,94b} B. Le,⁹¹ O. Le Dortz,⁸³ E. Le Guirriec,⁸⁸ E. P. Le Quilleuc,¹³⁸ M. LeBlanc,¹⁷² T. LeCompte,⁶ F. Ledroit-Guillon,⁵⁸ C. A. Lee,²⁷ G. R. Lee,^{34a} S. C. Lee,¹⁵³ L. Lee,⁵⁹ B. Lefebvre,⁹⁰ G. Lefebvre,⁸³ M. Lefebvre,¹⁷² F. Legger,¹⁰² C. Leggett,¹⁶ G. Lehmann Miotto,³² X. Lei,⁷ W. A. Leight,⁴⁵ M. A. L. Leite,^{26d} R. Leitner,¹³¹ D. Lellouch,¹⁷⁵ B. Lemmer,⁵⁷ K. J. C. Leney,⁸¹ T. Lenz,²³ B. Lenzi,³² R. Leone,⁷ S. Leone,^{126a,126b} C. Leonidopoulos,⁴⁹ G. Lerner,¹⁵¹ C. Leroy,⁹⁷ R. Les,¹⁶¹ A. A. J. Lesage,¹³⁸ C. G. Lester,³⁰ M. Levchenko,¹²⁵ J. Levêque,⁵ D. Levin,⁹² L. J. Levinson,¹⁷⁵ M. Levy,¹⁹ D. Lewis,⁷⁹ B. Li,^{36a,w} Changqiao Li,^{36a} H. Li,¹⁵⁰ L. Li,^{36c} Q. Li,^{35a} Q. Li,^{36a} S. Li,⁴⁸ X. Li,^{36c} Y. Li,¹⁴³ Z. Liang,^{35a} B. Liberti,^{135a} A. Liblong,¹⁶¹ K. Lie,^{62c} J. Liebal,²³ W. Liebig,¹⁵ A. Limosani,¹⁵² K. Lin,⁹³ S. C. Lin,¹⁸² T. H. Lin,⁸⁶ R. A. Linck,⁶⁴ B. E. Lindquist,¹⁵⁰ A. E. Lioni,⁵² E. Lipeles,¹²⁴ A. Lipniacka,¹⁵ M. Lisovyi,^{60b} T. M. Liss,^{169,ag} A. Lister,¹⁷¹ A. M. Litke,¹³⁹ B. Liu,⁶⁷ H. Liu,⁹² H. Liu,²⁷ J. K. K. Liu,¹²² J. Liu,^{36b} J. B. Liu,^{36a} K. Liu,⁸⁸ L. Liu,¹⁶⁹ M. Liu,^{36a} Y. L. Liu,^{36a} Y. Liu,^{36a} M. Livan,^{123a,123b} A. Lleres,⁵⁸ J. Llorente Merino,^{35a} S. L. Lloyd,⁷⁹ C. Y. Lo,^{62b} F. Lo Sterzo,⁴³ E. M. Lobodzinska,⁴⁵ P. Loch,⁷ F. K. Loebinger,⁸⁷ A. Loesle,⁵¹ K. M. Loew,²⁵ T. Lohse,¹⁷ K. Lohwasser,¹⁴¹ M. Lokajicek,¹²⁹ B. A. Long,²⁴ J. D. Long,¹⁶⁹ R. E. Long,⁷⁵ L. Longo,^{76a,76b} K. A.Looper,¹¹³ J. A. Lopez,^{34b} I. Lopez Paz,¹³ A. Lopez Solis,⁸³ J. Lorenz,¹⁰² N. Lorenzo Martinez,⁵ M. Losada,²¹ P. J. Lösel,¹⁰² X. Lou,^{35a} A. Lounis,¹¹⁹ J. Love,⁶ P. A. Love,⁷⁵ H. Lu,^{62a} N. Lu,⁹² Y. J. Lu,⁶³ H. J. Lubatti,¹⁴⁰ C. Luci,^{134a,134b} A. Lucotte,⁵⁸ C. Luedtke,⁵¹ F. Luehring,⁶⁴ W. Lukas,⁶⁵ L. Luminari,^{134a} O. Lundberg,^{148a,148b} B. Lund-Jensen,¹⁴⁹ M. S. Lutz,⁸⁹ P. M. Luzzi,⁸³ D. Lynn,²⁷ R. Lysak,¹²⁹ E. Lytken,⁸⁴ F. Lyu,^{35a} V. Lyubushkin,⁶⁸ H. Ma,²⁷ L. L. Ma,^{36b} Y. Ma,^{36b} G. Maccarrone,⁵⁰ A. Macchiolo,¹⁰³ C. M. Macdonald,¹⁴¹ B. Maček,⁷⁸ J. Machado Miguens,^{124,128b} D. Madaffari,¹⁷⁰ R. Madar,³⁷ W. F. Mader,⁴⁷ A. Madsen,⁴⁵ N. Madysa,⁴⁷ J. Maeda,⁷⁰ S. Maeland,¹⁵ T. Maeno,²⁷ A. S. Maevskiy,¹⁰¹ V. Magerl,⁵¹ C. Maiani,¹¹⁹ C. Maidantchik,^{26a} T. Maier,¹⁰² A. Maio,^{128a,128b,128d} O. Majersky,^{146a} S. Majewski,¹¹⁸ Y. Makida,⁶⁹ N. Makovec,¹¹⁹ B. Malaescu,⁸³ Pa. Malecki,⁴² V. P. Maleev,¹²⁵ F. Malek,⁵⁸ U. Mallik,⁶⁶ D. Malon,⁶ C. Malone,³⁰ S. Maltezos,¹⁰ S. Malyukov,³² J. Mamuzic,¹⁷⁰ G. Mancini,⁵⁰ I. Mandić,⁷⁸ J. Maneira,^{128a,128b} L. Manhaes de Andrade Filho,^{26b} J. Manjarres Ramos,⁴⁷ K. H. Mankinen,⁸⁴ A. Mann,¹⁰² A. Manoussos,³² B. Mansoulie,¹³⁸ J. D. Mansour,^{35a} R. Mantifel,⁹⁰ M. Mantoani,⁵⁷ S. Manzoni,^{94a,94b} L. Mapelli,³² G. Marceca,²⁹ L. March,⁵² L. Marchese,¹²² G. Marchiori,⁸³ M. Marcisovsky,¹²⁹ C. A. Marin Tobon,³² M. Marjanovic,³⁷ D. E. Marley,⁹² F. Marroquim,^{26a} S. P. Marsden,⁸⁷ Z. Marshall,¹⁶ M. U. F. Martensson,¹⁶⁸ S. Marti-Garcia,¹⁷⁰ C. B. Martin,¹¹³ T. A. Martin,¹⁷³ V. J. Martin,⁴⁹ B. Martin dit Latour,¹⁵ M. Martinez,^{13,v} V. I. Martinez Outschoorn,¹⁶⁹ S. Martin-Haugh,¹³³ V. S. Martoiu,^{28b} A. C. Martyniuk,⁸¹ A. Marzin,³² L. Masetti,⁸⁶ T. Mashimo,¹⁵⁷ R. Mashinistov,⁹⁸ J. Masik,⁸⁷ A. L. Maslennikov,^{111,c} L. H. Mason,⁹¹ L. Massa,^{135a,135b} P. Mastrandrea,⁵ A. Mastroberardino,^{40a,40b} T. Masubuchi,¹⁵⁷ P. Mättig,¹⁷⁸ J. Maurer,^{28b} S. J. Maxfield,⁷⁷ D. A. Maximov,^{111,c} R. Mazini,¹⁵³ I. Maznas,¹⁵⁶ S. M. Mazza,^{94a,94b} N. C. Mc Fadden,¹⁰⁷ G. Mc Goldrick,¹⁶¹ S. P. Mc Kee,⁹² A. McCarn,⁹² R. L. McCarthy,¹⁵⁰ T. G. McCarthy,¹⁰³ L. I. McClymont,⁸¹ E. F. McDonald,⁹¹ J. A. Mcfayden,³² G. Mchedlidze,⁵⁷ S. J. McMahon,¹³³ P. C. McNamara,⁹¹ C. J. McNicol,¹⁷³ R. A. McPherson,^{172,o} S. Meehan,¹⁴⁰ T. J. Megy,⁵¹ S. Mehlhase,¹⁰² A. Mehta,⁷⁷ T. Meideck,⁵⁸ K. Meier,^{60a} B. Meirose,⁴⁴ D. Melini,^{170,ah} B. R. Mellado Garcia,^{147c} J. D. Mellenthin,⁵⁷ M. Melo,^{146a} F. Meloni,¹⁸ A. Melzer,²³ S. B. Menary,⁸⁷ L. Meng,⁷⁷ X. T. Meng,⁹² A. Mengarelli,^{22a,22b} S. Menke,¹⁰³ E. Meoni,^{40a,40b} S. Mergelmeyer,¹⁷ C. Merlassino,¹⁸ P. Mermod,⁵² L. Merola,^{106a,106b} C. Meroni,^{94a} F. S. Merritt,³³ A. Messina,^{134a,134b} J. Metcalfe,⁶ A. S. Mete,¹⁶⁶ C. Meyer,¹²⁴ J-P. Meyer,¹³⁸ J. Meyer,¹⁰⁹ H. Meyer Zu Theenhausen,^{60a} F. Miano,¹⁵¹ R. P. Middleton,¹³³ S. Miglioranzi,^{53a,53b} L. Mijović,⁴⁹ G. Mikenberg,¹⁷⁵ M. Mikestikova,¹²⁹ M. Mikuž,⁷⁸ M. Milesi,⁹¹ A. Milic,¹⁶¹ D. A. Millar,⁷⁹ D. W. Miller,³³ C. Mills,⁴⁹ A. Milov,¹⁷⁵ D. A. Milstead,^{148a,148b} A. A. Minaenko,¹³² Y. Minami,¹⁵⁷ I. A. Minashvili,^{54b} A. I. Mincer,¹¹² B. Mindur,^{41a} M. Mineev,⁶⁸ Y. Minegishi,¹⁵⁷ Y. Ming,¹⁷⁶ L. M. Mir,¹³ A. Mirto,^{76a,76b} K. P. Mistry,¹²⁴ T. Mitani,¹⁷⁴ J. Mitrevski,¹⁰² V. A. Mitsou,¹⁷⁰

A. Miucci,¹⁸ P. S. Miyagawa,¹⁴¹ A. Mizukami,⁶⁹ J. U. Mjörnmark,⁸⁴ T. Mkrtchyan,¹⁸⁰ M. Mlynarikova,¹³¹ T. Moa,^{148a,148b}
 K. Mochizuki,⁹⁷ P. Mogg,⁵¹ S. Mohapatra,³⁸ S. Molander,^{148a,148b} R. Moles-Valls,²³ M. C. Mondragon,⁹³ K. Mönig,⁴⁵
 J. Monk,³⁹ E. Monnier,⁸⁸ A. Montalbano,¹⁵⁰ J. Montejo Berlingen,³² F. Monticelli,⁷⁴ S. Monzani,^{94a,94b} R. W. Moore,³
 N. Morange,¹¹⁹ D. Moreno,²¹ M. Moreno Llácer,³² P. Morettini,^{53a} S. Morgenstern,³² D. Mori,¹⁴⁴ T. Mori,¹⁵⁷ M. Morii,⁵⁹
 M. Morinaga,¹⁷⁴ V. Morisbak,¹²¹ A. K. Morley,³² G. Mornacchi,³² J. D. Morris,⁷⁹ L. Morvaj,¹⁵⁰ P. Moschovakos,¹⁰
 M. Mosidze,^{54b} H. J. Moss,¹⁴¹ J. Moss,^{145,ai} K. Motohashi,¹⁵⁹ R. Mount,¹⁴⁵ E. Mountricha,²⁷ E. J. W. Moyse,⁸⁹ S. Muanza,⁸⁸
 F. Mueller,¹⁰³ J. Mueller,¹²⁷ R. S. P. Mueller,¹⁰² D. Muenstermann,⁷⁵ P. Mullen,⁵⁶ G. A. Mullier,¹⁸ F. J. Munoz Sanchez,⁸⁷
 W. J. Murray,^{173,133} H. Musheghyan,³² M. Muškinja,⁷⁸ A. G. Myagkov,^{132,aj} M. Myska,¹³⁰ B. P. Nachman,¹⁶
 O. Nackenhorst,⁵² K. Nagai,¹²² R. Nagai,^{69,ae} K. Nagano,⁶⁹ Y. Nagasaka,⁶¹ K. Nagata,¹⁶⁴ M. Nagel,⁵¹ E. Nagy,⁸⁸
 A. M. Nairz,³² Y. Nakahama,¹⁰⁵ K. Nakamura,⁶⁹ T. Nakamura,¹⁵⁷ I. Nakano,¹¹⁴ R. F. Naranjo Garcia,⁴⁵ R. Narayan,¹¹
 D. I. Narrias Villar,^{60a} I. Naryshkin,¹²⁵ T. Naumann,⁴⁵ G. Navarro,²¹ R. Nayyar,⁷ H. A. Neal,⁹² P. Yu. Nechaeva,⁹⁸
 T. J. Neep,¹³⁸ A. Negri,^{123a,123b} M. Negrini,^{22a} S. Nektarijevic,¹⁰⁸ C. Nellist,⁵⁷ A. Nelson,¹⁶⁶ M. E. Nelson,¹²² S. Nemecek,¹²⁹
 P. Nemethy,¹¹² M. Nessi,^{32,ak} M. S. Neubauer,¹⁶⁹ M. Neumann,¹⁷⁸ P. R. Newman,¹⁹ T. Y. Ng,^{62c} T. Nguyen Manh,⁹⁷
 R. B. Nickerson,¹²² R. Nicolaidou,¹³⁸ J. Nielsen,¹³⁹ N. Nikiforou,¹¹ V. Nikolaenko,^{132,aj} I. Nikolic-Audit,⁸³
 K. Nikolopoulos,¹⁹ J. K. Nilsen,¹²¹ P. Nilsson,²⁷ Y. Ninomiya,¹⁵⁷ A. Nisati,^{134a} N. Nishu,^{36c} R. Nisius,¹⁰³ I. Nitsche,⁴⁶
 T. Nitta,¹⁷⁴ T. Nobe,¹⁵⁷ Y. Noguchi,⁷¹ M. Nomachi,¹²⁰ I. Nomidis,³¹ M. A. Nomura,²⁷ T. Nooney,⁷⁹ M. Nordberg,³²
 N. Norjoharuddeen,¹²² O. Novgorodova,⁴⁷ M. Nozaki,⁶⁹ L. Nozka,¹¹⁷ K. Ntekas,¹⁶⁶ E. Nurse,⁸¹ F. Nuti,⁹¹ K. O'Connor,²⁵
 D. C. O'Neil,¹⁴⁴ A. A. O'Rourke,⁴⁵ V. O'Shea,⁵⁶ F. G. Oakham,^{31,d} H. Oberlack,¹⁰³ T. Obermann,²³ J. Ocariz,⁸³ A. Ochi,⁷⁰
 I. Ochoa,³⁸ J. P. Ochoa-Ricoux,^{34a} S. Oda,⁷³ S. Odaka,⁶⁹ A. Oh,⁸⁷ S. H. Oh,⁴⁸ C. C. Ohm,¹⁴⁹ H. Ohman,¹⁶⁸ H. Oide,^{53a,53b}
 H. Okawa,¹⁶⁴ Y. Okumura,¹⁵⁷ T. Okuyama,⁶⁹ A. Olariu,^{28b} L. F. Oleiro Seabra,^{128a} S. A. Olivares Pino,^{34a}
 D. Oliveira Damazio,²⁷ A. Olszewski,⁴² J. Olszowska,⁴² A. Onofre,^{128a,128e} K. Onogi,¹⁰⁵ P. U. E. Onyisi,^{11,aa} H. Oppen,¹²¹
 M. J. Oreglia,³³ Y. Oren,¹⁵⁵ D. Orestano,^{136a,136b} N. Orlando,^{62b} R. S. Orr,¹⁶¹ B. Osculati,^{53a,53b,†} R. Ospanov,^{36a}
 G. Otero y Garzon,²⁹ H. Otono,⁷³ M. Ouchrif,^{137d} F. Ould-Saada,¹²¹ A. Ouraou,¹³⁸ K. P. Oussoren,¹⁰⁹ Q. Ouyang,^{35a}
 M. Owen,⁵⁶ R. E. Owen,¹⁹ V. E. Ozcan,^{20a} N. Ozturk,⁸ K. Pachal,¹⁴⁴ A. Pacheco Pages,¹³ L. Pacheco Rodriguez,¹³⁸
 C. Padilla Aranda,¹³ S. Pagan Griso,¹⁶ M. Paganini,¹⁷⁹ F. Paige,²⁷ G. Palacino,⁶⁴ S. Palazzo,^{40a,40b} S. Palestini,³² M. Palka,^{41b}
 D. Pallin,³⁷ E. St. Panagiotopoulou,¹⁰ I. Panagoulas,¹⁰ C. E. Pandini,⁵² J. G. Panduro Vazquez,⁸⁰ P. Pani,³² S. Panitkin,²⁷
 D. Pantea,^{28b} L. Paolozzi,⁵² Th. D. Papadopoulou,¹⁰ K. Papageorgiou,^{9,s} A. Paramonov,⁶ D. Paredes Hernandez,¹⁷⁹
 A. J. Parker,⁷⁵ M. A. Parker,³⁰ K. A. Parker,⁴⁵ F. Parodi,^{53a,53b} J. A. Parsons,³⁸ U. Parzefall,⁵¹ V. R. Pascuzzi,¹⁶¹
 J. M. Pasner,¹³⁹ E. Pasqualucci,^{134a} S. Passaggio,^{53a} Fr. Pastore,⁸⁰ S. Patariaia,⁸⁶ J. R. Pater,⁸⁷ T. Pauly,³² B. Pearson,¹⁰³
 S. Pedraza Lopez,¹⁷⁰ R. Pedro,^{128a,128b} S. V. Peleganchuk,^{111,c} O. Penc,¹²⁹ C. Peng,^{35a} H. Peng,^{36a} J. Penwell,⁶⁴
 B. S. Peralva,^{26b} M. M. Perego,¹³⁸ D. V. Perepelitsa,²⁷ F. Peri,¹⁷ L. Perini,^{94a,94b} H. Pernegger,³² S. Perrella,^{106a,106b}
 R. Peschke,⁴⁵ V. D. Peshekhonov,^{68,†} K. Peters,⁴⁵ R. F. Y. Peters,⁸⁷ B. A. Petersen,³² T. C. Petersen,³⁹ E. Petit,⁵⁸ A. Petridis,¹
 C. Petridou,¹⁵⁶ P. Petroff,¹¹⁹ E. Petrolo,^{134a} M. Petrov,¹²² F. Petrucci,^{136a,136b} N. E. Pettersson,⁸⁹ A. Peyaud,¹³⁸ R. Pezoa,^{34b}
 F. H. Phillips,⁹³ P. W. Phillips,¹³³ G. Piacquadio,¹⁵⁰ E. Pianori,¹⁷³ A. Picazio,⁸⁹ E. Piccaro,⁷⁹ M. A. Pickering,¹²² R. Piegaiia,²⁹
 J. E. Pilcher,³³ A. D. Pilkington,⁸⁷ M. Pinamonti,^{135a,135b} J. L. Pinfold,³ H. Pirumov,⁴⁵ M. Pitt,¹⁷⁵ L. Plazak,^{146a}
 M.-A. Pleier,²⁷ V. Pleskot,⁸⁶ E. Plotnikova,⁶⁸ D. Pluth,⁶⁷ P. Podberezko,¹¹¹ R. Poettgen,⁸⁴ R. Poggi,^{123a,123b} L. Poggioli,¹¹⁹
 I. Pogrebnyak,⁹³ D. Pohl,²³ I. Pokharel,⁵⁷ G. Polesello,^{123a} A. Poley,⁴⁵ A. Policicchio,^{40a,40b} R. Polifka,³² A. Polini,^{22a}
 C. S. Pollard,⁵⁶ V. Polychronakos,²⁷ K. Pommès,³² D. Ponomarenko,¹⁰⁰ L. Pontecorvo,^{134a} G. A. Popeneciu,^{28d}
 D. M. Portillo Quintero,⁸³ S. Pospisil,¹³⁰ K. Potamianos,⁴⁵ I. N. Potrap,⁶⁸ C. J. Potter,³⁰ H. Potti,¹¹ T. Poulsen,⁸⁴ J. Poveda,³²
 M. E. Pozo Astigarraga,³² P. Pralavorio,⁸⁸ A. Pranko,¹⁶ S. Prell,⁶⁷ D. Price,⁸⁷ M. Primavera,^{76a} S. Prince,⁹⁰ N. Proklova,¹⁰⁰
 K. Prokofiev,^{62c} F. Prokoshin,^{34b} S. Protopopescu,²⁷ J. Proudfoot,⁶ M. Przybycien,^{41a} A. Puri,¹⁶⁹ P. Puzo,¹¹⁹ J. Qian,⁹²
 G. Qin,⁵⁶ Y. Qin,⁸⁷ A. Quadt,⁵⁷ M. Queitsch-Maitland,⁴⁵ D. Quilty,⁵⁶ S. Raddum,¹²¹ V. Radeka,²⁷ V. Radescu,¹²²
 S. K. Radhakrishnan,¹⁵⁰ P. Radloff,¹¹⁸ P. Rados,⁹¹ F. Ragusa,^{94a,94b} G. Rahal,¹⁸¹ J. A. Raine,⁸⁷ S. Rajagopalan,²⁷
 C. Rangel-Smith,¹⁶⁸ T. Rashid,¹¹⁹ S. Raspopov,⁵ M. G. Ratti,^{94a,94b} D. M. Rauch,⁴⁵ F. Rauscher,¹⁰² S. Rave,⁸⁶
 I. Ravinovich,¹⁷⁵ J. H. Rawling,⁸⁷ M. Raymond,³² A. L. Read,¹²¹ N. P. Readioff,⁵⁸ M. Reale,^{76a,76b} D. M. Rebuzzi,^{123a,123b}
 A. Redelbach,¹⁷⁷ G. Redlinger,²⁷ R. Reece,¹³⁹ R. G. Reed,^{147c} K. Reeves,⁴⁴ L. Rehnisch,¹⁷ J. Reichert,¹²⁴ A. Reiss,⁸⁶
 C. Rembser,³² H. Ren,^{35a} M. Rescigno,^{134a} S. Resconi,^{94a} E. D. Resseguie,¹²⁴ S. Rettie,¹⁷¹ E. Reynolds,¹⁹
 O. L. Rezanova,^{111,c} P. Reznicek,¹³¹ R. Rezvani,⁹⁷ R. Richter,¹⁰³ S. Richter,⁸¹ E. Richter-Was,^{41b} O. Ricken,²³ M. Ridel,⁸³
 P. Rieck,¹⁰³ C. J. Riegel,¹⁷⁸ J. Rieger,⁵⁷ O. Rifki,¹¹⁵ M. Rijssenbeek,¹⁵⁰ A. Rimoldi,^{123a,123b} M. Rimoldi,¹⁸ L. Rinaldi,^{22a}

G. Ripellino,¹⁴⁹ B. Ristić,³² E. Ritsch,³² I. Riu,¹³ F. Rizatdinova,¹¹⁶ E. Rizvi,⁷⁹ C. Rizzi,¹³ R. T. Roberts,⁸⁷
 S. H. Robertson,^{90,o} A. Robichaud-Veronneau,⁹⁰ D. Robinson,³⁰ J. E. M. Robinson,⁴⁵ A. Robson,⁵⁶ E. Rocco,⁸⁶
 C. Roda,^{126a,126b} Y. Rodina,^{88,al} S. Rodriguez Bosca,¹⁷⁰ A. Rodriguez Perez,¹³ D. Rodriguez Rodriguez,¹⁷⁰ S. Roe,³²
 C. S. Rogan,⁵⁹ O. Røhne,¹²¹ J. Roloff,⁵⁹ A. Romaniouk,¹⁰⁰ M. Romano,^{22a,22b} S. M. Romano Saez,³⁷ E. Romero Adam,¹⁷⁰
 N. Rompotis,⁷⁷ M. Ronzani,⁵¹ L. Roos,⁸³ S. Rosati,^{134a} K. Rosbach,⁵¹ P. Rose,¹³⁹ N.-A. Rosien,⁵⁷ E. Rossi,^{106a,106b}
 L. P. Rossi,^{53a} J. H. N. Rosten,³⁰ R. Rosten,¹⁴⁰ M. Rotaru,^{28b} J. Rothberg,¹⁴⁰ D. Rousseau,¹¹⁹ A. Rozanov,⁸⁸ Y. Rozen,¹⁵⁴
 X. Ruan,^{147c} F. Rubbo,¹⁴⁵ F. Rühr,⁵¹ A. Ruiz-Martinez,³¹ Z. Rurikova,⁵¹ N. A. Rusakovich,⁶⁸ H. L. Russell,⁹⁰
 J. P. Rutherford,⁷ N. Ruthmann,³² Y. F. Ryabov,¹²⁵ M. Rybar,¹⁶⁹ G. Rybkin,¹¹⁹ S. Ryu,⁶ A. Ryzhov,¹³² G. F. Rzehorz,⁵⁷
 A. F. Saavedra,¹⁵² G. Sabato,¹⁰⁹ S. Sacerdoti,²⁹ H. F.-W. Sadrozinski,¹³⁹ R. Sadykov,⁶⁸ F. Safai Tehrani,^{134a} P. Saha,¹¹⁰
 M. Sahinsoy,^{60a} M. Saimpert,⁴⁵ M. Saito,¹⁵⁷ T. Saito,¹⁵⁷ H. Sakamoto,¹⁵⁷ Y. Sakurai,¹⁷⁴ G. Salamanna,^{136a,136b}
 J. E. Salazar Loyola,^{34b} D. Salek,¹⁰⁹ P. H. Sales De Bruin,¹⁶⁸ D. Salihagic,¹⁰³ A. Salnikov,¹⁴⁵ J. Salt,¹⁷⁰ D. Salvatore,^{40a,40b}
 F. Salvatore,¹⁵¹ A. Salvucci,^{62a-62c} A. Salzburger,³² D. Sammel,⁵¹ D. Sampsonidis,¹⁵⁶ D. Sampsonidou,¹⁵⁶ J. Sánchez,¹⁷⁰
 V. Sanchez Martinez,¹⁷⁰ A. Sanchez Pineda,^{167a,167c} H. Sandaker,¹²¹ R. L. Sandbach,⁷⁹ C. O. Sander,⁴⁵ M. Sandhoff,¹⁷⁸
 C. Sandoval,²¹ D. P. C. Sankey,¹³³ M. Sannino,^{53a,53b} Y. Sano,¹⁰⁵ A. Sansoni,⁵⁰ C. Santoni,³⁷ H. Santos,^{128a}
 I. Santoyo Castillo,¹⁵¹ A. Sapronov,⁶⁸ J. G. Saraiva,^{128a,128d} B. Sarrazin,²³ O. Sasaki,⁶⁹ K. Sato,¹⁶⁴ E. Sauvan,⁵ G. Savage,⁸⁰
 P. Savard,^{161,d} N. Savic,¹⁰³ C. Sawyer,¹³³ L. Sawyer,^{82,u} J. Saxon,³³ C. Sbarra,^{22a} A. Sbrizzi,^{22a,22b} T. Scanlon,⁸¹
 D. A. Scannicchio,¹⁶⁶ J. Schaarschmidt,¹⁴⁰ P. Schacht,¹⁰³ B. M. Schachtner,¹⁰² D. Schaefer,³³ L. Schaefer,¹²⁴ R. Schaefer,⁴⁵
 J. Schaeffer,⁸⁶ S. Schaepe,²³ S. Schaezel,^{60b} U. Schäfer,⁸⁶ A. C. Schaffer,¹¹⁹ D. Schaile,¹⁰² R. D. Schamberger,¹⁵⁰
 V. A. Schegelsky,¹²⁵ D. Scheirich,¹³¹ M. Schernau,¹⁶⁶ C. Schiavi,^{53a,53b} S. Schier,¹³⁹ L. K. Schildgen,²³ C. Schillo,⁵¹
 M. Schioppa,^{40a,40b} S. Schlenker,³² K. R. Schmidt-Sommerfeld,¹⁰³ K. Schmieden,³² C. Schmitt,⁸⁶ S. Schmitt,⁴⁵ S. Schmitz,⁸⁶
 U. Schnoor,⁵¹ L. Schoeffel,¹³⁸ A. Schoening,^{60b} B. D. Schoenrock,⁹³ E. Schopf,²³ M. Schott,⁸⁶ J. F. P. Schouwenberg,¹⁰⁸
 J. Schovancova,³² S. Schramm,⁵² N. Schuh,⁸⁶ A. Schulte,⁸⁶ M. J. Schultens,²³ H.-C. Schultz-Coulon,^{60a} H. Schulz,¹⁷
 M. Schumacher,⁵¹ B. A. Schumm,¹³⁹ Ph. Schune,¹³⁸ A. Schwartzman,¹⁴⁵ T. A. Schwarz,⁹² H. Schweiger,⁸⁷
 Ph. Schwemling,¹³⁸ R. Schwenhorst,⁹³ J. Schwindling,¹³⁸ A. Sciandra,²³ G. Sciolla,²⁵ M. Scornajenghi,^{40a,40b}
 F. Scuri,^{126a,126b} F. Scutti,⁹¹ J. Searcy,⁹² P. Seema,²³ S. C. Seidel,¹⁰⁷ A. Seiden,¹³⁹ J. M. Seixas,^{26a} G. Sekhniaidze,^{106a}
 K. Sekhon,⁹² S. J. Sekula,⁴³ N. Semprini-Cesari,^{22a,22b} S. Senkin,³⁷ C. Serfon,¹²¹ L. Serin,¹¹⁹ L. Serkin,^{167a,167b}
 M. Sessa,^{136a,136b} R. Seuster,¹⁷² H. Severini,¹¹⁵ T. Sfiligoi,⁷⁸ F. Sforza,¹⁶⁵ A. Sfyrla,⁵² E. Shabalina,⁵⁷ N. W. Shaikh,^{148a,148b}
 L. Y. Shan,^{35a} R. Shang,¹⁶⁹ J. T. Shank,²⁴ M. Shapiro,¹⁶ P. B. Shatalov,⁹⁹ K. Shaw,^{167a,167b} S. M. Shaw,⁸⁷
 A. Shcherbakova,^{148a,148b} C. Y. Shehu,¹⁵¹ Y. Shen,¹¹⁵ N. Sherafati,³¹ P. Sherwood,⁸¹ L. Shi,^{153,am} S. Shimizu,⁷⁰
 C. O. Shimmin,¹⁷⁹ M. Shimojima,¹⁰⁴ I. P. J. Shipsey,¹²² S. Shirabe,⁷³ M. Shiyakova,^{68,an} J. Shlomi,¹⁷⁵ A. Shmeleva,⁹⁸
 D. Shoaleh Saadi,⁹⁷ M. J. Shochet,³³ S. Shojaii,^{94a,94b} D. R. Shope,¹¹⁵ S. Shrestha,¹¹³ E. Shulga,¹⁰⁰ M. A. Shupe,⁷ P. Sicho,¹²⁹
 A. M. Sickles,¹⁶⁹ P. E. Sidebo,¹⁴⁹ E. Sideras Haddad,^{147c} O. Sidiropoulou,¹⁷⁷ A. Sidoti,^{22a,22b} F. Siegert,⁴⁷ Dj. Sijacki,¹⁴
 J. Silva,^{128a,128d} S. B. Silverstein,^{148a} V. Simak,¹³⁰ L. Simic,⁶⁸ S. Simion,¹¹⁹ E. Simioni,⁸⁶ B. Simmons,⁸¹ M. Simon,⁸⁶
 P. Sinervo,¹⁶¹ N. B. Sinev,¹¹⁸ M. Sioli,^{22a,22b} G. Siragusa,¹⁷⁷ I. Siral,⁹² S. Yu. Sivoklov,¹⁰¹ J. Sjölin,^{148a,148b} M. B. Skinner,⁷⁵
 P. Skubic,¹¹⁵ M. Slater,¹⁹ T. Slavicek,¹³⁰ M. Slawinska,⁴² K. Sliwa,¹⁶⁵ R. Slovak,¹³¹ V. Smakhtin,¹⁷⁵ B. H. Smart,⁵
 J. Smiesko,^{146a} N. Smirnov,¹⁰⁰ S. Yu. Smirnov,¹⁰⁰ Y. Smirnov,¹⁰⁰ L. N. Smirnova,^{101,ao} O. Smirnova,⁸⁴ J. W. Smith,⁵⁷
 M. N. K. Smith,³⁸ R. W. Smith,³⁸ M. Smizanska,⁷⁵ K. Smolek,¹³⁰ A. A. Snesarev,⁹⁸ I. M. Snyder,¹¹⁸ S. Snyder,²⁷
 R. Sobie,^{172,o} F. Socher,⁴⁷ A. Soffer,¹⁵⁵ A. Søggaard,⁴⁹ D. A. Soh,¹⁵³ G. Sokhrannyi,⁷⁸ C. A. Solans Sanchez,³² M. Solar,¹³⁰
 E. Yu. Soldatov,¹⁰⁰ U. Soldevila,¹⁷⁰ A. A. Solodkov,¹³² A. Soloshenko,⁶⁸ O. V. Solovyanov,¹³² V. Solovyev,¹²⁵ P. Sommer,⁵¹
 H. Son,¹⁶⁵ A. Sopczak,¹³⁰ D. Sosa,^{60b} C. L. Sotiropoulou,^{126a,126b} S. Sottocornola,^{123a,123b} R. Soualah,^{167a,167c}
 A. M. Soukharev,^{111,c} D. South,⁴⁵ B. C. Sowden,⁸⁰ S. Spagnolo,^{76a,76b} M. Spalla,^{126a,126b} M. Spangenberg,¹⁷³ F. Spanò,⁸⁰
 D. Sperlich,¹⁷ F. Spettel,¹⁰³ T. M. Spieker,^{60a} R. Spighi,^{22a} G. Spigo,³² L. A. Spiller,⁹¹ M. Spousta,¹³¹ R. D. St. Denis,^{56,†}
 A. Stabile,^{94a} R. Stamen,^{60a} S. Stamm,¹⁷ E. Stanecka,⁴² R. W. Stanek,⁶ C. Stanescu,^{136a} M. M. Stanitzki,⁴⁵ B. S. Stapf,¹⁰⁹
 S. Stapnes,¹²¹ E. A. Starchenko,¹³² G. H. Stark,³³ J. Stark,⁵⁸ S. H. Stark,³⁹ P. Staroba,¹²⁹ P. Starovoitov,^{60a} S. Stärz,³²
 R. Staszewski,⁴² M. Stegler,⁴⁵ P. Steinberg,²⁷ B. Stelzer,¹⁴⁴ H. J. Stelzer,³² O. Stelzer-Chilton,^{163a} H. Stenzel,⁵⁵
 G. A. Stewart,⁵⁶ M. C. Stockton,¹¹⁸ M. Stoebe,⁹⁰ G. Stoicea,^{28b} P. Stolte,⁵⁷ S. Stonjek,¹⁰³ A. R. Stradling,⁸ A. Straessner,⁴⁷
 M. E. Stramaglia,¹⁸ J. Strandberg,¹⁴⁹ S. Strandberg,^{148a,148b} M. Strauss,¹¹⁵ P. Strizenec,^{146b} R. Ströhmer,¹⁷⁷ D. M. Strom,¹¹⁸
 R. Stroynowski,⁴³ A. Strubig,⁴⁹ S. A. Stucci,²⁷ B. Stugu,¹⁵ N. A. Styles,⁴⁵ D. Su,¹⁴⁵ J. Su,¹²⁷ S. Suchek,^{60a} Y. Sugaya,¹²⁰
 M. Suk,¹³⁰ V. V. Sulin,⁹⁸ DMS Sultan,^{162a,162b} S. Sultansoy,^{4c} T. Sumida,⁷¹ S. Sun,⁵⁹ X. Sun,³ K. Suruliz,¹⁵¹ C. J. E. Suster,¹⁵²

M. R. Sutton,¹⁵¹ S. Suzuki,⁶⁹ M. Svatos,¹²⁹ M. Swiatlowski,³³ S. P. Swift,² I. Sykora,^{146a} T. Sykora,¹³¹ D. Ta,⁵¹ K. Tackmann,⁴⁵ J. Taenzer,¹⁵⁵ A. Taffard,¹⁶⁶ R. Tafirout,^{163a} E. Tahirovic,⁷⁹ N. Taiblum,¹⁵⁵ H. Takai,²⁷ R. Takashima,⁷² E. H. Takasugi,¹⁰³ K. Takeda,⁷⁰ T. Takeshita,¹⁴² Y. Takubo,⁶⁹ M. Talby,⁸⁸ A. A. Talyshv,^{111,c} J. Tanaka,¹⁵⁷ M. Tanaka,¹⁵⁹ R. Tanaka,¹¹⁹ S. Tanaka,⁶⁹ R. Tanioka,⁷⁰ B. B. Tannenwald,¹¹³ S. Tapia Araya,^{34b} S. Tapprogge,⁸⁶ S. Tarem,¹⁵⁴ G. F. Tartarelli,^{94a} P. Tas,¹³¹ M. Tasevsky,¹²⁹ T. Tashiro,⁷¹ E. Tassi,^{40a,40b} A. Tavares Delgado,^{128a,128b} Y. Tayalati,^{137e} A. C. Taylor,¹⁰⁷ A. J. Taylor,⁴⁹ G. N. Taylor,⁹¹ P. T. E. Taylor,⁹¹ W. Taylor,^{163b} P. Teixeira-Dias,⁸⁰ D. Temple,¹⁴⁴ H. Ten Kate,³² P. K. Teng,¹⁵³ J. J. Teoh,¹²⁰ F. Tepel,¹⁷⁸ S. Terada,⁶⁹ K. Terashi,¹⁵⁷ J. Terron,⁸⁵ S. Terzo,¹³ M. Testa,⁵⁰ R. J. Teuscher,^{161,o} T. Thevenaux-Pelzer,⁸⁸ F. Thiele,³⁹ J. P. Thomas,¹⁹ J. Thomas-Wilsker,⁸⁰ P. D. Thompson,¹⁹ A. S. Thompson,⁵⁶ L. A. Thomsen,¹⁷⁹ E. Thomson,¹²⁴ Y. Tian,³⁸ M. J. Tibbetts,¹⁶ R. E. Tice Torres,⁸⁸ V. O. Tikhomirov,^{98,ap} Yu. A. Tikhonov,^{111,c} S. Timoshenko,¹⁰⁰ P. Tipton,¹⁷⁹ S. Tisserant,⁸⁸ K. Todome,¹⁵⁹ S. Todorova-Nova,⁵ S. Todt,⁴⁷ J. Tojo,⁷³ S. Tokár,^{146a} K. Tokushuku,⁶⁹ E. Tolley,¹¹³ L. Tomlinson,⁸⁷ M. Tomoto,¹⁰⁵ L. Tompkins,^{145,aq} K. Toms,¹⁰⁷ B. Tong,⁵⁹ P. Tornambe,⁵¹ E. Torrence,¹¹⁸ H. Torres,⁴⁷ E. Torró Pastor,¹⁴⁰ J. Toth,^{88,ar} F. Touchard,⁸⁸ D. R. Tovey,¹⁴¹ C. J. Treado,¹¹² T. Trefzger,¹⁷⁷ F. Tresoldi,¹⁵¹ A. Tricoli,²⁷ I. M. Trigger,^{163a} S. Trincaz-Duvold,⁸³ M. F. Tripiana,¹³ W. Trischuk,¹⁶¹ B. Trocmé,⁵⁸ A. Trofymov,⁴⁵ C. Troncon,^{94a} M. Trotter-McDonald,¹⁶ M. Trovatelli,¹⁷² L. Truong,^{147b} M. Trzebinski,⁴² A. Trzupek,⁴² K. W. Tsang,^{62a} J. C.-L. Tseng,¹²² P. V. Tsiarehka,⁹⁵ G. Tsipolitis,¹⁰ N. Tsirintanis,⁹ S. Tsiskaridze,¹³ V. Tsiskaridze,⁵¹ E. G. Tskhadadze,^{54a} I. I. Tsukerman,⁹⁹ V. Tsulaia,¹⁶ S. Tsuno,⁶⁹ D. Tsybychev,¹⁵⁰ Y. Tu,^{62b} A. Tudorache,^{28b} V. Tudorache,^{28b} T. T. Tulbure,^{28a} A. N. Tuna,⁵⁹ S. Turchikhin,⁶⁸ D. Turgeman,¹⁷⁵ I. Turk Cakir,^{4b,as} R. Turra,^{94a} P. M. Tuts,³⁸ G. Uccielli,^{22a,22b} I. Ueda,⁶⁹ M. Ughetto,^{148a,148b} F. Ukegawa,¹⁶⁴ G. Unal,³² A. Undrus,²⁷ G. Unel,¹⁶⁶ F. C. Ungaro,⁹¹ Y. Unno,⁶⁹ K. Uno,¹⁵⁷ C. Unverdorben,¹⁰² J. Urban,^{146b} P. Urquijo,⁹¹ P. Urrejola,⁸⁶ G. Usai,⁸ J. Usui,⁶⁹ L. Vacavant,⁸⁸ V. Vacek,¹³⁰ B. Vachon,⁹⁰ K. O. H. Vadla,¹²¹ A. Vaidya,⁸¹ C. Valderanis,¹⁰² E. Valdes Santurio,^{148a,148b} M. Valente,⁵² S. Valentinetti,^{22a,22b} A. Valero,¹⁷⁰ L. Valéry,¹³ S. Valkar,¹³¹ A. Vallier,⁵ J. A. Valls Ferrer,¹⁷⁰ W. Van Den Wollenberg,¹⁰⁹ H. van der Graaf,¹⁰⁹ P. van Gemmeren,⁶ J. Van Nieuwkoop,¹⁴⁴ I. van Vulpen,¹⁰⁹ M. C. van Woerden,¹⁰⁹ M. Vanadia,^{135a,135b} W. Vandelli,³² A. Vaniachine,¹⁶⁰ P. Vankov,¹⁰⁹ G. Vardanyan,¹⁸⁰ R. Vari,^{134a} E. W. Varnes,⁷ C. Varni,^{53a,53b} T. Varol,⁴³ D. Varouchas,¹¹⁹ A. Vartapetian,⁸ K. E. Varvell,¹⁵² J. G. Vasquez,¹⁷⁹ G. A. Vasquez,^{34b} F. Vazeille,³⁷ D. Vazquez Furelos,¹³ T. Vazquez Schroeder,⁹⁰ J. Veatch,⁵⁷ V. Veeraraghavan,⁷ L. M. Veloce,¹⁶¹ F. Veloso,^{128a,128c} S. Veneziano,^{134a} A. Ventura,^{76a,76b} M. Venturi,¹⁷² N. Venturi,³² A. Venturini,²⁵ V. Vercesi,^{123a} M. Verducci,^{136a,136b} W. Verkerke,¹⁰⁹ A. T. Vermeulen,¹⁰⁹ J. C. Vermeulen,¹⁰⁹ M. C. Vetterli,^{144,d} N. Viaux Maira,^{34b} O. Viazlo,⁸⁴ I. Vichou,^{169,†} T. Vickey,¹⁴¹ O. E. Vickey Boeriu,¹⁴¹ G. H. A. Viehhauser,¹²² S. Viel,¹⁶ L. Vigani,¹²² M. Villa,^{22a,22b} M. Villaplana Perez,^{94a,94b} E. Vilucchi,⁵⁰ M. G. Vincter,³¹ V. B. Vinogradov,⁶⁸ A. Vishwakarma,⁴⁵ C. Vittori,^{22a,22b} I. Vivarelli,¹⁵¹ S. Vlachos,¹⁰ M. Vogel,¹⁷⁸ P. Vokac,¹³⁰ G. Volpi,¹³ H. von der Schmitt,¹⁰³ E. von Toerne,²³ V. Vorobel,¹³¹ K. Vorobev,¹⁰⁰ M. Vos,¹⁷⁰ R. Voss,³² J. H. Vosseveld,⁷⁷ N. Vranjes,¹⁴ M. Vranjes Milosavljevic,¹⁴ V. Vrba,¹³⁰ M. Vreeswijk,¹⁰⁹ R. Vuillermet,³² I. Vukotic,³³ P. Wagner,²³ W. Wagner,¹⁷⁸ J. Wagner-Kuhr,¹⁰² H. Wahlberg,⁷⁴ S. Wahrmund,⁴⁷ J. Walder,⁷⁵ R. Walker,¹⁰² W. Walkowiak,¹⁴³ V. Wallangen,^{148a,148b} C. Wang,^{35b} C. Wang,^{36b,at} F. Wang,¹⁷⁶ H. Wang,¹⁶ H. Wang,³ J. Wang,⁴⁵ J. Wang,¹⁵² Q. Wang,¹¹⁵ R.-J. Wang,⁸³ R. Wang,⁶ S. M. Wang,¹⁵³ T. Wang,³⁸ W. Wang,^{153,au} W. Wang,^{36a,av} Z. Wang,^{36c} C. Wanotayaroj,⁴⁵ A. Warburton,⁹⁰ C. P. Ward,³⁰ D. R. Wardrope,⁸¹ A. Washbrook,⁴⁹ P. M. Watkins,¹⁹ A. T. Watson,¹⁹ M. F. Watson,¹⁹ G. Watts,¹⁴⁰ S. Watts,⁸⁷ B. M. Waugh,⁸¹ A. F. Webb,¹¹ S. Webb,⁸⁶ M. S. Weber,¹⁸ S. M. Weber,^{60a} S. W. Weber,¹⁷⁷ S. A. Weber,³¹ J. S. Webster,⁶ A. R. Weidberg,¹²² B. Weinert,⁶⁴ J. Weingarten,⁵⁷ M. Weirich,⁸⁶ C. Weiser,⁵¹ H. Weits,¹⁰⁹ P. S. Wells,³² T. Wenaus,²⁷ T. Wengler,³² S. Wenig,³² N. Vermes,²³ M. D. Werner,⁶⁷ P. Werner,³² M. Wessels,^{60a} T. D. Weston,¹⁸ K. Whalen,¹¹⁸ N. L. Whallon,¹⁴⁰ A. M. Wharton,⁷⁵ A. S. White,⁹² A. White,⁸ M. J. White,¹ R. White,^{34b} D. Whiteson,¹⁶⁶ B. W. Whitmore,⁷⁵ F. J. Wickens,¹³³ W. Wiedenmann,¹⁷⁶ M. Wielers,¹³³ C. Wiglesworth,³⁹ L. A. M. Wiik-Fuchs,⁵¹ A. Wildauer,¹⁰³ F. Wilk,⁸⁷ H. G. Wilkens,³² H. H. Williams,¹²⁴ S. Williams,¹⁰⁹ C. Willis,⁹³ S. Willocq,⁸⁹ J. A. Wilson,¹⁹ I. Wingerter-Seez,⁵ E. Winkels,¹⁵¹ F. Winklmeier,¹¹⁸ O. J. Winston,¹⁵¹ B. T. Winter,²³ M. Wittgen,¹⁴⁵ M. Wobisch,^{82,u} T. M. H. Wolf,¹⁰⁹ R. Wolff,⁸⁸ M. W. Wolter,⁴² H. Wolters,^{128a,128c} V. W. S. Wong,¹⁷¹ N. L. Woods,¹³⁹ S. D. Worm,¹⁹ B. K. Wosiek,⁴² J. Wotschack,³² K. W. Wozniak,⁴² M. Wu,³³ S. L. Wu,¹⁷⁶ X. Wu,⁵² Y. Wu,⁹² T. R. Wyatt,⁸⁷ B. M. Wynne,⁴⁹ S. Xella,³⁹ Z. Xi,⁹² L. Xia,^{35c} D. Xu,^{35a} L. Xu,²⁷ T. Xu,¹³⁸ B. Yabsley,¹⁵² S. Yacoob,^{147a} D. Yamaguchi,¹⁵⁹ Y. Yamaguchi,¹⁵⁹ A. Yamamoto,⁶⁹ S. Yamamoto,¹⁵⁷ T. Yamanaka,¹⁵⁷ F. Yamane,⁷⁰ M. Yamatani,¹⁵⁷ Y. Yamazaki,⁷⁰ Z. Yan,²⁴ H. Yang,^{36c} H. Yang,¹⁶ Y. Yang,¹⁵³ Z. Yang,¹⁵ W.-M. Yao,¹⁶ Y. C. Yap,⁴⁵ Y. Yasu,⁶⁹ E. Yatsenko,⁵ K. H. Yau Wong,²³ J. Ye,⁴³ S. Ye,²⁷ I. Yeletsikh,⁶⁸ E. Yigitbasi,²⁴ E. Yildirim,⁸⁶ K. Yorita,¹⁷⁴ K. Yoshihara,¹²⁴ C. Young,¹⁴⁵ C. J. S. Young,³² J. Yu,⁸ J. Yu,⁶⁷

S. P. Y. Yuen,²³ I. Yusuff,^{30,aw} B. Zabinski,⁴² G. Zacharis,¹⁰ R. Zaidan,¹³ A. M. Zaitsev,^{132,aj} N. Zakharchuk,⁴⁵ J. Zalieckas,¹⁵ A. Zaman,¹⁵⁰ S. Zambito,⁵⁹ D. Zanzi,⁹¹ C. Zeitnitz,¹⁷⁸ G. Zemaityte,¹²² A. Zemla,^{41a} J. C. Zeng,¹⁶⁹ Q. Zeng,¹⁴⁵ O. Zenin,¹³² T. Ženiš,^{146a} D. Zerwas,¹¹⁹ D. Zhang,^{36b} D. Zhang,⁹² F. Zhang,¹⁷⁶ G. Zhang,^{36a,av} H. Zhang,¹¹⁹ J. Zhang,⁶ L. Zhang,⁵¹ L. Zhang,^{36a} M. Zhang,¹⁶⁹ P. Zhang,^{35b} R. Zhang,²³ R. Zhang,^{36a,at} X. Zhang,^{36b} Y. Zhang,^{35a} Z. Zhang,¹¹⁹ X. Zhao,⁴³ Y. Zhao,^{36b,ax} Z. Zhao,^{36a} A. Zhemchugov,⁶⁸ B. Zhou,⁹² C. Zhou,¹⁷⁶ L. Zhou,⁴³ M. Zhou,^{35a} M. Zhou,¹⁵⁰ N. Zhou,^{35c} Y. Zhou,⁷ C. G. Zhu,^{36b} H. Zhu,^{35a} J. Zhu,⁹² Y. Zhu,^{36a} X. Zhuang,^{35a} K. Zhukov,⁹⁸ A. Zibell,¹⁷⁷ D. Zieminska,⁶⁴ N. I. Zimine,⁶⁸ C. Zimmermann,⁸⁶ S. Zimmermann,⁵¹ Z. Zinonos,¹⁰³ M. Zinser,⁸⁶ M. Ziolkowski,¹⁴³ L. Živković,¹⁴ G. Zoernig,¹⁷⁶ A. Zoccoli,^{22a,22b} R. Zou,³³ M. zur Nedden,¹⁷ and L. Zwalinski³²

(ATLAS Collaboration)

¹*Department of Physics, University of Adelaide, Adelaide, Australia*

²*Physics Department, SUNY Albany, Albany New York, USA*

³*Department of Physics, University of Alberta, Edmonton Alberta, Canada*

^{4a}*Department of Physics, Ankara University, Ankara, Turkey*

^{4b}*Istanbul Aydin University, Istanbul, Turkey*

^{4c}*Division of Physics, TOBB University of Economics and Technology, Ankara, Turkey*

⁵*LAPP, CNRS/IN2P3 and Université Savoie Mont Blanc, Annecy-le-Vieux, France*

⁶*High Energy Physics Division, Argonne National Laboratory, Argonne Illinois, USA*

⁷*Department of Physics, University of Arizona, Tucson Arizona, USA*

⁸*Department of Physics, The University of Texas at Arlington, Arlington Texas, USA*

⁹*Physics Department, National and Kapodistrian University of Athens, Athens, Greece*

¹⁰*Physics Department, National Technical University of Athens, Zografou, Greece*

¹¹*Department of Physics, The University of Texas at Austin, Austin Texas, USA*

¹²*Institute of Physics, Azerbaijan Academy of Sciences, Baku, Azerbaijan*

¹³*Institut de Física d'Altes Energies (IFAE), The Barcelona Institute of Science and Technology, Barcelona, Spain*

¹⁴*Institute of Physics, University of Belgrade, Belgrade, Serbia*

¹⁵*Department for Physics and Technology, University of Bergen, Bergen, Norway*

¹⁶*Physics Division, Lawrence Berkeley National Laboratory and University of California, Berkeley California, USA*

¹⁷*Department of Physics, Humboldt University, Berlin, Germany*

¹⁸*Albert Einstein Center for Fundamental Physics and Laboratory for High Energy Physics, University of Bern, Bern, Switzerland*

¹⁹*School of Physics and Astronomy, University of Birmingham, Birmingham, United Kingdom*

^{20a}*Department of Physics, Bogazici University, Istanbul, Turkey*

^{20b}*Department of Physics Engineering, Gaziantep University, Gaziantep, Turkey*

^{20d}*Istanbul Bilgi University, Faculty of Engineering and Natural Sciences, Istanbul, Turkey*

^{20c}*Bahcesehir University, Faculty of Engineering and Natural Sciences, Istanbul, Turkey*

²¹*Centro de Investigaciones, Universidad Antonio Narino, Bogota, Colombia*

^{22a}*INFN Sezione di Bologna, Italy*

^{22b}*Dipartimento di Fisica e Astronomia, Università di Bologna, Bologna, Italy*

²³*Physikalisches Institut, University of Bonn, Bonn, Germany*

²⁴*Department of Physics, Boston University, Boston Massachusetts, USA*

²⁵*Department of Physics, Brandeis University, Waltham Massachusetts, USA*

^{26a}*Universidade Federal do Rio De Janeiro COPPE/EE/IF, Rio de Janeiro, Brazil*

^{26b}*Electrical Circuits Department, Federal University of Juiz de Fora (UFJF), Juiz de Fora, Brazil*

^{26c}*Federal University of Sao Joao del Rei (UFSJ), Sao Joao del Rei, Brazil*

^{26d}*Instituto de Física, Universidade de Sao Paulo, Sao Paulo, Brazil*

²⁷*Physics Department, Brookhaven National Laboratory, Upton New York, USA*

^{28a}*Transilvania University of Brasov, Brasov, Romania*

^{28b}*Horia Hulubei National Institute of Physics and Nuclear Engineering, Bucharest, Romania*

^{28c}*Department of Physics, Alexandru Ioan Cuza University of Iasi, Iasi, Romania*

^{28d}*National Institute for Research and Development of Isotopic and Molecular Technologies, Physics Department, Cluj Napoca, Romania*

^{28e}*University Politehnica Bucharest, Bucharest, Romania*

^{28f}*West University in Timisoara, Timisoara, Romania*

²⁹*Departamento de Física, Universidad de Buenos Aires, Buenos Aires, Argentina*

- ³⁰*Cavendish Laboratory, University of Cambridge, Cambridge, United Kingdom*
- ³¹*Department of Physics, Carleton University, Ottawa Ontario, Canada*
- ³²*CERN, Geneva, Switzerland*
- ³³*Enrico Fermi Institute, University of Chicago, Chicago Illinois, USA*
- ^{34a}*Departamento de Física, Pontificia Universidad Católica de Chile, Santiago, Chile*
- ^{34b}*Departamento de Física, Universidad Técnica Federico Santa María, Valparaíso, Chile*
- ^{35a}*Institute of High Energy Physics, Chinese Academy of Sciences, Beijing, China*
- ^{35b}*Department of Physics, Nanjing University, Jiangsu, China*
- ^{35c}*Physics Department, Tsinghua University, Beijing 100084, China*
- ^{36a}*Department of Modern Physics and State Key Laboratory of Particle Detection and Electronics, University of Science and Technology of China, Anhui, China*
- ^{36b}*School of Physics, Shandong University, Shandong, China*
- ^{36c}*Department of Physics and Astronomy, Key Laboratory for Particle Physics, Astrophysics and Cosmology, Ministry of Education; Shanghai Key Laboratory for Particle Physics and Cosmology, Shanghai Jiao Tong University, Shanghai(also at PKU-CHEP), China*
- ³⁷*Université Clermont Auvergne, CNRS/IN2P3, LPC, Clermont-Ferrand, France*
- ³⁸*Nevis Laboratory, Columbia University, Irvington New York, USA*
- ³⁹*Niels Bohr Institute, University of Copenhagen, Kobenhavn, Denmark*
- ^{40a}*INFN Gruppo Collegato di Cosenza, Laboratori Nazionali di Frascati, Italy*
- ^{40b}*Dipartimento di Fisica, Università della Calabria, Rende, Italy*
- ^{41a}*AGH University of Science and Technology, Faculty of Physics and Applied Computer Science, Krakow, Poland*
- ^{41b}*Marian Smoluchowski Institute of Physics, Jagiellonian University, Krakow, Poland*
- ⁴²*Institute of Nuclear Physics Polish Academy of Sciences, Krakow, Poland*
- ⁴³*Physics Department, Southern Methodist University, Dallas Texas, USA*
- ⁴⁴*Physics Department, University of Texas at Dallas, Richardson Texas, USA*
- ⁴⁵*DESY, Hamburg and Zeuthen, Germany*
- ⁴⁶*Lehrstuhl für Experimentelle Physik IV, Technische Universität Dortmund, Dortmund, Germany*
- ⁴⁷*Institut für Kern- und Teilchenphysik, Technische Universität Dresden, Dresden, Germany*
- ⁴⁸*Department of Physics, Duke University, Durham North Carolin, USA*
- ⁴⁹*SUPA—School of Physics and Astronomy, University of Edinburgh, Edinburgh, United Kingdom*
- ⁵⁰*INFN e Laboratori Nazionali di Frascati, Frascati, Italy*
- ⁵¹*Fakultät für Mathematik und Physik, Albert-Ludwigs-Universität, Freiburg, Germany*
- ⁵²*Departement de Physique Nucleaire et Corpusculaire, Université de Genève, Geneva, Switzerland*
- ^{53a}*INFN Sezione di Genova, Italy*
- ^{53b}*Dipartimento di Fisica, Università di Genova, Genova, Italy*
- ^{54a}*E. Andronikashvili Institute of Physics, Iv. Javakhishvili Tbilisi State University, Tbilisi, Georgia*
- ^{54b}*High Energy Physics Institute, Tbilisi State University, Tbilisi, Georgia*
- ⁵⁵*II Physikalisches Institut, Justus-Liebig-Universität Giessen, Giessen, Germany*
- ⁵⁶*SUPA—School of Physics and Astronomy, University of Glasgow, Glasgow, United Kingdom*
- ⁵⁷*II Physikalisches Institut, Georg-August-Universität, Göttingen, Germany*
- ⁵⁸*Laboratoire de Physique Subatomique et de Cosmologie, Université Grenoble-Alpes, CNRS/IN2P3, Grenoble, France*
- ⁵⁹*Laboratory for Particle Physics and Cosmology, Harvard University, Cambridge Massachusetts, USA*
- ^{60a}*Kirchhoff-Institut für Physik, Ruprecht-Karls-Universität Heidelberg, Heidelberg, Germany*
- ^{60b}*Physikalisches Institut, Ruprecht-Karls-Universität Heidelberg, Heidelberg, Germany*
- ⁶¹*Faculty of Applied Information Science, Hiroshima Institute of Technology, Hiroshima, Japan*
- ^{62a}*Department of Physics, The Chinese University of Hong Kong, Shatin, N.T., Hong Kong, China*
- ^{62b}*Department of Physics, The University of Hong Kong, Hong Kong, China*
- ^{62c}*Department of Physics and Institute for Advanced Study, The Hong Kong University of Science and Technology, Clear Water Bay, Kowloon, Hong Kong, China*
- ⁶³*Department of Physics, National Tsing Hua University, Taiwan, Taiwan*
- ⁶⁴*Department of Physics, Indiana University, Bloomington Indiana, USA*
- ⁶⁵*Institut für Astro- und Teilchenphysik, Leopold-Franzens-Universität, Innsbruck, Austria*
- ⁶⁶*University of Iowa, Iowa City Iowa, USA*
- ⁶⁷*Department of Physics and Astronomy, Iowa State University, Ames Iowa, USA*
- ⁶⁸*Joint Institute for Nuclear Research, JINR Dubna, Dubna, Russia*
- ⁶⁹*KEK, High Energy Accelerator Research Organization, Tsukuba, Japan*
- ⁷⁰*Graduate School of Science, Kobe University, Kobe, Japan*
- ⁷¹*Faculty of Science, Kyoto University, Kyoto, Japan*

- ⁷²Kyoto University of Education, Kyoto, Japan
- ⁷³Research Center for Advanced Particle Physics and Department of Physics, Kyushu University, Fukuoka, Japan
- ⁷⁴Instituto de Física La Plata, Universidad Nacional de La Plata and CONICET, La Plata, Argentina
- ⁷⁵Physics Department, Lancaster University, Lancaster, United Kingdom
- ^{76a}INFN Sezione di Lecce, Italy
- ^{76b}Dipartimento di Matematica e Fisica, Università del Salento, Lecce, Italy
- ⁷⁷Oliver Lodge Laboratory, University of Liverpool, Liverpool, United Kingdom
- ⁷⁸Department of Experimental Particle Physics, Jožef Stefan Institute and Department of Physics, University of Ljubljana, Ljubljana, Slovenia
- ⁷⁹School of Physics and Astronomy, Queen Mary University of London, London, United Kingdom
- ⁸⁰Department of Physics, Royal Holloway University of London, Surrey, United Kingdom
- ⁸¹Department of Physics and Astronomy, University College London, London, United Kingdom
- ⁸²Louisiana Tech University, Ruston Louisiana, USA
- ⁸³Laboratoire de Physique Nucléaire et de Hautes Energies, UPMC and Université Paris-Diderot and CNRS/IN2P3, Paris, France
- ⁸⁴Fysiska institutionen, Lunds universitet, Lund, Sweden
- ⁸⁵Departamento de Física Teórica C-15, Universidad Autónoma de Madrid, Madrid, Spain
- ⁸⁶Institut für Physik, Universität Mainz, Mainz, Germany
- ⁸⁷School of Physics and Astronomy, University of Manchester, Manchester, United Kingdom
- ⁸⁸CPPM, Aix-Marseille Université and CNRS/IN2P3, Marseille, France
- ⁸⁹Department of Physics, University of Massachusetts, Amherst Massachusetts, USA
- ⁹⁰Department of Physics, McGill University, Montreal Québec, Canada
- ⁹¹School of Physics, University of Melbourne, Victoria, Australia
- ⁹²Department of Physics, The University of Michigan, Ann Arbor Michigan, USA
- ⁹³Department of Physics and Astronomy, Michigan State University, East Lansing Michigan, USA
- ^{94a}INFN Sezione di Milano, Italy
- ^{94b}Dipartimento di Fisica, Università di Milano, Milano, Italy
- ⁹⁵B.I. Stepanov Institute of Physics, National Academy of Sciences of Belarus, Minsk, Republic of Belarus
- ⁹⁶Research Institute for Nuclear Problems of Byelorussian State University, Minsk, Republic of Belarus
- ⁹⁷Group of Particle Physics, University of Montreal, Montreal Québec, Canada
- ⁹⁸P.N. Lebedev Physical Institute of the Russian Academy of Sciences, Moscow, Russia
- ⁹⁹Institute for Theoretical and Experimental Physics (ITEP), Moscow, Russia
- ¹⁰⁰National Research Nuclear University MEPhI, Moscow, Russia
- ¹⁰¹D.V. Skobeltsyn Institute of Nuclear Physics, M.V. Lomonosov Moscow State University, Moscow, Russia
- ¹⁰²Fakultät für Physik, Ludwig-Maximilians-Universität München, München, Germany
- ¹⁰³Max-Planck-Institut für Physik (Werner-Heisenberg-Institut), München, Germany
- ¹⁰⁴Nagasaki Institute of Applied Science, Nagasaki, Japan
- ¹⁰⁵Graduate School of Science and Kobayashi-Maskawa Institute, Nagoya University, Nagoya, Japan
- ^{106a}INFN Sezione di Napoli, Italy
- ^{106b}Dipartimento di Fisica, Università di Napoli, Napoli, Italy
- ¹⁰⁷Department of Physics and Astronomy, University of New Mexico, Albuquerque New Mexico, USA
- ¹⁰⁸Institute for Mathematics, Astrophysics and Particle Physics, Radboud University Nijmegen/Nikhef, Nijmegen, Netherlands
- ¹⁰⁹Nikhef National Institute for Subatomic Physics and University of Amsterdam, Amsterdam, Netherlands
- ¹¹⁰Department of Physics, Northern Illinois University, DeKalb Illinois, USA
- ¹¹¹Budker Institute of Nuclear Physics, SB RAS, Novosibirsk, Russia
- ¹¹²Department of Physics, New York University, New York, USA
- ¹¹³Ohio State University, Columbus Ohio, USA
- ¹¹⁴Faculty of Science, Okayama University, Okayama, Japan
- ¹¹⁵Homer L. Dodge Department of Physics and Astronomy, University of Oklahoma, Norman Oklahoma, USA
- ¹¹⁶Department of Physics, Oklahoma State University, Stillwater Oklahoma, USA
- ¹¹⁷Palacký University, RCPTM, Olomouc, Czech Republic
- ¹¹⁸Center for High Energy Physics, University of Oregon, Eugene Oregon, USA
- ¹¹⁹LAL, Univ. Paris-Sud, CNRS/IN2P3, Université Paris-Saclay, Orsay, France
- ¹²⁰Graduate School of Science, Osaka University, Osaka, Japan
- ¹²¹Department of Physics, University of Oslo, Oslo, Norway
- ¹²²Department of Physics, Oxford University, Oxford, United Kingdom

- ^{123a}*INFN Sezione di Pavia, Italy*
- ^{123b}*Dipartimento di Fisica, Università di Pavia, Pavia, Italy*
- ¹²⁴*Department of Physics, University of Pennsylvania, Philadelphia Pennsylvania, USA*
- ¹²⁵*National Research Centre “Kurchatov Institute” B.P.Konstantinov Petersburg Nuclear Physics Institute, St. Petersburg, Russia*
- ^{126a}*INFN Sezione di Pisa, Italy*
- ^{126b}*Dipartimento di Fisica E. Fermi, Università di Pisa, Pisa, Italy*
- ¹²⁷*Department of Physics and Astronomy, University of Pittsburgh, Pittsburgh Pennsylvania, USA*
- ^{128a}*Laboratório de Instrumentação e Física Experimental de Partículas—LIP, Lisboa, Portugal*
- ^{128b}*Faculdade de Ciências, Universidade de Lisboa, Lisboa, Portugal*
- ^{128c}*Department of Physics, University of Coimbra, Coimbra, Portugal*
- ^{128d}*Centro de Física Nuclear da Universidade de Lisboa, Lisboa, Portugal*
- ^{128e}*Departamento de Física, Universidade do Minho, Braga, Portugal*
- ^{128f}*Departamento de Física Teórica y del Cosmos, Universidad de Granada, Granada, Portugal*
- ^{128g}*Dep Física and CEFITEC of Faculdade de Ciências e Tecnologia, Universidade Nova de Lisboa, Caparica, Portugal*
- ¹²⁹*Institute of Physics, Academy of Sciences of the Czech Republic, Praha, Czech Republic*
- ¹³⁰*Czech Technical University in Prague, Praha, Czech Republic*
- ¹³¹*Charles University, Faculty of Mathematics and Physics, Prague, Czech Republic*
- ¹³²*State Research Center Institute for High Energy Physics (Protvino), NRC KI, Russia*
- ¹³³*Particle Physics Department, Rutherford Appleton Laboratory, Didcot, United Kingdom*
- ^{134a}*INFN Sezione di Roma, Italy*
- ^{134b}*Dipartimento di Fisica, Sapienza Università di Roma, Roma, Italy*
- ^{135a}*INFN Sezione di Roma Tor Vergata, Italy*
- ^{135b}*Dipartimento di Fisica, Università di Roma Tor Vergata, Roma, Italy*
- ^{136a}*INFN Sezione di Roma Tre, Italy*
- ^{136b}*Dipartimento di Matematica e Fisica, Università Roma Tre, Roma, Italy*
- ^{137a}*Faculté des Sciences Ain Chock, Réseau Universitaire de Physique des Hautes Energies—Université Hassan II, Casablanca, Morocco*
- ^{137b}*Centre National de l’Energie des Sciences Techniques Nucleaires, Rabat, Morocco*
- ^{137c}*Faculté des Sciences Semlalia, Université Cadi Ayyad, LPHEA-Marrakech, Morocco*
- ^{137d}*Faculté des Sciences, Université Mohamed Premier and LPTPM, Oujda, Morocco*
- ^{137e}*Faculté des sciences, Université Mohammed V, Rabat, Morocco*
- ¹³⁸*DSM/IRFU (Institut de Recherches sur les Lois Fondamentales de l’Univers), CEA Saclay (Commissariat à l’Energie Atomique et aux Energies Alternatives), Gif-sur-Yvette, France*
- ¹³⁹*Santa Cruz Institute for Particle Physics, University of California Santa Cruz, Santa Cruz California, USA*
- ¹⁴⁰*Department of Physics, University of Washington, Seattle Washington, USA*
- ¹⁴¹*Department of Physics and Astronomy, University of Sheffield, Sheffield, United Kingdom*
- ¹⁴²*Department of Physics, Shinshu University, Nagano, Japan*
- ¹⁴³*Department Physik, Universität Siegen, Siegen, Germany*
- ¹⁴⁴*Department of Physics, Simon Fraser University, Burnaby British Columbia, Canada*
- ¹⁴⁵*SLAC National Accelerator Laboratory, Stanford California, USA*
- ^{146a}*Faculty of Mathematics, Physics & Informatics, Comenius University, Bratislava, Slovak Republic*
- ^{146b}*Department of Subnuclear Physics, Institute of Experimental Physics of the Slovak Academy of Sciences, Kosice, Slovak Republic*
- ^{147a}*Department of Physics, University of Cape Town, Cape Town, South Africa*
- ^{147b}*Department of Physics, University of Johannesburg, Johannesburg, South Africa*
- ^{147c}*School of Physics, University of the Witwatersrand, Johannesburg, South Africa*
- ^{148a}*Department of Physics, Stockholm University, Sweden*
- ^{148b}*The Oskar Klein Centre, Stockholm, Sweden*
- ¹⁴⁹*Physics Department, Royal Institute of Technology, Stockholm, Sweden*
- ¹⁵⁰*Departments of Physics & Astronomy and Chemistry, Stony Brook University, Stony Brook New York, USA*
- ¹⁵¹*Department of Physics and Astronomy, University of Sussex, Brighton, United Kingdom*
- ¹⁵²*School of Physics, University of Sydney, Sydney, Australia*
- ¹⁵³*Institute of Physics, Academia Sinica, Taipei, Taiwan*
- ¹⁵⁴*Department of Physics, Technion: Israel Institute of Technology, Haifa, Israel*
- ¹⁵⁵*Raymond and Beverly Sackler School of Physics and Astronomy, Tel Aviv University, Tel Aviv, Israel*
- ¹⁵⁶*Department of Physics, Aristotle University of Thessaloniki, Thessaloniki, Greece*

- ¹⁵⁷*International Center for Elementary Particle Physics and Department of Physics,
The University of Tokyo, Tokyo, Japan*
- ¹⁵⁸*Graduate School of Science and Technology, Tokyo Metropolitan University, Tokyo, Japan*
- ¹⁵⁹*Department of Physics, Tokyo Institute of Technology, Tokyo, Japan*
- ¹⁶⁰*Tomsk State University, Tomsk, Russia*
- ¹⁶¹*Department of Physics, University of Toronto, Toronto Ontario, Canada*
- ^{162a}*INFN-TIFPA, Italy*
- ^{162b}*University of Trento, Trento, Italy*
- ^{163a}*TRIUMF, Vancouver British Columbia, Canada*
- ^{163b}*Department of Physics and Astronomy, York University, Toronto Ontario, Canada*
- ¹⁶⁴*Faculty of Pure and Applied Sciences, and Center for Integrated Research in Fundamental Science and
Engineering, University of Tsukuba, Tsukuba, Japan*
- ¹⁶⁵*Department of Physics and Astronomy, Tufts University, Medford Massachusetts, USA*
- ¹⁶⁶*Department of Physics and Astronomy, University of California Irvine, Irvine California, USA*
- ^{167a}*INFN Gruppo Collegato di Udine, Sezione di Trieste, Udine, Italy*
- ^{167b}*ICTP, Trieste, Italy*
- ^{167c}*Dipartimento di Chimica, Fisica e Ambiente, Università di Udine, Udine, Italy*
- ¹⁶⁸*Department of Physics and Astronomy, University of Uppsala, Uppsala, Sweden*
- ¹⁶⁹*Department of Physics, University of Illinois, Urbana Illinois, USA*
- ¹⁷⁰*Instituto de Fisica Corpuscular (IFIC), Centro Mixto Universidad de Valencia—CSIC, Spain*
- ¹⁷¹*Department of Physics, University of British Columbia, Vancouver British Columbia, Canada*
- ¹⁷²*Department of Physics and Astronomy, University of Victoria, Victoria British Columbia, Canada*
- ¹⁷³*Department of Physics, University of Warwick, Coventry, United Kingdom*
- ¹⁷⁴*Waseda University, Tokyo, Japan*
- ¹⁷⁵*Department of Particle Physics, The Weizmann Institute of Science, Rehovot, Israel*
- ¹⁷⁶*Department of Physics, University of Wisconsin, Madison Wisconsin, USA*
- ¹⁷⁷*Fakultät für Physik und Astronomie, Julius-Maximilians-Universität, Würzburg, Germany*
- ¹⁷⁸*Fakultät für Mathematik und Naturwissenschaften, Fachgruppe Physik,
Bergische Universität Wuppertal, Wuppertal, Germany*
- ¹⁷⁹*Department of Physics, Yale University, New Haven Connecticut, USA*
- ¹⁸⁰*Yerevan Physics Institute, Yerevan, Armenia*
- ¹⁸¹*Centre de Calcul de l'Institut National de Physique Nucléaire et de Physique des Particules (IN2P3),
Villeurbanne, France*
- ¹⁸²*Academia Sinica Grid Computing, Institute of Physics, Academia Sinica, Taipei, Taiwan*

[†]Deceased.

^aAlso at Department of Physics, King's College London, London, United Kingdom.

^bAlso at Institute of Physics, Azerbaijan Academy of Sciences, Baku, Azerbaijan.

^cAlso at Novosibirsk State University, Novosibirsk, Russia.

^dAlso at TRIUMF, Vancouver BC, Canada.

^eAlso at Department of Physics & Astronomy, University of Louisville, Louisville, KY, USA.

^fAlso at Physics Department, An-Najah National University, Nablus, Palestine.

^gAlso at Department of Physics, California State University, Fresno CA, USA.

^hAlso at Department of Physics, University of Fribourg, Fribourg, Switzerland.

ⁱAlso at II Physikalisches Institut, Georg-August-Universität, Göttingen, Germany.

^jAlso at Departament de Fisica de la Universitat Autònoma de Barcelona, Barcelona, Spain.

^kAlso at Departamento de Fisica e Astronomia, Faculdade de Ciencias, Universidade do Porto, Portugal.

^lAlso at Tomsk State University, Tomsk, and Moscow Institute of Physics and Technology State University, Dolgoprudny, Russia.

^mAlso at The Collaborative Innovation Center of Quantum Matter (CICQM), Beijing, China.

ⁿAlso at Università di Napoli Parthenope, Napoli, Italy.

^oAlso at Institute of Particle Physics (IPP), Canada.

^pAlso at Horia Hulubei National Institute of Physics and Nuclear Engineering, Bucharest, Romania.

^qAlso at Department of Physics, St. Petersburg State Polytechnical University, St. Petersburg, Russia.

^rAlso at Borough of Manhattan Community College, City University of New York, New York City, USA.

^sAlso at Department of Financial and Management Engineering, University of the Aegean, Chios, Greece.

^tAlso at Centre for High Performance Computing, CSIR Campus, Rosebank, Cape Town, South Africa.

^uAlso at Louisiana Tech University, Ruston LA, USA.

^vAlso at Institutio Catalana de Recerca i Estudis Avancats, ICREA, Barcelona, Spain.

^wAlso at Department of Physics, The University of Michigan, Ann Arbor MI, USA.

^xAlso at Graduate School of Science, Osaka University, Osaka, Japan.

- ^y Also at Fakultät für Mathematik und Physik, Albert-Ludwigs-Universität, Freiburg, Germany.
- ^z Also at Institute for Mathematics, Astrophysics and Particle Physics, Radboud University Nijmegen/Nikhef, Nijmegen, Netherlands.
- ^{aa} Also at Department of Physics, The University of Texas at Austin, Austin TX, USA.
- ^{ab} Also at Institute of Theoretical Physics, Ilia State University, Tbilisi, Georgia.
- ^{ac} Also at CERN, Geneva, Switzerland.
- ^{ad} Also at Georgian Technical University (GTU), Tbilisi, Georgia.
- ^{ae} Also at Ochadai Academic Production, Ochanomizu University, Tokyo, Japan.
- ^{af} Also at Manhattan College, New York NY, USA.
- ^{ag} Also at The City College of New York, New York NY, USA.
- ^{ah} Also at Departamento de Física Teórica y del Cosmos, Universidad de Granada, Granada, Portugal.
- ^{ai} Also at Department of Physics, California State University, Sacramento CA, USA.
- ^{aj} Also at Moscow Institute of Physics and Technology State University, Dolgoprudny, Russia.
- ^{ak} Also at Département de Physique Nucleaire et Corpusculaire, Université de Genève, Geneva, Switzerland.
- ^{al} Also at Institut de Física d'Altes Energies (IFAE), The Barcelona Institute of Science and Technology, Barcelona, Spain.
- ^{am} Also at School of Physics, Sun Yat-sen University, Guangzhou, China.
- ^{an} Also at Institute for Nuclear Research and Nuclear Energy (INRNE) of the Bulgarian Academy of Sciences, Sofia, Bulgaria.
- ^{ao} Also at Faculty of Physics, M.V.Lomonosov Moscow State University, Moscow, Russia.
- ^{ap} Also at National Research Nuclear University MEPhI, Moscow, Russia.
- ^{aq} Also at Department of Physics, Stanford University, Stanford CA, USA.
- ^{ar} Also at Institute for Particle and Nuclear Physics, Wigner Research Centre for Physics, Budapest, Hungary.
- ^{as} Also at Giresun University, Faculty of Engineering, Turkey.
- ^{at} Also at CPPM, Aix-Marseille Université and CNRS/IN2P3, Marseille, France.
- ^{au} Also at Department of Physics, Nanjing University, Jiangsu, China.
- ^{av} Also at Institute of Physics, Academia Sinica, Taipei, Taiwan.
- ^{aw} Also at University of Malaya, Department of Physics, Kuala Lumpur, Malaysia.
- ^{ax} Also at LAL, Univ. Paris-Sud, CNRS/IN2P3, Université Paris-Saclay, Orsay, France.